STRUCTURAL AND FUNCTIONAL DEVELOPMENT OF THE MARSUPIAL RESPIRATORY SYSTEM

SUBMITTED BY

SHANNON JADE SIMPSON

B. SC. (MEDICAL SCIENCE) (*HONS*)

A THESIS SUBMITTED IN FULFILMENT OF THE REQUIREMENTS FOR THE DEGREE OF DOCTOR OF PHILOSOPHY

UNIVERSITY OF TASMANIA

NOVEMBER, 2010

ABSTRACT

Marsupials are born with structurally immature lungs and rely, to varying degrees, on cutaneous gas exchange. The fat-tailed dunnart (*Sminthopsis crassicaudata*) is one of the smallest and most immature marsupial newborns having a gestation period of just 13 days, a birth weight of 13 mg and a delay in the onset of ventilation. This thesis (1) documents the structure and function of the respiratory system in the fat-tailed dunnart throughout the first weeks of life; (2) investigates possible causes for the necessity of cutaneous gas exchange including structural, neural, and mechanical constraints, and (3) explores changes in the control of breathing.

The skin is almost solely responsible for gas exchange in the newborn fat-tailed dunnart. Indeed, less than 35 % of newborn dunnarts were observed to make any respiratory effort on the day of birth. "Breathing", if seen, was usually accompanied by gross body movements, prolonged periods of apnoea, and tidal volumes and frequencies unlikely to result in efficient gas exchange. As a result of a poor breathing pattern, pulmonary ventilation did not meet the demand for oxygen until approximately 35 days postpartum.

Electron microscopy demonstrated that despite a general absence of breathing on the day of birth, the respiratory epithelium was well developed, containing both Type-I and Type-II (surfactant producing) alveolar epithelial cells. While surfactant coils were detected in the airways of the newborn marsupial it is likely that low diffusibility for oxygen contributes to the functional inadequacy of the lungs in the newborn; low diffusibility resulting from high diffusion distance caused by underdeveloped vasculature, small surface area and volumes available for gas exchange, and thickened singular cytoplasmic extensions of the gas exchanging Type-I epithelial cells. In addition, poor muscle co-ordination, chest wall distortion, and the absence of alveoli until after 40 days postpartum impede efficient pulmonary gas exchange in the newborn. All the above factors force the neonatal fat-tailed dunnart to rely predominately on its skin for gas exchange which is supported by a low metabolic rate and small size, hence large general surface area. In addition, the afferent input from chemoreceptors, and subsequent ability to mount a ventilatory response when challenged with hypoxia or hypercapnia, seems poorly developed in the neonatal period, and may contribute to the low convective requirement and need for cutaneous gas exchange in these neonates.

With much of the structural and functional development of the respiratory system occurring in the extra-uterine environment, the newborn marsupial challenges the traditional view that the mammalian respiratory system must be adequately developed to act as the sole organ of gas exchange at birth.

STATEMENT OF ORIGINALITY

This thesis contains no material that has been accepted for a degree or diploma by the University, or any other institution, except by way of background information and duly acknowledged in the thesis. To the best of my knowledge and belief, this thesis contains no material previously published or written by another person, except where due acknowledgement is made in the text, nor does the thesis contain any material that infringes copyright.

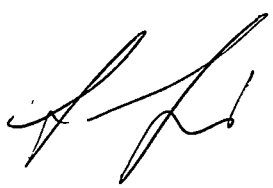

SHANNON JADE SIMPSON

NOVEMBER 2010

STATEMENT OF AUTHORITY OF ACCESS

This thesis may be available for loan and limited copying in accordance with the Copyright Act 1968.

SHANNON JADE SIMPSON

NOVEMBER 2010

ANIMAL ETHICS

The research associated with this thesis abides by the international and Australian codes on animal experimentation. All animals used in experimentation were done so under the approval and guidelines of La Trobe University Animal Ethics Committee permit LTU AEC 04/37(L). All animal experimentation was completed prior to the Frappell laboratory moving to the University of Tasmania.

SHANNON JADE SIMPSON

NOVEMBER 2010

FORMAT OF THESIS

THIS THESIS IS WRITTEN SUCH THAT EACH CHAPTER IS THE BASIS FOR A MANUSCRIPT THAT IS EITHER SUBMITTED OR IN PREPARATION WITH SHANNON J SIMPSON AS THE FIRST AUTHOR.

ACKNOWLEDGEMENTS

I would like to start by acknowledging the guidance provided to me by my supervisor Peter "Frapps" Frappell. I recall you saying when I first came into the lab that you would "allow me enough rope to hang myself". And I nearly did, several times! However I am extremely grateful for the freedom that you gave me during my PhD to explore the things that were of interest to me, and to change my mind along the path. Your enthusiasm for science is infectious and I thank you for introducing me to comparative and respiratory physiology. I truly value all the good times we had (who can forget the muffin bandage, firefly squid or your amazing dance moves...), the serious times too, the things I have learnt from you, and the friendship we have grown; I hope this molecular biology trained physiologist has done her 'academic dad' proud.

I would also like to thank Frapps' family, Deirdre, Claire and Huon; not just for putting up with us, but for welcoming us into your lives and home.

The administrative staff of the Department of Zoology at La Trobe University are sincerely thanked for all the 'behind the scenes' support they gave, particularly Fran Pizzey, June Cheah and Michelle Skicko. A special thank you is also extended to Mark Wilson for IT support (and answering a million questions) and to Eva Suric and Tobie Cousipetcos for the care they provided to the animal colonies.

I would not have made it through many a day without the love and support of my "lab sisters" Sarah Andrewartha and Lyndal Horne, and the music of Ryan Adams. We all celebrated the highs and suffered the lows of a PhD (and life!), and we always looked out

for each other. Josh Edwards; you are included as a 'lab sister' due to the surrogate arrangement you have with our lab...

I would also like to thank a few very special postdocs who have helped me in too many ways to mention here, and have become great friends along the way. Very special thanks to Kevin Cummings, Angelina Fong and Sharon Flecknoe for all that you have done. Kevin, I'm not sure this would have happened without you!

I also extend thanks to the external labs who allowed me to complete various aspects of this project with them, especially the laboratories of Stuart Hooper and John Greer. I would also like to thank the physicists who worked insane hours with us at SPring8 to collect the synchrotron images, especially Karen Siu who helped me to make sense of the data.

The support provided to me by my good friends (especially Victoria) and my amazing family (Mum, Amber-Lee and the wonderful John) brings a tear to my eye. I know it's not always easy to be around a stressed PhD student, especially one that goes through a cancer diagnosis, surgery and chemotherapy while trying to write up. So, thanks for always encouraging me to reach for the stars no matter what stands in my way, and for always being there on the occasions when I came crashing down.

I dedicate the completion of this thesis to all those who are not as lucky as I have been, and to those people who helped get me through. I fought to get this done- not just for myself, but as a way to say thanks to all of you.

TABLE OF CONTENTS

LIST OF FIGURES

LIST OF TABLES

LIST OF ABBREVIATIONS

Δ	(delta) change in
AEC(s)	alveolar epithelial cell(s)
ATP	adenosine triphosphate
CO_2	carbon dioxide
C_{rs}	compliance of the respiratory system
^oC	degrees Celsius
E	embryonic
f	frequency of breathing
$FADH_2$	flavin adenine dinucleotide
FBM	fetal breathing movement
FRC	functional residual capacity
g	gram
GABA	γ-aminobutyric acid
H_2O	water
Hz	hertz
keV	kilo electron volt
mg	milligram
min	minute
ml	millilitre
mm	millimetre

NADH	nicotinamide adenine dinucleotide
O_2	oxygen
P	days postpartum
P_{O_2}	partial pressure of O_2
P_{CO_2}	partial pressure of CO_2
pre-BötC	pre-Bötzinger complex
S.E.M	standard error of the mean
T_E	expiratory time
T_I	inspiratory time
T_I/T_{TOT}	duty cycle
T_P	post-inspiratory pause
T_{TOT}	total breath time
µl	microlitre
$\dot{V}_{CO_2}$	total rate of carbon dioxide production
$\dot{V}_E$	rate of pulmonary ventilation (minute ventilation)
$\dot{V}_{O_2}$	total rate of oxygen consumption (*i.e. skin + lungs*)
Vr	resting volume
V_T	tidal volume
V_T/T_I	inspiratory drive

1 STRUCTURAL AND FUNCTIONAL DEVELOPMENT OF THE RESPIRATORY SYSTEM: AN INTRODUCTION

Birth is perhaps the most physiologically challenging event in the life of any mammal. The fetal lung must undergo extensive structural, physiological and biochemical maturation *in utero* so that it can function as an effective organ for gas exchange during postnatal life. Air breathing requires the clearance of fetal lung liquid, the onset of a rhythmic breathing pattern and the establishment of a functional residual capacity (FRC). In addition, the lung must be able to provide a large surface area for gas exchange, a thin air-blood barrier for diffusion, appropriate vascularisation and a functioning surfactant system, which together support oxygen demands and maintenance of acid-base balance. Once established, the breathing pattern can be modified by the integration of central and peripheral feedback to maintain homeostatic control over blood gases and pH.

1.1 STRUCTURAL DEVELOPMENT OF THE RESPIRATORY SYSTEM

To support gas exchange, the mammalian lung must undergo significant morphological changes prior to and at birth. This section describes the morphological features characterising the stages of lung development, as well as describing epithelial cell differentiation and maturation of the pulmonary vasculature.

1.1.1 Stages of lung development

While lung development is a continuous process, six well-defined stages have been delineated based on anatomical and histological characteristics: embryonic, pseudoglandular, canalicular, saccular, alveolar, and microvascular maturation (Zeltner and Burri, 1987). The timing of these stages relative to birth can vary considerably between species (Zoetis and Hurtt, 2003). For example, human infants are born with

lungs that have just entered the alveolar stage, while other species have been shown to be more developed (*e.g.* sheep) or less developed (*e.g.* opossum) at birth (Thurlbeck, 1975). The lungs of the newborn quokka wallaby are at the canalicular stage (Makanya et al., 2007), making it to date the most primitive newborn lung.

1.1.1.1 The prenatal embryonic and pseudoglandular stages of lung development

During the embryonic stage of lung development, the lung buds from the primitive gut and gives rise to two primary bronchial buds, from which arises the respiratory tree (Burri, 1984). Simultaneously, the vasculature, which will become the pulmonary arteries and veins, buds off from the sixth pair of aortic arches and the atrial portion of the heart, respectively (Burri, 1984). The embryonic stage leads into the pseudoglandular stage of lung development, when branching morphogenesis occurs. All airway divisions are complete by the end of this period, with branching taking on the adult pattern (Bucher and Reid, 1961a). The airway tubes are lined proximally with glycogen-containing high columnar cells, and distally by cuboidal, epithelial cells (Bucher and Reid, 1961b).

1.1.1.2 Canalicular stage of lung development

This canalicular stage is so named because the lung parenchyma lining the potential airspaces is being "canalised" by a network of capillaries. Simultaneously, the glycogen-rich epithelial cells lining the tubules begin to flatten out, so that regions with a thin air-blood barrier begin to appear in preparation for gas exchange (Burri, 1997). The capillaries, which previously formed a loose network in the mesenchyme, begin to arrange themselves around the airspaces, subsequently establishing close contact with

the overlying epithelium (Burri, 1984). Differentiation into Type-I or Type-II alveolar epithelial cells (AECs) from the progenitor Type-II stem cell has commenced (Mercurio and Rhodin, 1976) and lamellar bodies, which are associated with surfactant production, begin to appear in the Type-II AECs .

1.1.1.3 Saccular stage of lung development

At the transition from the canalicular stage to the saccular stage of lung development, the peripheral airways end in clusters of widened airspaces called saccules, which represent the future alveolar ducts and alveoli (Boyden, 1977). As a result of this airspace widening, the volume of the interstitial tissue between air sacs greatly decreases, which in turn alters the capillary arrangement such that a capillary bi-layer is seen at the intersaccular septa (Burri, 1984). The AECs undergo further differentiation, with the Type-I AECs becoming the most abundant epithelial cell type in the lung. The Type-II AECs increase in number, size and surfactant stores, while the amount of cytoplasmic glycogen decreases (Deutsch and Pinar, 2002).

1.1.1.4 Alveolar stage of lung development and the role of elastin

During normal alveolarisation, new inter-alveolar walls within the terminal saccules arise from secondary septa; which are derived from the intersaccular walls, or primary septa. As with the primary septa, a double capillary layer is present (Burri, 2006). The secondary septa are characterised by a deposition of elastin fibres at the tip of the secondary septal crest. Elastin is critically important for the development of alveoli in the lung (Starcher, 2000); such that mice deficient in elastin are unable to commence the alveolar stage of

lung development (Bostrom et al., 1996; Lindahl et al., 1997). The packet of elastin at the apex of the septa is produced by differentiating fibroblasts in the central portion of the septum (McGowan, 1992). While elastin in imperative for alveolarisation within the developing lung, it is also important for maintaining the structural and functional integrity of the lung. For example, elastin supports the changes in compliance occurring in the mature lung across the normal breathing range (Mercer and Crapo, 1990).

1.1.1.5 Stage of microvascular maturation

Following alveolar formation, the capillary networks of the pulmonary parenchyma must mature morphologically, termed the stage of microvascular maturation. During this final stage of lung development, the double-capillary network is transformed into a single capillary network by thinning of the intervening connective tissue layer. In this way, the capillaries on both sides of the septum come in close contact with each other and merge their lumina (Burri, 2006).

1.1.2 Structural development of the cardio-respiratory system in the newborn marsupial

The newborn marsupial lung is the most primitive mammalian lung that has been described (Makanya et al., 2001) In fact, marsupials are born with a number of organ systems at a very rudimentary stage of development, with much of the organogenesis and differentiation occurring within the pouch.

1.1.2.1 Development of the respiratory system in the marsupial

Despite its relative immaturity, the epiglottis and pharynx of the marsupial respiratory system is sufficiently developed to allow simultaneous suckling and breathing in early postnatal life (Hill and Hill, 1955; Hughes et al., 1989). The ribs and tracheal rings of the tammar wallaby are composed of hyaline cartilage (Hughes and Hall, 1988) and the relatively well-developed intercostal muscles are thought to be the driving force behind respiratory movements. The diaphragm, a thin sheet of muscle that divides the thoracic and abdominal cavities just three days prior to birth, probably has very little role in breathing during this period (Hughes et al., 1989).

When compared to eutherians, a comparatively under-developed lung has been described in the newborn marsupials, with the tammar wallaby (Runciman et al., 1996), brushtail possum (Gemmell and Nelson, 1988) and bandicoot (Gemmell, 1986) born at the saccular stage of lung development. The low birth weight marsupials, such as the northern native cat (Gemmell and Nelson, 1988), the Tasmanian devil (Tyndale-Biscoe and Janssens, 1988), and the American opossum (Krause and Leeson, 1975) have an even more immature lung at birth, composed of simple branching airways ending in a number of terminal air chambers and a double capillary network. In contrast to all other mammals, the quokka wallaby is born with lungs in the canalicular stage of development (Makanya et al., 2007), not making the transition to the saccular stage until approximately four postnatal days (Makanya et al., 2001). Birth at this incredibly early stage of development would lead to respiratory dysfunction and possibly death in many other newborn mammals. This is potentially less problematic for the newborn marsupial

since, unlike eutherians with a smaller surface area-volume ratio, the skin can also be used as a surface for gas exchange (Mortola et al., 1999; Frappell and Mortola, 2000; MacFarlane and Frappell, 2001).

Alveolarisation does not commence until well after birth in marsupials (Gemmell, 1986; Runciman et al., 1996; Makanya et al., 2001), and a lung that is adult in appearance is generally not observed until just prior to pouch vacation. In the tammar wallaby, alveoli formation commenced at around 70 days postpartum (P70) (Runciman et al., 1996), roughly equivalent to a P5-10 rat (Burri et al., 1974). Despite this, both Type-I and Type-II AECs are present in marsupials at birth (Runciman et al., 1999; Makanya et al., 2001; Makanya et al., 2003). In addition, surfactant proteins have been immunohistochemically detected in the tammar wallaby (Miller et al., 2001), implying that at this age functional surfactant is lowering surface tension at the air-gas interface to effectively increase lung compliance.

1.1.2.2 Cardiovascular circulation in the developing marsupial

The ductus arteriosus closes within hours after birth in the newborn marsupial (Runciman et al., 1995). In contrast to other mammals, however, the inter-atrial connection is still open until at least 4 days after birth, indicative of mixing of the pulmonary and systemic blood supply until this age (Baudinette et al., 1988b; Runciman et al., 1995). As is often the case in reptiles (Wang and Hicks, 1996), this right-to-left shunting would be expected to dilute the arterial oxygen (O_2), leading to decreased haemoglobin O_2 saturation and arterial O_2 content.

The blood of newborn marsupials is reminiscent of eutherian embryonic blood, including large nucleated red blood cells and also contains several haemoglobin subtypes distinct from those observed in adults (Baudinette et al., 1988a; Holland et al., 1988; Tibben et al., 1991; Holland et al., 1998). With the exception of the fat-tailed dunnart (Holland et al., 1994), the oxygen affinity of the fetal and newborn marsupial blood is less than that of the adult (Baudinette et al., 1988a; Holland et al., 1988; Calvert et al., 1993; Calvert et al., 1994), which is in stark contrast to the increased O_2 affinity observed in fetal and newborn eutherians. The reason for the difference between marsupials and eutherians is not entirely known, however, while high O_2 affinity is advantageous to combat the lower O_2 tension experienced *in utero* by eutherian mammals, it is presumably not required in the well oxygenated (and relatively hyperoxic to the eutherian) environment (Baudinette et al., 1988a) experienced in the maternal pouch of the marsupial.

1.2 FUNCTIONAL DEVELOPMENT OF THE RESPIRATORY SYSTEM

Except for some very small newborn marsupials, a functional lung at birth is essential for survival. This section addresses the role of the lungs and the important physiological aspects that lead to a functional lung at birth.

1.2.1 The oxygen cascade

The energetic needs of cells are predominantly met by the synthesis of high energy phosphate molecules (adenosine triphosphate, ATP) by the aerobic process of oxidative phosphorylation, which involves the reduction of O_2 to water (H_2O) with electrons donated by nicotinamide adenine dinucleotide (NADH) and flavin adenine dinucleotide

($FADH_2$) in the mitochondria (Kennedy and Lehninger, 1948). Oxygen is transported to the site of oxidation via a number of convective and diffusive steps in a process known as the oxygen cascade (or respiratory cascade) (Taylor and Weibel, 1981). In mammals, O_2 from environmental air is moved into the lungs via inspiration and subsequently diffuses from the alveoli to the circulation via the capillary network, driven by the maintenance of the O_2 partial pressure gradient. Oxygen is predominantly carried through the circulation for transfer to tissues bound to haemoglobin in erythrocytes, though a small amount is dissolved in the plasma. The oxygenated blood is then moved into the tissues by the circulation, and finally reaches the cells and their mitochondria by diffusion (Dejours, 1975) (see Figure 1.1 for model). The carbon dioxide (CO_2) produced during metabolism is removed by essentially the same mechanism in the reverse direction, with the exception that most of the CO_2 is transported as HCO_3^- rather than combined with haemoglobin. The flow of O_2 through the cascade is determined by the O_2 required for energy conversion in the respiratory chain of the mitochondria; i.e. the mitochondria behave like a "sink" for O_2. Any step in this pathway could potentially limit the overall O_2 flow into the mitochondrial sink and thus the O_2 available for aerobic metabolism (Taylor and Weibel, 1981).

1.2.2 Metabolic-ventilatory coupling

When the lung is the sole source for gas exchange, it is reasonable to expect a tight coupling between aerobic metabolism and pulmonary ventilation as O_2 demand must be met by supply (Taylor and Weibel, 1981). In fact, the tight coupling is maintained irrespective of animal size, such that the ratio of ventilation ($\dot{V}_E$) to metabolic rate ($\dot{V}_{O_2}$)

(convective requirement) for any mammal is mass independent and should be in the range of 32-41 ml air/ml O_2 under normal conditions (Stahl, 1967; Frappell and Baudinette, 1995). If $\dot{V}_E/\dot{V}_{O_2}$ was not universal , then animals with high $\dot{V}_E/\dot{V}_{O_2}$ would have lower alveolar (and arterial) CO_2 partial pressures (P_{CO_2}) and higher partial pressures of O_2 (P_{O_2}) than animals with low $\dot{V}_E/\dot{V}_{O_2}$, which, would be contrary to the observation that alveolar and arterial blood gases are similar among species (Reeves, 1977).

Other animal groups have different $\dot{V}_E/\dot{V}_{O_2}$ ratios depending on the efficiency of the gas exchange surface *e.g.* birds (Frappell et al., 2001) or their ability to utilise the skin for gas exchange *e.g.* most amphibians, aquatic reptiles and some fishes (Piiper and Scheid, 1992). In addition, $\dot{V}_E/\dot{V}_{O_2}$ varies with temperature in amphibians and reptiles as a means of regulating blood acid-base balance (Reeves, 1977).

1.2.3 The onset of breathing

Fetal breathing movements (FBMs) play an important role in stimulating lung growth and preparing the respiratory muscles for the first breath. FBMs have been demonstrated in a large number of mammalian species (Jansen and Chernick, 1983). Fetal breathing, unlike breathing in postnatal life, is often rapid, very irregular, episodic and highly sleep-state dependent (Jansen and Chernick, 1991).

For the newborn to survive, ventilation must be established immediately at birth and continuously maintained. At birth, the airways must be cleared of fetal lung liquid to allow the entry of air.

Figure 1.1. A model of the oxygen (respiratory) cascade.

In the interest of maintaining steady state conditions, flow of O_2 is equal at each step and is dictated by the rate of oxygen consumption ($\dot{V}O_2$) at the mitochondrial sink.. Flow rates can be expressed at each step of the pathway as the product of the O_2 partial pressure gradient (ΔPO_2) and the associated conductance term, as described by variations in the Fick Equation. For convective transfer, the conductance is equivalent to the mass flow rate multiplied by the capacitance (β) of the medium for O_2. Abbreviations: $\dot{V}E$ is pulmonary ventilation; $P_{insp}O_2$ is inspired PO_2; $P_{exp}O_2$ is expired PO_2; D_{LO_2} is the lung diffusing capacity for O_2; P_{AO_2} is alveolar PO_2; $P_{\bar{v}O_2}$ is blood PO_2; $\dot{Q}T$ is total cardiac output; P_{aO_2} is arterial PO_2; $P_{\bar{v}O_2}$ is mixed venous PO_2; D_{TO_2} is tissue diffusing capacity for O_2; $P_{\bar{c}O_2}$ is mixed capillary PO_2; ADP is adenosine diphosphate; ATP is adenosine triphosphate.

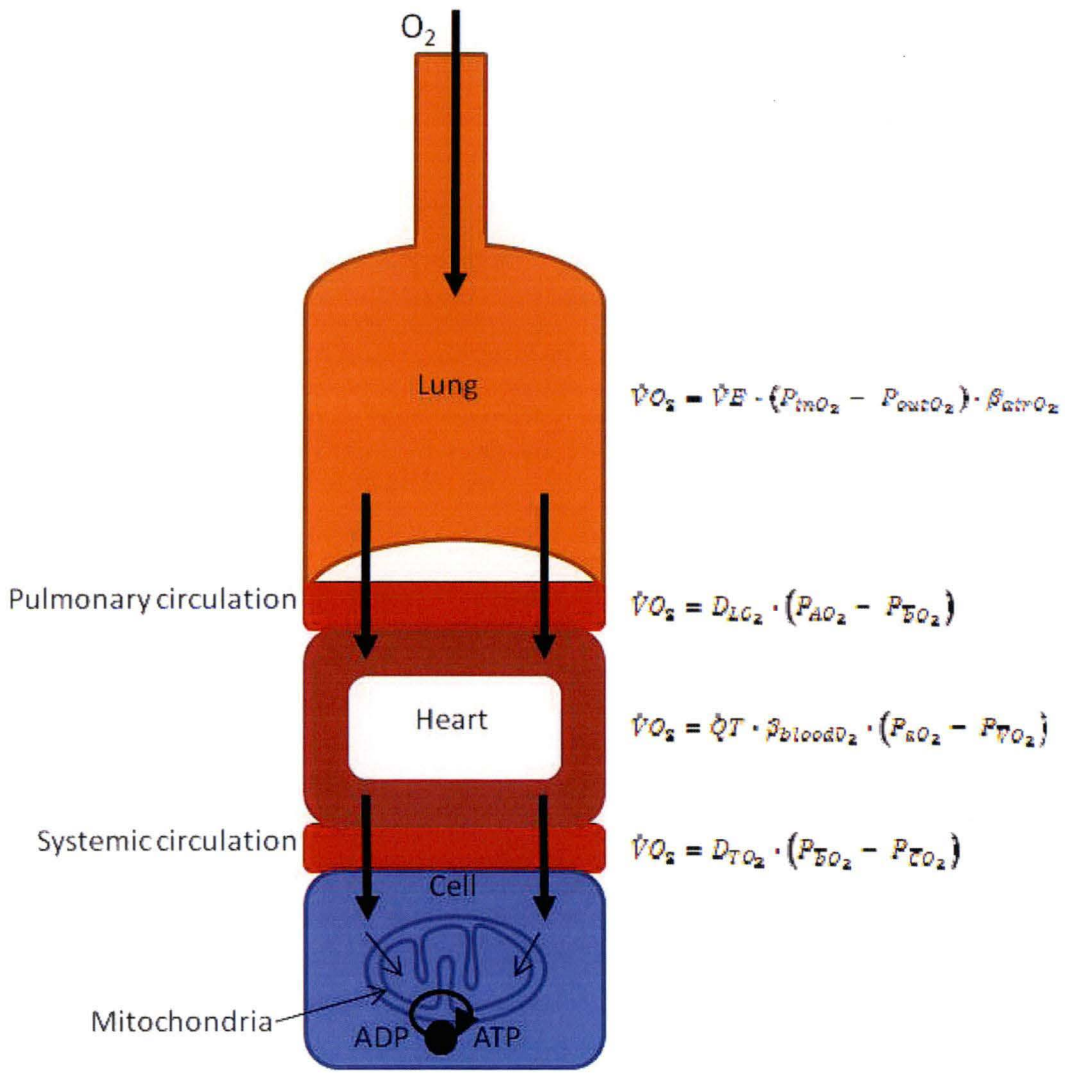
O_2
Lung
Pulmonary circulation
Heart
Systemic circulation
Cell
Mitochondria
ADP
ATP
$\dot{V}O_2 = \dot{V}E \cdot (P_{inO_2} - P_{outO_2}) \cdot \beta_{atrO_2}$
$\dot{V}O_2 = D_{LO_2} \cdot (P_{AO_2} - P_{\bar{P}O_2})$
$\dot{V}O_2 = \dot{Q}T \cdot \beta_{bloodO_2} \cdot (P_{aO_2} - P_{\bar{T}O_2})$
$\dot{V}O_2 = D_{TO_2} \cdot (P_{\bar{P}O_2} - P_{\bar{T}O_2})$

The suggested mechanisms for clearance include; mechanical forces imposed on the fetus during labour (Vyas et al., 1981; te Pas et al., 2008), transepithelial osmotic gradients generated by sodium re-absorption from the airways (Strang, 1991; Olver et al., 2004), and the trans-pulmonary pressures generated by inspiration which provide a hydrostatic pressure gradient for the movement of fluid out of the airways and into the surrounding lung tissue after birth (Hooper et al., 2007; Hooper et al., 2009). The first postnatal breath may result from a combination of lung expansion, oxygen levels, CO_2 chemoreceptor activation, thermal, tactile and pressure stimuli, and the activation of the sympatho-adrenal system, and will consequently 'reset' the carotid body chemoreceptors to their adult values because of the relative increase in P_{O_2} from fetal life (Randall, 1992). Some air remains in the lungs after this first breath (indicative of alveolar stability attributable to the presence of surfactant) and the establishment of functional residual capacity (FRC) is commenced. Newborns are inclined to maintain FRC above the relaxation volume of the lung (Vr) by narrowing the upper airways during expiration, predominantly at the laryngeal level, and/or recruiting post-inspiratory muscle activity (Mortola, 1985). Expiratory 'braking' often results in complete post-inspiratory obstruction (or pauses) which can be favourable for the newborn by raising intra-pulmonary pressure to help generate uniform lung expansion and prevention of atelectasis (Kosch and Stark, 1984). Such a strategy may not be desirable in species with high metabolic rates due to the increase in expiratory time and consequent decrease in breathing frequency (and subsequently $\dot{V}_E$) (Mortola et al., 1985a).

1.2.4 The breathing pattern of newborn marsupials

A post-inspiratory pause (T_P) is prominent in the breathing pattern of neonatal marsupials (Frappell and MacFarlane, 2006), where the respiratory system relaxes passively against a closed glottis (Farber, 1972). The only phase in which diaphragmatic activity occurs throughout the entire breath cycle (T_{TOT}) is during the time of inspiration (T_I) and thus T_P represents the static component of expiration. At the end of the pause, the glottis opens and the lungs deflate (deflation time is T_E). Tidal volume (V_T) is determined from the inflation phase of the cycle, and these variables are used to derive the duty cycle (T_I/T_{TOT}), inspiratory drive (V_T/T_I), breathing frequency ($f = 60/T_{TOT}$), and minute ventilation ($\dot{V}_E = V_T.f$). The breathing pattern undergoes changes with postnatal development, including the cessation of T_P in the case of marsupials, as well as a progressive lengthening of T_I as shown in neonates of several species, including the opossum (Farber, 1988), mice and rabbits (Mortola, 1984; Hilaire and Duron, 1999).

1.3 RESPIRATORY CONTROL IN THE NEWBORN

The regulation of breathing during the neonatal period undergoes dramatic changes with the maturation of the neurophysiological, metabolic and mechanical components of the respiratory control system (Bonora et al., 1994). Coordinated ventilation relies on the generation of spontaneous rhythms from brainstem respiratory neurons (a "central rhythm generator"), maturation of the respiratory motoneurones and muscles, as well as increased feedback from peripheral and central chemoreceptors and lung and airway mechanoreceptors (Feldman et al., 2003). The effectiveness of ventilation depends not

only on neural control but also on the mechanical properties of the respiratory system, which allow the neural output to be converted to effective ventilation. To add to the complexity, breathing pattern may be further modified by sleep-wake state, sighing, yawning or swallowing. The interplay of these factors is subject to maturational changes and neonatal breathing is inherently variable due to the immature state of integration between these components. While the neural and muscular components of the respiratory system mature postnatally, they must be sufficiently developed to function at birth, and allow generation of a rhythm that allows for ventilation in a highly compliant chest wall (Greer et al., 2006). This section will address some of the elements that contribute to respiratory control in the newborn.

1.3.1 Respiratory rhythmogenesis

Tidal breathing results from the intermittent activation of the respiratory muscles by neural output from the respiratory centres, but can be overridden by higher parts of the brain such as the cortex (West, 1995). In mammals, the central role of the pre-Bötzinger complex (pre-BötC) for inspiratory rhythmogenesis (Smith et al., 1991) is now widely accepted. Considerable debate does however remain about the cellular mechanisms and whether the pre-BötC co-operates with neurons in the parafacial respiratory group (Feldman and Janczewski, 2006; Onimaru and Homma, 2006). The parafacial group is thought to control the expiratory musculature, especially during periods of high ventilatory demand. Like the pre-BötC, neurons in this group are intrinsically rhythmogenic. Unlike the pre-BötC, however, neurons in the parafacial nucleus are opiate insensitive (Janczewski et al., 2002).

Innervation of the diaphragm is important for expression of the respiratory rhythm. Respiratory rhythmogenesis first emerges in the rat at embryonic day (E) 16.5-17 (Greer et al., 1992) and the mouse at E15 (Viemari et al., 2003) despite the phrenic axons reaching the primordial diaphragm by E13.5 (Allan and Greer, 1997a, 1998). Approximately 24 hours after initial contact, intramuscular branching commences within the diaphragm so that the phrenic nerve establishes the characteristic bilateral entry points and subsequent tertiary intramuscular branching pattern (Laskowski and Owens, 1994).

1.3.2 Neurotransmitters in neonates

Neurotransmitters are important in the generation, transmission and modulation of respiratory rhythm, and often elicit a different response in neonates than they do in adults (Bonham, 1995). Glutamate is the key neurotransmitter mediating excitatory synaptic input to virtually all brain stem respiratory neurons and is required for the transmission of inspiratory drive (Wong-Riley and Liu, 2005). The expression of glutamate immunoreactivity increases with postnatal days from P2 to P21 in several brain stem nuclei of the rat, however a distinct reduction in glutamate immunoreactivity is evident at P12 (Liu and Wong-Riley, 2002), implying that the neurons are engaged in more glutamatergic neurotransmission as they mature, with a critical developmental period at P12. Interestingly, glutamate injected into the brainstem of the newborn opossum induces respiratory pauses, however when injected into older animals glutamate is clearly stimulatory (Farber, 1990). Inhibitory neurotransmitters such as γ-aminobutyric acid (GABA) also have age-dependent effects in the opossum and many other species.

GABA has been shown to have an excitatory effect in the neurons of the newborn, switching to an inhibitory effect in the mature neuron (Michelson and Wong, 1991). A distinct rise in GABA immunoreactivity in rats at P12 has also been demonstrated (Liu and Wong-Riley, 2002) further identifying this as a critical developmental period.

1.3.3 Respiratory mechanics

The mechanical properties of the respiratory system determine how effectively the neural output translates into a ventilatory response. The surfactant layer lining the respiratory epithelium plays a vital role in this by reducing surface tension within the alveoli (Clements et al., 1961). The resting lung volume (Vr) is an important feature that helps maintain blood-gas homeostasis by maintaining air in the lung allowing O_2 and CO_2 exchange to continue in the absence of active breathing. Resting lung volume depends on the mechanical interaction between the lungs and chest wall; specifically, the opposing outward recoil of the chest wall (dependent on the elastic properties of the diaphragm and rib cage), and the inward recoil of the lung (dependent on the viscoelastic properties of the lung). The elastic characteristics are normally defined as compliance (C), determined by the pressure required to achieve a given change in volume ($C=\Delta V/\Delta P$) (Mortola, 2001). The compliance of the respiratory system (C_{rs}) can be broken down into its constituents, the lung (C_L) and the chest wall (C_{CW}). In the tidal volume range of newborns, C_{rs} does not differ much from that of the lung alone (C_L) (Avery and Cook, 1961; Fisher and Mortola, 1980; Mortola, 1987), indicating that the compliance of the chest wall ($C_{CW}=1/C_{rs} - 1/C_L$) must be higher than that of the lung. Consequently, chest wall distortion is common during inspiration, resulting in a loss of lung volume and

inefficient ventilation (Mortola et al., 1985b; Frappell and Mortola, 1989; Frappell and Mortola, 2000).

The resistance of the respiratory system is often measured and describes the airflow characteristics defined by the pressure required to generate a unit change in flow (Mortola et al., 1987). Newborns have a comparatively higher resistance and therefore must generate more pressure to achieve the same amount of airflow when compared to adults. Quantifying these mechanical characteristics can provide information about the functional capabilities of the respiratory system and the efficiency of breathing (Mortola, 2001).

1.3.4 Chemosensitivity

While afferent information to the respiratory centres from chemoreceptors and mechanoreceptors is not essential for neuronal rhythmicity, it is important for the modulation of the depth, timing and pattern of respiration (Milsom, 1990). Chemoreceptors provide essential information about O_2, CO_2 and pH (Nattie, 1999). Chemoreceptors located in the carotid bodies, while able to detect CO_2 and pH, mainly detect O_2. Additional chemoreceptors in the brain detect CO_2/pH (Nattie, 1999). The respiratory activity in response to changes in O_2 or CO_2 (*i.e.* hypoxia or hypercapnia, respectively) generally increases with postnatal age and is dependent on the relative size and maturity at birth (Bonora et al., 1994).

1.3.4.1 Hypoxia

The carotid body glomus cells are the primary mediators of the increase in breathing during acute hypoxia, though accessory receptors like the aortic chemoreceptors can play a role (Comroe, 1939). Generally, ventilatory chemosensitivity is low in newborns; the response to hypoxia increases with age, probably as the sensitivity of the glomus cells reset to the relatively hyperoxic conditions of the extra-uterine environment (Hanson et al., 1989). In contrast to the adult, the newborn does not sustain an increase in ventilation (hyperpnoea) in response to hypoxia, and the ventilatory response is often a biphasic one where there is an initial increase in minute ventilation, followed by a decline, in some cases to below the pre-hypoxic levels (Neubauer et al., 1990).

The overall lack of hyperpnoea during hypoxia in newborns implies that either the chemoafferent input is minimal, or that their inputs are suppressed centrally. The secondary ventilatory depression has been studied extensively, but no definitive causes have been revealed. Central neural inhibition has been suggested (Blanco et al., 1984), as has the effects of hypoxic hypometabolism. Contributions from the fatigue of the respiratory muscles, changes in compliance, depression of the respiratory neurons, or failure of the peripheral chemoreceptors have all been discounted (Lawson and Long, 1983; Blanco et al., 1984). It should however be noted that all animals used in these studies were anesthetised, which changes the activity of respiratory neurons, and the responsiveness of the chemoreceptors.

Despite the reduced breathing in newborns with acute hypoxia, an increase in the convective requirement is still observed because of disproportionate drop in $\dot{V}O_2$ (Mortola, 1993). Thus, hypometabolism plays an important role in neonates for mitigating the effects of hypoxia (Mortola, 2004).

1.3.4.2 Hypercapnia

Similar to the hypoxic response, newborns also show an attenuated ventilatory response to hypercapnia compared to adults (Carroll et al., 1993; Carroll and Fitzgerald, 1993; Davis et al., 2006). In general, newborn mammals respond to CO_2 with a sustained hyperventilation (Saetta and Mortola, 1987), with little or no hypometabolic response (Mortola and Lanthier, 1996; Saiki and Mortola, 1996). Increases in both V_T and f contribute to the initial hyperventilation in response to increasing CO_2. With time, f returns to baseline and the hyperventilation is sustained solely by the increase in V_T (Bonora et al., 1994). While term neonates and adults can increase their ventilation through an increase in both tidal volume and frequency, preterm infants to not appear to be able to increase breathing frequency in response to CO_2 (Martin et al., 1985; Eichenwald et al., 1993), presumably as a result of both mechanical and neuronal factors (Krauss et al., 1965).

1.4 DIRECTIONS OF THE THESIS

1.4.1 Gas exchange in the newborn marsupial

While cutaneous gas exchange is common in amphibians, aquatic reptiles and some fishes, the skin contributes very little to the gas exchange required to meet total metabolic requirements of the adult mammal. The possible exception is the bat which can utilise the large surface area on its highly vascularised wings for a maximum of 11.5 % CO_2 elimination (Onimaru and Homma, 2006; Makanya and Mortola, 2007). To enable cutaneous respiration, the skin must be highly vascularised and have high gas diffusion properties. In addition, the animal must have metabolic requirements (often low) that can be met through this avenue and a high surface area to volume ratio (Feder and Burggren, 1985).

Marsupials are generally born small and with low metabolic demands. Despite this, initial measurements in one week-old tammar wallabies weighing over 1 gram showed that the skin accounted for only 3-4 % of the total O_2 uptake (Baudinette et al., 1988a). Later, the newborn Julia Creek dunnart was shown to rely almost entirely on the skin for respiration and displayed no evidence of ventilation during the first days of life (Mortola et al., 1999; Frappell and Mortola, 2000). This challenged the notion that the lungs are always the sole contributor to gas exchange in mammals, and prompted re-examination of cutaneous gas exchange in other marsupials. MacFarlane and Frappell (2001) subsequently demonstrated that the skin did contribute ~30 % of the oxygen to meet the metabolic requirements of the newborn tammar wallaby (400 mg). However, there was

no longer significant contribution by the skin when the animal reached a body mass of 1 gram, supporting the speculation that 1 gram was close to the upper weight limit, after which cutaneous gas exchange could no longer occur in the newborn marsupial (Frappell and Mortola, 2000).

With a delay in the onset of ventilation and subsequent development of the breathing pattern, the level of lung ventilation in the Julia Creek dunnart is insufficient to sustain total metabolic rate during the first weeks of life (Frappell and MacFarlane, 2006). Interestingly, the newborn opossum also yielded a convective requirement lower than that which would be expected based on the allometric relationship relating $\dot{V}_E$ to $\dot{V}_{O_2}$.

Although disputed, this might be indicative of cutaneous gas exchange (Farber, 1972). In contrast, the total convective requirement in the newborn tammar wallaby is close to that of the adult, despite a substantial contribution from the skin to gas exchange (MacFarlane and Frappell, 2001). The presence of an underdeveloped lung and superficial capillaries suggest a participation by the skin in gas exchange of the newborn quokka wallaby (Makanya et al., 2007), however, neither skin nor lung gas exchange have been measured in this species.

Pulmonary ventilation in newborn marsupials is characterised by post-inspiratory pauses, brought about by relaxation of the diaphragm against a closed glottis (Farber, 1978). This potentially serves to increase the efficiency of gas exchange in a structurally immature lung as large alveoli and thickened blood-gas barriers require longer times for gas transfer to and from the pulmonary capillaries. Additionally, augmented breaths or sighs

are frequent in marsupial neonates (Farber, 1972; Frappell and MacFarlane, 2006). Sighs have been observed in a number of other newborns (Bartlett, 1971; Flecknoe et al., 2003) and are thought to prevent lung collapse (De Leo et al., 2006).

In marsupials, the transition to the lung as the sole organ of gas exchange has been attributed to larger body mass (and smaller surface area to mass ratio), the increasing metabolic needs of the growing offspring and thus a need for a more efficient gas exchange strategy.

CUTANEOUS GAS EXCHANGE, THE DEVELOPMENT OF THE BREATHING PATTERN AND THE ESTABLISHMENT OF THE CONVECTIVE REQUIREMENT WERE INVESTIGATED IN ONE OF THE SMALLEST NEONATES, THE FAT-TAILED DUNNART (13 MILLIGRAMS TO 1 GRAM).

1.4.2 Why don't newborn marsupials breathe? Possible constraints to lung gas exchange

The immediate transition to air breathing reflects the state of maturation of the entire cardiorespiratory system at birth: lungs, diaphragm and accessory muscles, circulation and the neural control of breathing.

1.4.2.1 The structure of the lungs

The relevant morphological features of the functioning lung are a large gas exchange surface area, a thin air-blood barrier, a surfactant system, a conductive airway tree and a sufficiently developed vascular network.

The lungs of some low-birth weight marsupials, such as the northern native cat (Gemmell and Nelson, 1988), the Tasmanian devil (Tyndale-Biscoe and Janssens, 1988), and the American opossum (Krause and Leeson, 1975) have been described as incredibly under-developed at the time of birth, with only a few simple vascularised air chambers. The quokka wallaby is born with lungs at the canalicular stage of development- more immature than those of any other mammal that have been described to date. These lungs also have a thick air-blood barrier, indicating that some level of cutaneous respiration is likely required to meet metabolic demands.

Other (larger) marsupial newborns such as the tammar wallaby (Runciman et al., 1996), brushtail possum (Gemmell and Nelson, 1988) and bandicoot (Gemmell, 1986) are all born with lungs at the saccular stage of development, and while still underdeveloped by eutherian standards, have much more complex lungs than the low birth weight marsupials.

The formation of true alveoli and subsequent reorganisation of the pulmonary vasculature does not occur until well after birth in the newborn marsupial, around 70 postnatal days in the tammar wallaby (Runciman et al., 1998a). However, the respiratory epithelium appears sufficiently developed to support gas exchange at birth, with both Type-I and -II AECs present and surfactant secreted over the lung surface in a number of marsupials (Krause et al., 1976; Walker and Gemmell, 1983; Miller et al., 2001).

To date, there has been just one study comparing lung structure and function in marsupials, (Szdzuy et al., 2008) with the authors concluding that the immature structure

of the newborn marsupial lung can support only a relatively low metabolic rate at birth. Indeed, the metabolic rate in marsupial newborns is lower than that of similarly sized eutherian newborns and that predicted from allometric relationships. It is equally likely that this is the consequence of being essentially ectothermic in the pouch rather than the presence of O_2 limitation as suggested by these authors. In addition, while the lung might limit O_2 availability, the use of the skin to assist, and in some cases as the sole source of gas exchange, does not lend weight to the idea that they are limited by total O_2 availability.

IN ORDER TO SHED LIGHT ON WHY THE NEWBORN DUNNART RELIES STRICTLY ON THE SKIN FOR GAS EXCHANGE AT BIRTH, THE STRUCTURAL DEVELOPMENT OF THE RESPIRATORY SYSTEM WAS INVESTIGATED DURING THE NEONATAL PERIOD. OF PARTICULAR INTEREST WAS THE STAGE OF LUNG DEVELOPMENT AT BIRTH, INCLUDING THAT OF THE RESPIRATORY EPITHELIUM AND SURFACTANT SYSTEM. IN ADDITION, POSTNATAL DEVELOPMENT OF THE LUNG IS A FOCUS, INCLUDING ASPECTS OF ALVEOLARISATION, THE INCREASE IN LUNG SURFACE AREA AND VOLUME, AND THE CORRELATION OF THESE VARIABLES WITH RESPIRATORY FUNCTION.

1.4.2.2 The diaphragm

In fetal rats and mice, the phrenic nerve makes contact with the primordial diaphragm between 13 and 14 days gestation (Greer et al., 1992). Despite this, the first rhythmic bursts of activity could not be detected until E16-17 (Greer et al., 1992; Allan and Greer,

1997a, 1998). This prompts the question: does the phrenic nerve innervate the diaphragm to provide inspiratory drive in a newborn marsupial born after just 13 days gestation?

THIS THESIS ALSO ASKS: CAN THE LACK OF CO-ORDINATED BREATHING AT BIRTH BE ATTRIBUTED TO A NON-MUSCULARISED DIAPHRAGM AND/OR A LACK OF INNERVATION BY THE PHRENIC NERVE?

1.4.2.3 Respiratory system mechanics

An inadequately developed lung or chest wall could hinder breathing and thus negatively affect gas exchange. Respiratory system compliance has been measured in the newborn opossum (Frappell and Mortola, 1989), tammar wallaby (MacFarlane et al., 2002) and Julia Creek dunnart (Frappell and Mortola, 2000), with values close to those predicted from allometric relationships. This suggests that, rather than constraints from the passive mechanical properties of the respiratory system, constraints from the active dynamic properties of the respiratory system may be inhibitory to effective ventilation. A substantial chest wall distortion during inspiration in the tammar wallaby has been reported as the major mechanical constraint to breathing (MacFarlane et al., 2002).

THIS THESIS ALSO ASKS WHETHER THE LACK OF VENTILATION IN THE NEWBORN FAT-TAILED DUNNART CAN BE ATTRIBUTED TO THE COMPLIANCE OF THE RESPIRATORY SYSTEM.

1.4.2.4 Control of breathing: The development of the hypoxic and hypercapnic responses

Blood gas homeostasis is maintained by the co-ordinated action of central (caudal brainstem) and peripheral (carotid body) chemoreceptors. The carotid bodies are responsible mainly (but not entirely) for O_2 homeostasis, while the brainstem chemoreceptors maintain CO_2 homeostasis. The main effect of chemoreception is the alteration of the level of lung ventilation to maintain constant O_2 and CO_2 levels in the blood. However, as mentioned previously, the typical response of a newborn mammal to hypoxia is a hyperventilation through a hypometabolism rather than a hyperpnoea. While generally blunted in the neonate, the opossum had an unusually large hyperventilatory response to hypoxia during the early neonatal period, which attenuated with age (Farber et al., 1972). The hypometabolic response is unique to hypoxia; hypercapnic conditions generally elicit an increase in breathing in most neonatal mammals, with minimal effects on metabolic rate (Mortola and Lanthier, 1996), again with the exception of the opossum neonate which experienced hypometabolism in response to CO_2 (Farber, 1972).

THIS THESIS ALSO CHARACTERISED THE VENTILATORY AND METABOLIC RESPONSES TO HYPOXIA AND HYPERCAPNIA IN ONE OF THE SMALLEST AND IMMATURE NEWBORN MAMMALS, WITH PARTICULAR EMPHASIS ON HOW THESE RESPONSES CHANGE THROUGH POSTNATAL DEVELOPMENT.

1.5 THESIS OVERVIEW AND HYPOTHESES

With relatively low oxygen demands, a high surface area-to-volume ratio and well vascularised skin observed in other marsupial neonates, we hypothesised that cutaneous gas exchange would dominate in the neonatal fat-tailed dunnart with a body mass of only 13 mg. We hypothesised that cutaneous gas exchange was required due to the under-developed structure of the respiratory system, including the lung parenchyma and diaphragm, in conjunction with a mechanical constraint to breathe. Furthermore, we hypothesised that the immature newborn fat-tailed dunnart would display under-developed chemoreflexes.

Therefore, this thesis intends to document both the functional and structural characteristics of the respiratory system, and how these change through postnatal development in one of the smallest and most immature newborn mammals; the fat-tailed dunnart.

2 THE MARSUPIAL AS A MODEL FOR DEVELOPMENTAL STUDIES

Eutheria and marsupials (metatheria) represent the two major evolutionary lines of mammalian species that diverged from a common pantotherian ancestor 130-180 million years ago (Wakefield and Graves, 2003). The reproductive strategies of marsupials differ markedly from the true placental mammals, as marsupials undergo a brief gestation period and bear almost embryonic young (Tyndale-Biscoe and Janssens, 1988). They are born with precocious forelimbs that are used to climb to the pouch where they undergo most of their basic development, including that of the respiratory system (Baudinette et al., 1988b; Runciman et al., 1996), during a long period of lactation. The fact that marsupials are born under-developed, with the development of their organ systems occurring predominantly in the extrauterine environment (*i.e.* easily accessible to the researcher) makes them an ideal model for developmental studies (Andrewartha et al., 2008). This study will utilise the tammar wallaby (*Macropus eugenii*) and the fat-tailed dunnart (*Sminthopsis crassicaudata*) to examine development of the respiratory system.

2.1 TAMMAR WALLABY, *Macropus eugenii*

The laboratory maintained an outdoor self-sustaining colony of tammar wallabies at La Trobe University, which was occasionally restocked with wild caught animals from Kangaroo Island. The tammar wallaby breeds after the summer solstice, and gives birth to a single young 28 days later weighing 350-400 milligrams (mg) or about 0.01 % of its mother's weight (Tyndale-Biscoe and Janssens, 1988). Parturition is followed by a postpartum oestrus and ovulation. If conception occurs, the embryo develops to a blastocyst of around 100 cells and then enters diapause (Saunders and Hinds, 1997). It is kept in this state as long as the previous offspring continues to suckle. During this period

(known as lactational quiescence) loss or removal of the pouch young induces reactivation of the blastocyst, with birth occurring 26 days later (Merchant, 1979) between January and June (Murphy and Smith, 1970). Removal of suckling pouch young allows births to be timed in experimental animals, with the day of birth defined as postpartum day 0 (P0).

2.2 FAT-TAILED DUNNART, *Sminthopsis crassicaudata*

A Poiley outbred colony of fat-tailed dunnarts was maintained by the laboratory, with animals housed at 22ºC in a harem. The small nocturnal insectivorous marsupial gives birth to a litter size between one and eight after a mere 13.5 days, with the average birth weight being 16 mg (Bennett et al., 1990). In the wild, commencement of breeding coincides with the winter solstice and litters are normally produced between July and February (Morton, 1978). However, alteration of day length with artificial lighting in captivity allows breeding year-round. Breeding harems were therefore housed on a 16L: 8D light cycle. Similarly, the day of birth is also defined as postpartum day 0 (P0).

3 STRUCTURE AND FUNCTION OF THE RESPIRATORY SYSTEM DURING POSTNATAL DEVELOPMENT IN THE FAT-TAILED DUNNART, *SMINTHOPSIS CRASSICAUDATA*.

3.1 INTRODUCTION:

3.1.1 Functional lung development in marsupials

Marsupials, when compared to eutherians, are born after a relatively short gestation. Consequently, much of their growth and development, including that of the lung, occurs in the extrauterine pouch environment (Tyndale-Biscoe and Renfree, 1987; Baudinette et al., 1988b; Runciman et al., 1996).

The fat-tailed dunnart *(Sminthopsis crassicaudata),* a small nocturnal insectivorous marsupial, gives birth to young after 13.5 days gestation with a birth weight of just 13-16 mg, making them one of the smallest newborns (Bennett et al., 1990). Other newborn marsupials, the tammar wallaby, 380 mg (MacFarlane and Frappell, 2001) and the Julia Creek dunnart, 17-20 mg (Frappell and Mortola, 2000), have been shown to undergo various degrees of cutaneous respiration in the neonatal period, as well as a delay in the onset of ventilation in the case of the Julia Creek dunnart. Such dependence on the skin for gas exchange is an indication that the respiratory system is structurally or functionally underdeveloped at the time of birth. In addition, a number of other factors are thought to contribute to the presence of cutaneous respiration in the newborn marsupial. These factors include: the large surface area to volume ratio that is inherent with a small body size (Mortola et al., 1999); the properties of the skin (Randall et al., 1984; Makanya et al., 2007); the low oxygen demands of the pouch young; neural, mechanical or chemical constraints on ventilation; and, the presence of cardiac shunts (Sevcik et al., 1955; Frappell and MacFarlane, 2006).

3.1.2 Structural lung development in marsupials

It is generally considered that the marsupial respiratory system is sufficiently mature at the time of birth to allow simultaneous suckling and breathing (Hill and Hill, 1955). Indeed, in the tammar wallaby, the epiglottis and pharyngeal region are reasonably well developed (Hughes et al., 1989) and the ribs and tracheal rings are composed of hyaline cartilage (Hughes and Hall, 1988). Further, the intercostal muscles are well developed in the newborn wallaby. In contrast, the diaphragm is relatively underdeveloped and is first observed just 3 days prior to the birth of the wallaby neonate. On the day of birth it consists of a thin sheet of muscle which is capable of separating the thoracic and abdominal cavities, but is unlikely to play a large role in respiration (Hughes et al., 1989).

While lung development is a continuous process, 6 well-defined stages have been delineated based on anatomical and histological characteristics: embryonic, pseudoglandular, canalicular, saccular, alveolar, and microvascular maturation (Zeltner and Burri, 1987) as discussed in Chapter 1. Briefly, during the embryonic stage of lung development, the lung buds from the primitive gut and gives rise to two primary bronchial buds, from which arises the respiratory tree (Burri, 1984) with all airway divisions complete by the end of the pseudoglandular period (Bucher and Reid, 1961a). At this point, the airway tubes are lined proximally with glycogen-containing epithelial cells, (Bucher and Reid, 1961b) which begin to flatten out in the canalicular stage so that regions with a thin air-blood barrier begin to appear in preparation for gas exchange (Burri, 1997). Simultaneously, the potential airspaces are being "canalised" by a network of capillaries and differentiation into Type-I or Type-II alveolar epithelial cells (AECs) from

the progenitor Type-II stem cell has commenced (Mercurio and Rhodin, 1976). At the transition from the canalicular stage to the saccular stage of lung development, the peripheral airways end in clusters of widened airspaces called saccules, which represent the future alveolar ducts and alveoli (Boyden, 1977). The capillary arrangement alters such that a capillary bilayer is seen at the intersaccular septa (Burri, 1984). The Type-II AECs have increased in number, size and surfactant stores, while the amount of cytoplasmic glycogen has decreased (Deutsch and Pinar, 2002). During normal alveolarisation, new inter-alveolar walls within the terminal saccules arise from secondary septa; which are derived from the intersaccular walls, or primary septa. As with the primary septa, a double capillary layer is present (Burri, 2006). The secondary septa are characterised by a deposition of elastic fibres at the tip of the secondary septal crest, with elastin critically important for the development of alveoli in the lung (Starcher, 2000). Finally, the capillary networks of the pulmonary parenchyma mature morphologically with the double-capillary network transformed into a single capillary network by thinning of the intervening connective tissue layer in the stage termed microvascular maturation.

The lung tissue in a range of newborn marsupials is comparatively less developed than eutherian mammals at the time of birth. For example, the tammar wallaby (29 days gestation, 370 mg at birth) (Runciman et al., 1996), brushtail possum (17.5 days, 200 mg) (Gemmell and Nelson, 1988) and bandicoot (12.5 days, 180 mg) (Gemmell, 1986) are born with saccular lungs that are inefficient at gas exchange (MacFarlane and Frappell, 2001). Newborns born during the saccular stage have lungs with small surface areas and

thick blood-gas barriers, potentially limiting gas exchange. The low birth weight marsupials, such as the northern native cat (21 days, 18 mg) (Gemmell and Nelson, 1988), the Tasmanian devil (21 days, 18 mg) (Tyndale-Biscoe and Janssens, 1988), and the North American opossum (13 days, 130 mg) (Krause and Leeson, 1975) have been shown to possess further under-developed lungs at the time of birth. In these low birth-weight marsupials, the simple airways end in a number of terminal air chambers, with capillaries on either side of the primary septa.

Showing a similar level of development to the marsupial, the lungs of newly hatched monotremes are structurally underdeveloped when compared to those of eutherian species; with the differences relating to the timing of each developmental stage (Ferner et al., 2009). To date, it is unknown whether the skin contributes to gas exchange in newborn monotremes.

In contrast to other mammals, the quokka wallaby (27 days, 350 mg) is born in the canalicular stage of lung development (Makanya et al., 2007), making the transition to the saccular stage approximately 4 days after birth (Makanya et al., 2001). By the end of the canalicular stage, the air-blood barrier is theoretically thin enough to support gas exchange, although gas exchange is likely to be very inefficient. In fact, human infants born at this stage (17-26 weeks gestation) often do not survive. In addition, the epidermis of the newborn quokka wallaby is poorly developed, has a thickness of 29.97 ± 4.88 μm, and is closely associated superficial capillaries (Makanya et al., 2007). While not measured, the immaturity of the lung and the poorly developed skin, indicate that the

quokka probably undergoes some level of cutaneous respiration in order to meet metabolic demands.

To date, there has been just one study comparing the immature lung structure and impaired lung function in marsupials, (Szdzuy et al., 2008), with the authors concluding that the immature structure of the newborn marsupial lung can support only a relatively low metabolic rate at birth. Szdzuy et al., (2008) examined the lungs of the much larger tammar wallaby and North American opossum, largely dismissing the contribution of cutaneous gas exchange in the animals' ability to meet metabolic demands. These larger species presumably show increased structural and functional development of the respiratory system when compared to the minute newborn fat-tailed dunnart. Therefore, the aim of this study was to use physiological, histological and ultrastructural studies to determine the role of the lungs and skin in gas exchange and whether mechanical and structural immaturity of the respiratory system accounts for the cutaneous gas exchange in the early neonatal period of the developing fat-tailed dunnart.

3.2 MATERIALS & METHODS:

3.2.1 Dual-Chamber Respirometry

Fat-tailed dunnart pouch young were analysed for skin and lung respiration using a closed respirometry system (Frappell et al., 1989) (Figure 3.1). A tiny mask was constructed from a short piece of polyethylene tubing that enclosed the nostrils and mouth. The mask was sealed to the skin using a non-toxic polyether material (Impregum, 3M ESPE) and the mask then inserted through a 10 ml syringe thermoplastic elastomer

gasket (Terumo Medical, Japan) (see Figure 3.1). The masked animal and gasket were inserted into a water-jacketed chamber maintained at a constant temperature of 36 °C (pouch temperature) and 100 % relative humidity; the gasket effectively dividing the chamber into two, a body and head side. Each compartment was sealed by a similar gasket at either end of the chamber. After an equilibration time, the compartments were sealed for a known period of time depending on the mass and, hence, metabolic rate of the animal (5 – 15 minutes). After which, the compartments were flushed individually with a known flow (20-25 $ml.min^{-1}$), and the gas from each compartment passed through Nafion® tubing (dead space 0.6 ml) surrounded by a molecular sieve desiccant (crystalline metal aluminosilicate zeolite) prior to being analysed for fractional concentrations of O_2 and CO_2 by gas analysers (ADInstruments, ML205). The output of each gas analyser was recorded at 200 Hz (Chart 4.2 and PowerLab, ADInstruments). The rates of oxygen consumption ($\dot{V}_{O_2}$) and carbon dioxide production ($\dot{V}_{CO_2}$) were calculated for each compartment (*i.e.* that across the lungs and body, with the sum of both being the total $\dot{V}_{O_2}$) from the time integral of the gas concentration curves multiplied by the flow and the reciprocal of the time for which each compartment was sealed (Frappell and Mortola, 2000). Gaseous metabolism was measured in animals ranging from P0 (0 days postpartum) (13mg) to P44 (~1.2 g).

Ventilation ($\dot{V}_E$) was measured when the chamber was sealed via a pressure transducer (Spirometer ML141, ADInstruments) connected to the head compartment, and the pressure oscillations were acquired at 200 Hz (Chart 4.2 and PowerLab, ADInstruments). The pressure oscillations associated with breathing were calibrated for volume by

repeated injection and withdrawal of 2 µl of air. The stability of the pressure change with each injection was also used to indicate the integrity of the seal for the chamber. Ventilation was analysed in animals at P0, P5, P12 and P23, with at least 50 consecutive breaths analysed for tidal volume (V_T), frequency ($f = 60/T_{TOT}$), and ventilation ($\dot{V}_E = V_T \times f$). All recorded breaths (not necessarily consecutive) were analysed in P0 animals as a stable ventilatory rhythm was not exhibited. Animals that did not show any discernable breaths were common in this age group and were therefore not included in the analysis of ventilatory components.

3.2.2 Mechanics of the respiratory system

The respirometry chamber described above was modified to allow pressure-volume (P-V) curves to be constructed for P0 and P8 fat-tailed dunnarts. A vacuum was connected to the body side of the chamber and negative pressures applied to the body, corresponding to positive transpulmonary pressures, from 0 to 25 cmH_2O in 5 cmH_2O steps during inflation and deflation, following conditioning of the lung by two inflations to 20 cmH_2O. These negative body surface pressures were calibrated with a water manometer and controlled by variance of the size of the leak that had been incorporated into the chamber. The corresponding change in pressure across the lung was measured using a pressure transducer, calibrated for volume using injection and withdrawal of 2 µl of air. The passive compliance of the respiratory system (C_{rs}) was determined from the change in lung volume (ΔV) associated with the corresponding change in pressure (ΔP) ($C_{rs} = \Delta V/\Delta P$) on the inflation limb at 15 cmH_2O.

Figure 3.1 Schematic of the dual-chamber respirometry apparatus.

A mask (attached to the gasket) was sealed over the face of the animal, and the animal placed into a chamber (pouch temperature, 36 °C, and 100 % relative humidity), separating the chamber into body and head sides. Following an equilibration time, the compartments were sealed for between 5 and 15 min and ventilation measured during this time. The compartments were then flushed (20-25 $ml.min^{-1}$) and the gas from each was analysed, allowing rates of oxygen consumption ($\dot{V}o_2$) and carbon dioxide production ($\dot{V}co_2$) to be calculated.

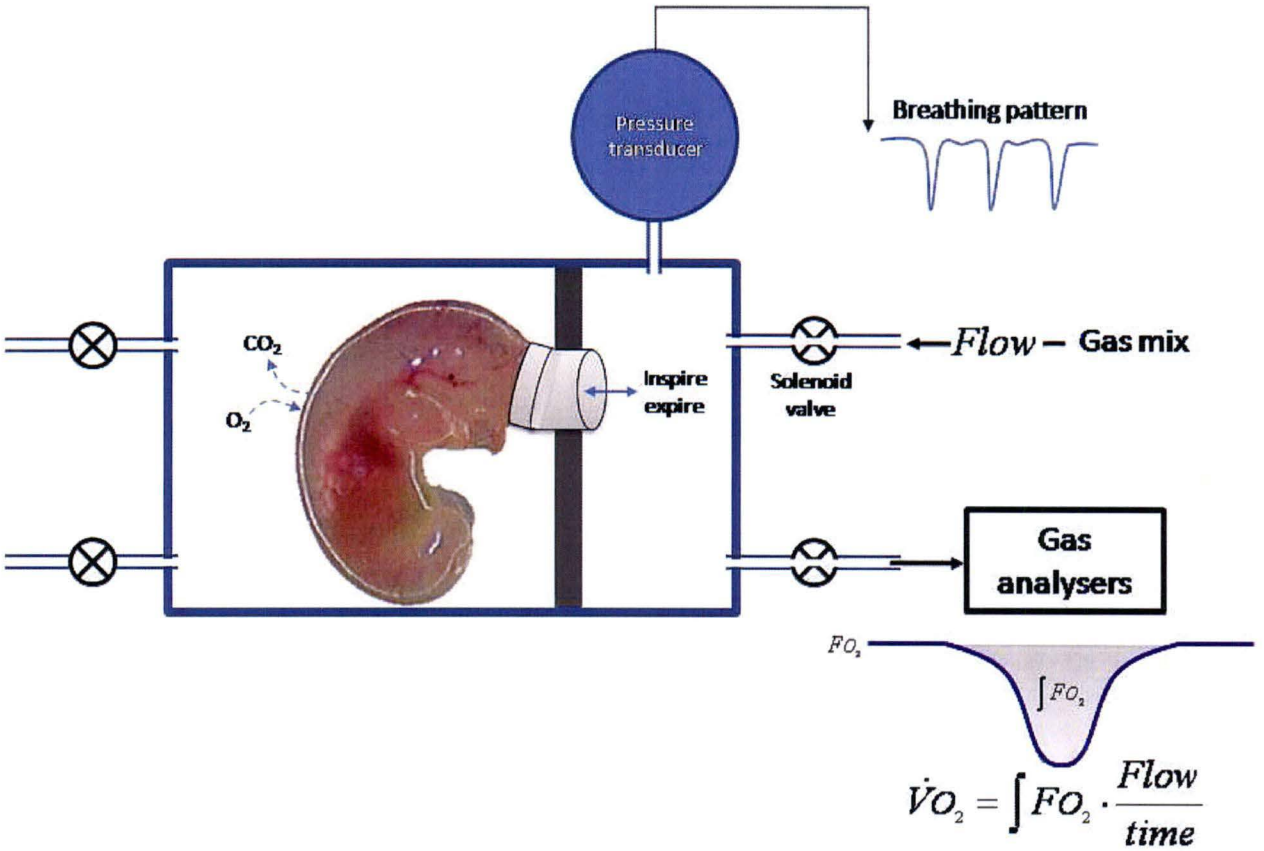
Pressure transducer
Breathing pattern
CO_2
O_2
Inspire expire
Solenoid valve
Flow – Gas mix
Gas analysers
FO_2
$\int FO_2$
$\dot{V}O_2 = \int FO_2 \cdot \frac{Flow}{time}$

3.2.3 Tissue Fixation

A minimum of three pouch young, from at least two different litters were collected at numerous ages ranging from the time of birth to P125. Pouch young in the early postnatal stages had the whole torso fixed, while the lungs were isolated in animals older than P20 prior to immersion fixation. Samples were fixed using 4 % paraformaldehyde in 0.1 M phosphate buffer for 24 hours at 4 °C.

3.2.4 Light Microscopy

Following fixation with paraformaldehyde, tissues were transferred to Zamboni's solution as a secondary fixative. The tissue was then dehydrated using an alcohol gradient, and embedded in paraffin wax (Histokinette 2000). Tissue blocks were serially sectioned at 5 μm and the subsequent slides baked. Baked slides were de-waxed with xylene (3 x 5 min) and rehydrated through a graded series of ethanol and washed in distilled water prior to staining for elastin using a modified Weigert's resorcin fuchsin method, including Hart's recommendations. Sections were counter-stained with 0.25 % tartrazine in saturated picric acid, dehydrated, mounted and viewed under a light microscope. Images were captured using the 20x objective, and the saved images were de-identified so as the density of secondary septal crests (a measure of alveolarisation) could be determined using a point counting method, without knowledge of the age of the neonate. Using this method, a point grid was applied to the captured image and the number of times the point fell on an elastin containing crest was expressed as a proportion of the number of times the point grid fell on lung parenchyma for each field

of view. A minimum of 3 captured images per animal were counted in all animals whose lungs were large enough to allow for 3 fields of view at 200x magnification.

3.2.5 Electron Microscopy

Following paraformaldehyde fixation, the tissue was cut into small cubes of approximately 1-2 mm^3 and then immersion-fixed in 4 % glutaraldehyde overnight at 4 °C. The tissue was processed for electron microscopy using a Pelco Biowave Microwave Processor. Tissue was washed in 0.1 M cacodylate buffer (5 min) and incubated in 4 % osmium tetroxide (4 x 2 min OsO_4, in 0.2 M cacodylate buffer with a vacuum and microwave set at 80 W) prior to undergoing a series of graded ethanol/acetone washes (45 sec each, 250 W). Following this, the lung tissue was embedded in epoxy resin (Procure 812) with a 3 min 1:1 acetone: procure, and two 3 min 100 % procure steps in the resin infiltration, all with the aid of a vacuum (250 W). The resin was then polymerised (90 min at 650 W) prior to the cutting of ultra-thin sections (70–90 nm) with a diamond knife. Sections were mounted on mesh copper grids, and stained with uranyl acetate and lead citrate. Tissue ultrastructure was viewed using a transmission electron microscope (TEM). Alveolar epithelial cells were identified (using a strict set of morphological criteria described in Chapter 1, based on the ultrastructural features of each cell type) and counted.

3.2.6 Immunohistochemistry

P0 fat-tailed dunnarts were fixed following the method outlined above for light microscopy. Paraffin sections were deparaffinised and rehydrated. Slides were

microwaved in 0.01 M sodium citrate buffer (pH 6.0) at 600 W for 5 minutes, and once cooled, were treated with 1 % hydrogen peroxide in methanol containing 0.4 % Triton X-100 for 45 minutes. Following three 5 minute PBS washes, sections were blocked with 1 % bovine serum albumin in 0.4 % Triton X-100/PBS for 1 hour, and incubated overnight at room temperature with anti-mouse neurofilament 2H3 primary antibody (1:100) (Hybridoma Bank). After three 10 minute PBS washes, tissues were incubated with goat anti-mouse IgG secondary antibody for 1 hour, washed again in PBS and incubated in an avidin biotinylated peroxidise solution (Vectastain ABC kit) for a further hour. After PBS washes, tissues were incubated with 3,3-diaminobenzidine tetrahydrochloride (DAB) with ammonium nickel sulphate for 5-15 minutes at room temperature, and underwent thorough washes and counter staining with Cresyl violet prior to dehydration and Entellan mounting. Positive control was provided with sectioned rat tissue which is known to express neurofilament 2H3 and negative control by omission of primary antibody.

3.2.7 Statistics

Significant changes in variables across developmental time-points were assessed by one way analysis of variance (ANOVA) with Tukey post hoc comparisons. Volume differences between P0 and P8 (P-V curve) were assessed using a student T-test at each pressure. Significance was considered at $P < 0.05$ for all tests.

3.3 RESULTS:

3.3.1 Functional development of the dunnart respiratory system

At P0 no discernable ventilatory pattern was observed in 2/3 of neonates (N=12), with any small deflections in pressure being accompanied by gross body movements (Figure 3.2). In the one-third of P0 neonates where a more rhythmic pattern was detected, the frequency (55 ± 4 breaths.min^{-1} within an episode of breathing) and tidal volume (0.11 ± 0.08 µl) were low (Figure 3.4) and this "breathing" was often accompanied by extended periods of apnoea (in excess of 15 minutes). By P5, a regular breathing pattern was established, characterised by a post-inspiratory pause (also present in the P0 "breaths") and frequent augmented breaths or sighs, as reported in other studies (Frappell and MacFarlane, 2006). However, it should be noted that periods of respiratory instability were common in this age group (Figure 3.2). P12 appears to be a period of transition from the immature breathing pattern with the post-inspiratory pauses to the adult breathing pattern which is detected in the P23 neonates (Figure 3.3). The two extremes of the P12 breathing patterns are shown in Figure 3.3, however it should be noted that some intermediate patterns were observed with the consequence of variability in the breathing pattern of the P12 neonates. Metabolic rate and pulmonary minute ventilation increased with age; with increases in both tidal volume and breathing frequency (Figure 3.4).

Given the lack of ventilation in the newborn fat-tailed dunnart, it is not surprising that the newborn is almost solely reliant upon its skin for gas exchange (Figure 3.5). While

cutaneous respiration constitutes almost 100 % of total gas exchange at birth, the rate of cutaneous oxygen consumption diminishes as the newborn develops, decreasing markedly as the animal approaches 0.2 grams (~25 postnatal days) and barely contributes by a body mass of 1 gram (~40 postnatal days). A similar trend exists for the rate of cutaneous exchange of CO_2.

The P-V curves of the respiratory system at P0 and P8 (Figure 3.6) demonstrate a hysteresis, with lung volume being maintained above resting volume after deflation back to 0 cmH_20. Worth noting is that positive transpulmonary pressures (and resultant lung inflation) led to a cessation of breathing in the P8 animals. In fact, at pressures greater than 10 cmH_20 breathing was slow to return and in some cases did not return until deflation pressure was less than 5 cmH_2O. The cessation of breathing following lung inflation is indicative of the presence of the Hering-Bruer inflation reflex. The compliance of the respiratory system averaged 2.5 ± 0.6 $ml.kg^{-1}.cmH_2O^{-1}$ at P0 and 1.8 ± 0.4 $ml.kg^{-1}.cmH_2O^{-1}$ at P8, demonstrating a highly compliant lung at birth.

3.3.2 Structural development of the dunnart respiratory system

The diaphragm is present at P0, though only a few cells thick. Immunohistochemistry for neurofilament demonstrated that the phrenic nerve had made contact with the diaphragm via the characteristic bilateral entry points (Figure 3.7) described by (Laskowski and Owens, 1994).

At P0 the lungs were characterised by a few large tubular like structures, perhaps reminiscent of primitive airways that one would expect to be present in the early

canalicular stage (see Figure 3.8). The septal walls dividing these primitive airways were thick and separated by a double capillary network (Figure 3.9). Despite the primitive structure of the lung parenchyma, the epithelial lining of these airways was surprisingly mature. Most of the epithelial cells exhibited characteristics of mature Type-I or –II AECs (Figure 3.10), with less than 7 % of the cells resembling an undifferentiated alveolar epithelial precursor cell (Figure 3.11). The presence of Type-I AECs was indicated by relatively thickened (when compared to a mature Type-I AEC) cytoplasmic extensions that projected from the perinuclear cytoplasm, many of which were thick enough to contain organelles such as mitochondria and rough endoplasmic reticulum.

Interestingly, many of these cells demonstrated only a single cytoplasmic projection, with the lateral border of the other side of the cell being closely flanked by the nuclear region of the adjacent epithelial cell (as seen in Figure 3.10); in most cases this was a Type-II or undifferentiated AEC, but occasionally, this was the perinuclear region of another asymmetrical Type-I AEC with the cytoplasm extending on only one side. Residual cytoplasmic glycogen was present in many of the cells displaying characteristics of Type-I and –II AECs, highlighting their recent state of differentiation from the undifferentiated phenotype. Type-II AECs were demarcated by the presence of well developed lamellar bodies, some of which had recently secreted contents into the airspace (Figure 3.10), which were present as tight coils or had begun to form tubular myelin.

Figure 3.2 The breathing pattern of fat-tailed dunnart neonates at 0 and 5 days postpartum (P).

At P0 no discernable ventilatory pattern was observed in 67 % of the neonates (top). Rather, any small deflections in pressure were accompanied by gross body movements as indicated by the arrows. In the P0 neonates where a ventilatory pattern was detected, tidal volume and frequency are low. By P5, a continuous regular breathing pattern was established, consisting of the characteristic post inspiratory pause, however, it should be noted that periods of respiratory instability (bottom) were common. Inspiration is upwards.

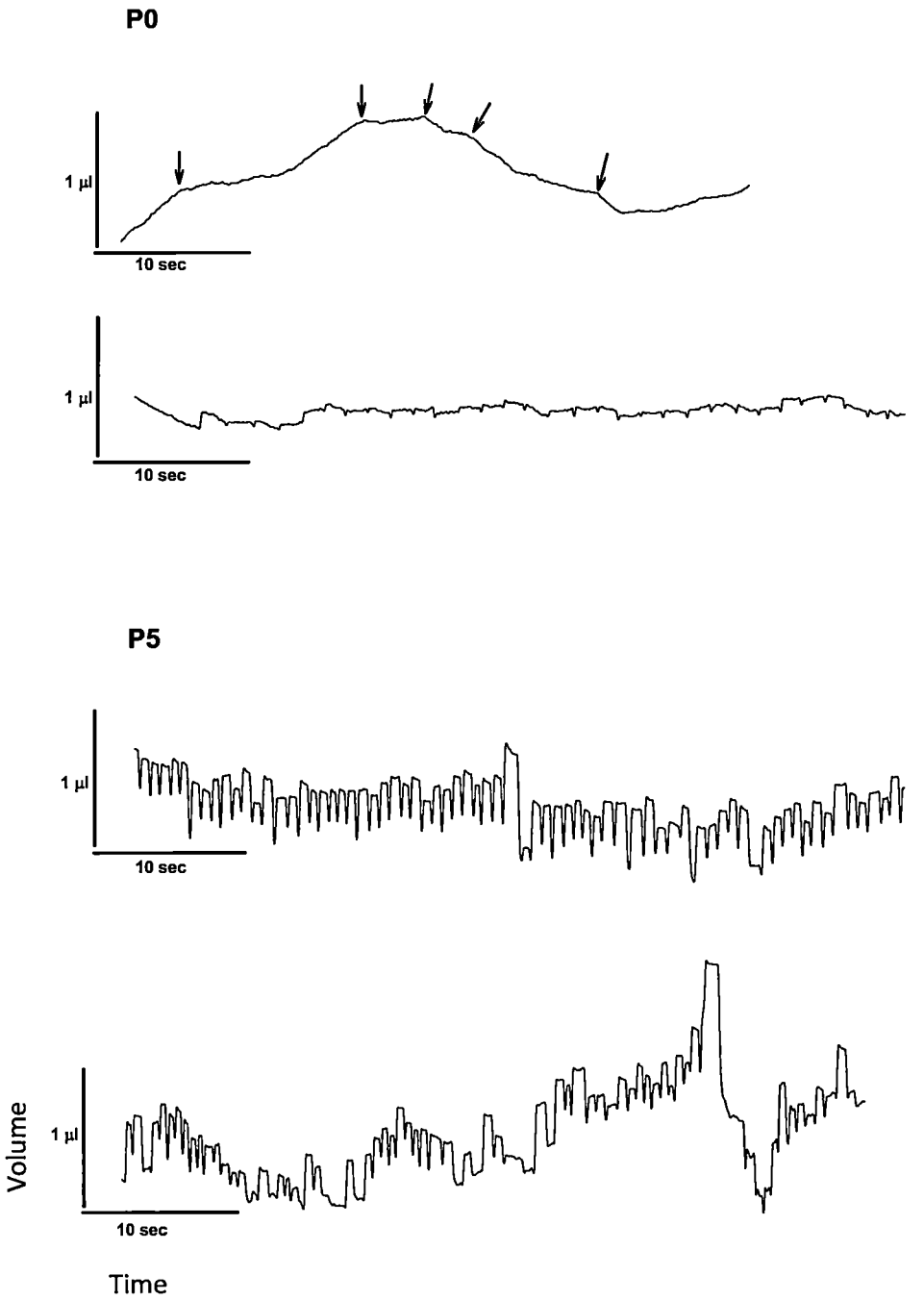
P0
1 µl
10 sec
1 µl
10 sec
P5
1 µl
10 sec
Volume
1 µl
10 sec
Time

Figure 3.3 The breathing pattern of fat-tailed dunnart neonates at 12 and 23 days postpartum (P).

Neonates which were 12 days postpartum exhibited both immature and adult breathing patterns (top) indicating that P12 appears to be around the transition from the immature pattern with the post inspiratory pauses to the adult breathing pattern which was always detected in the P23 neonates (bottom). The two extremes of the P12 breathing patterns are shown here in the top panel, however it should be noted that some intermediate patterns were observed. Inspiration is upwards.

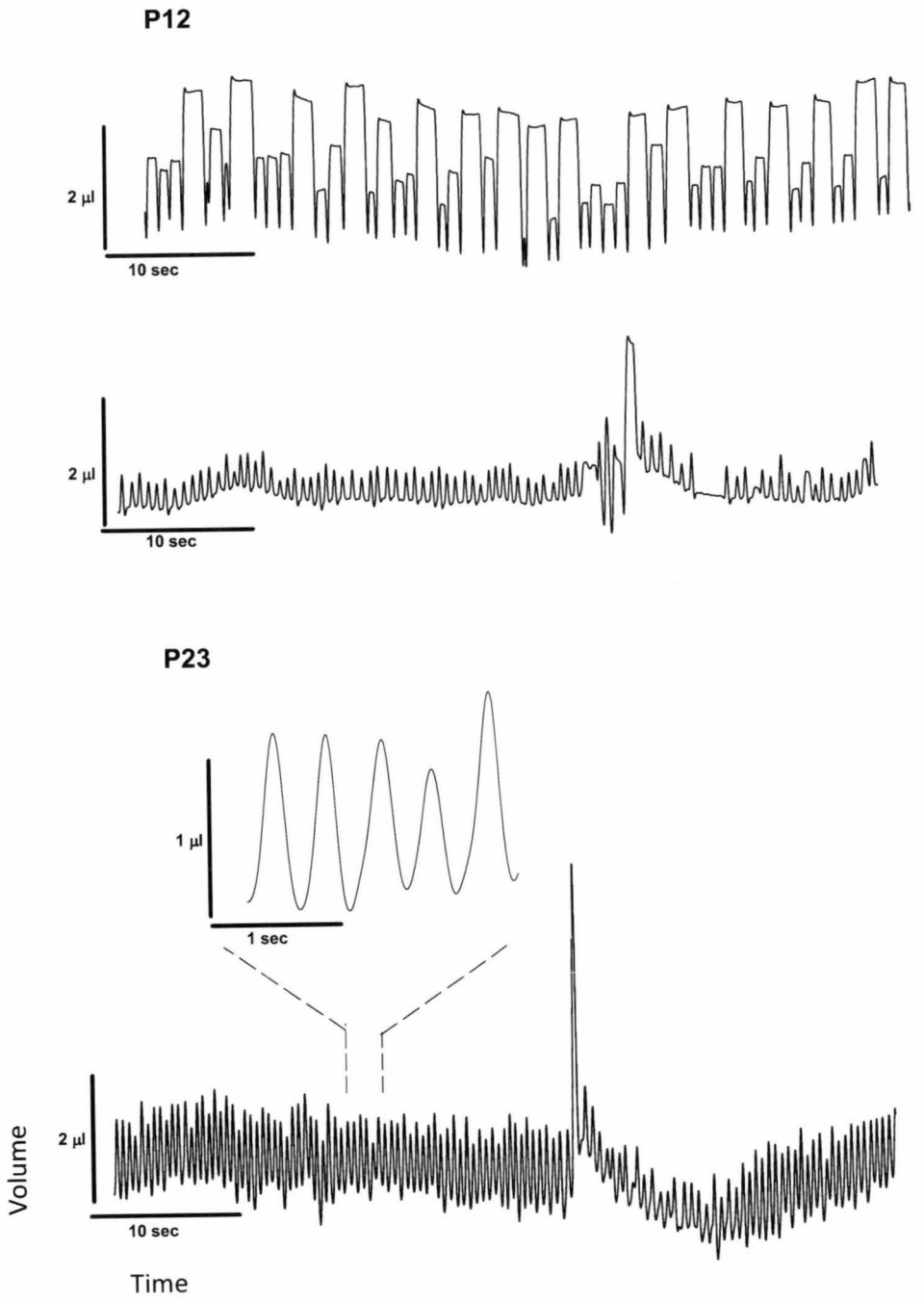
P12
2 µl
10 sec
2 µl
10 sec
P23
1 µl
1 sec
2 µl
10 sec
Volume
Time

Figure 3.4 Ventilation and metabolism in the neonatal fat-tailed dunnart.

During development, the newborn dunnart undergoes an increase in the rate of oxygen consumption and pulmonary minute ventilation ($\dot{V}_E$). The increase in $\dot{V}_E$ can be attributed to an increase in both of its components, breathing frequency and tidal volume. P0 is unfilled, as a reminder that breathing was only observed in 33 % of newborns for a period of time. N = 12, 7, 9 and 9 for P0, 5, 12 and 23 respectively. Values are means ± 1 S.E.M. Values indicated by a different letter are significantly different from each other.

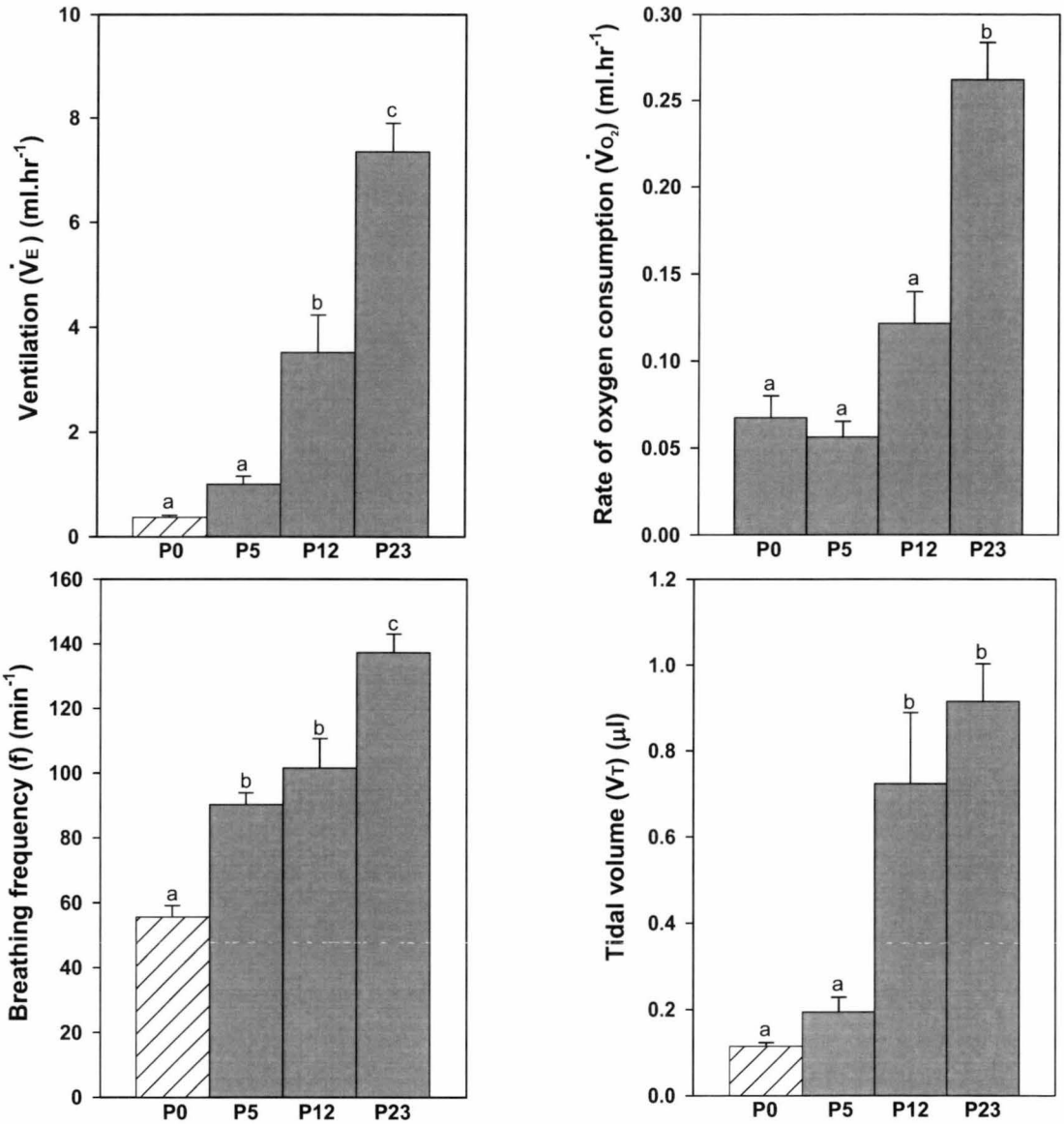
Ventilation ($\dot{V}_E$) (ml.hr^{-1})
10
8
6
4
2
0
a
a
b
c
P0
P5
P12
P23
Rate of oxygen consumption ($\dot{V}O_2$) (ml.hr^{-1})
0.30
0.25
0.20
0.15
0.10
0.05
0.00
a
a
a
b
P0
P5
P12
P23
Breathing frequency (f) (min^{-1})
160
140
120
100
80
60
40
20
0
a
b
b
c
P0
P5
P12
P23
Tidal volume (V_T) (µl)
1.2
1.0
0.8
0.6
0.4
0.2
0.0
a
a
b
b
P0
P5
P12
P23

Figure 3.5 Cutaneous gas exchange in the postnatal fat-tailed dunnart.

Exchange of oxygen (closed circles) and carbon dioxide (open circles) across the skin in dunnart pouch young is expressed as a percentage of the total rate of oxygen consumption or carbon dioxide production respectively, presented as a function of mass. Indicative ages are shown in postpartum (P) days.

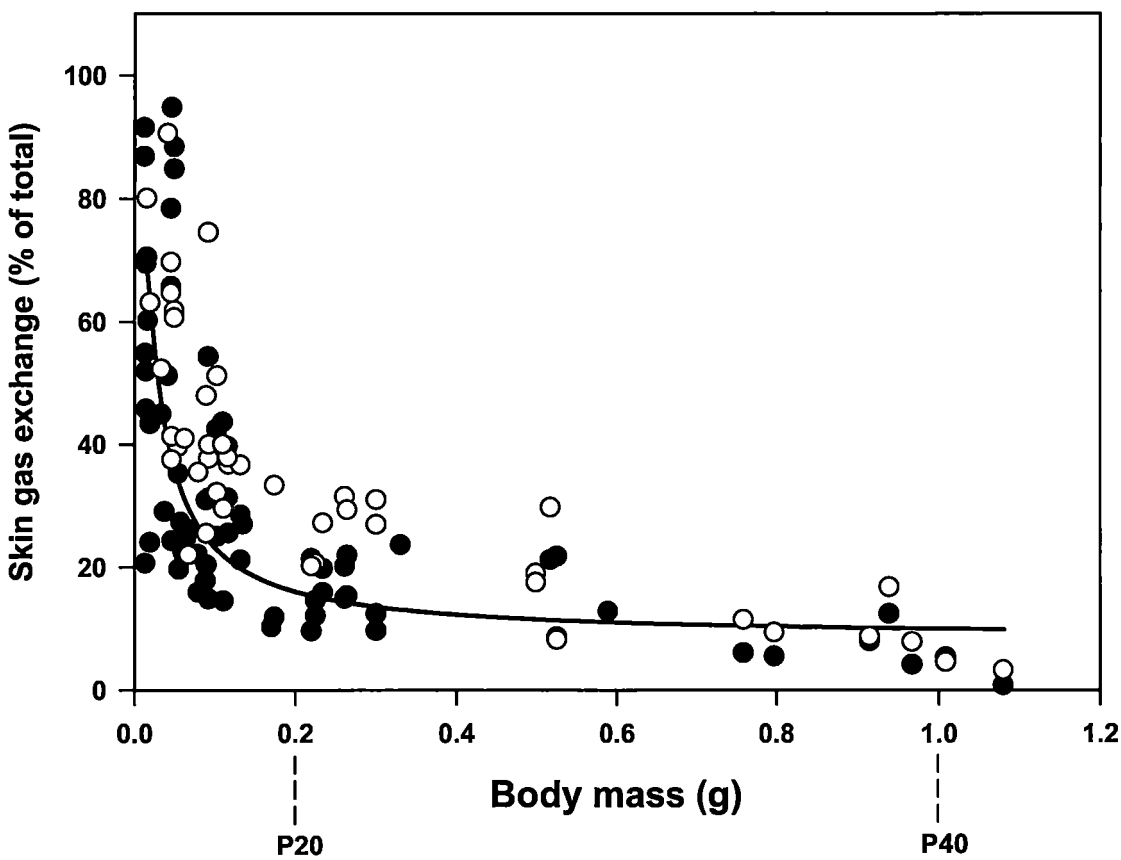

Figure 3.6 Pressure-volume (P-V) curve of the respiratory system in the fat-tailed dunnart on the day of birth (P0) and 8 days postpartum (P8).

Volume (V) is that above resting lung volume when airway pressure is zero 0 and is normalised by the mass of the animal. The P-V curve demonstrates a hysteresis, with lung volume being maintained above resting volume after deflation. Arrows indicate inflation/deflation. Symbols are mean values and error bars represent 1 S.E.M. N=5 for both ages. * represents significant difference between P0 and P8 at that given pressure.

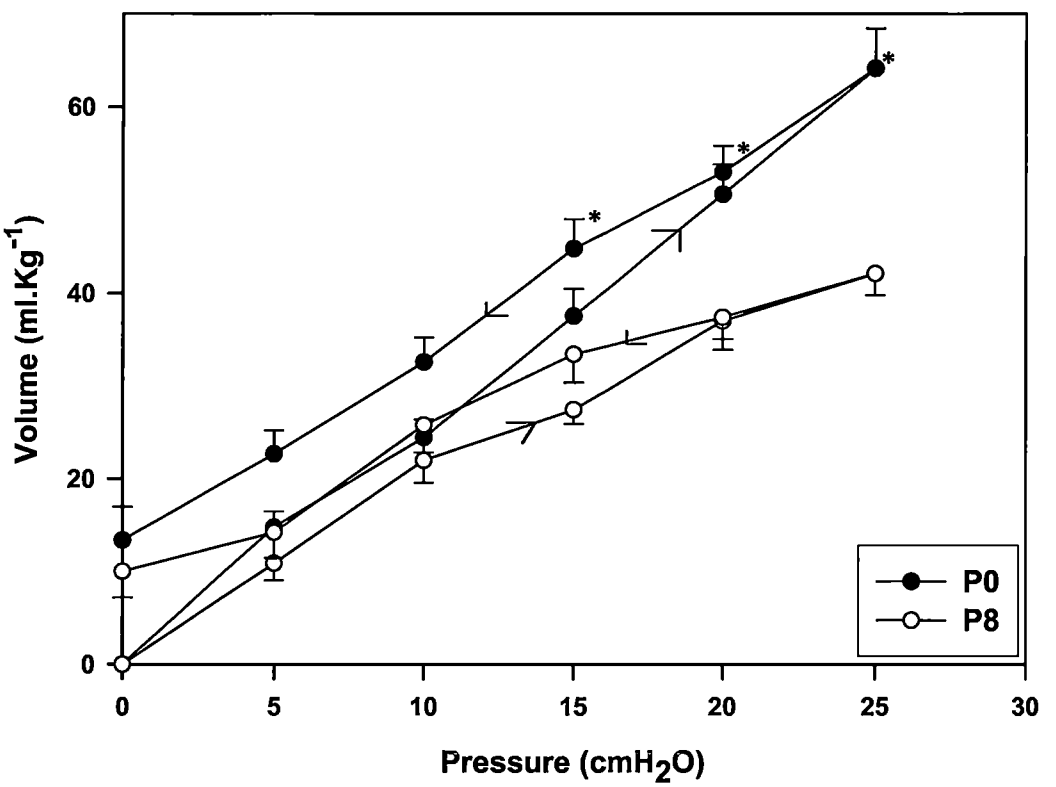
Volume (ml.Kg-1)
60
40
20
0
0
5
10
15
20
25
30
Pressure (cmH2O)
P0
P8
*
*
*
*

By P4, the lung had become more compartmentalised (Figure 3.8) and the number of lamellar bodies in each Type-II AEC appeared to double (from 4 lamellar bodies per cross-sectional area to 8 lamellar bodies per cross-sectional area, however it is important to note that slight increases in lamellar body size with increased development may have affected the chance of counting them). Furthermore, the airways now held increased supplies of secreted surfactant. Interestingly, Type-II AECs were commonly seen in pairs, triplets and quadruplets at this age; that is, they were seldom interspersed by other AEC types, indicating that these cells may be the product of recent proliferation. In contrast, the cytoplasmic extensions of Type-I AECs had begun to thin, however, many Type-I AECs still exhibited uni-lateral projections.

At P10, lung morphology remained relatively similar to that at P4. Noteworthy, however, was the apparent flattening of Type-II AECs; rather than being rounded and protruding into the airspace, the nucleus of many of these cells had become flattened. Tight junctions close to the perinuclear lateral membranes of these cells and the subsequent lack of cytoplasmic extensions precluded these cells from be classified as intermediate cells.

Between P27 and P45, the interstitium began to thin and the parenchymal structure appeared to increase slightly in complexity; the lung no longer appeared as large open sacs, with more complex structures being identified. By P45 many of the capillaries were positioned in close proximity to the overlying epithelial cells on both sides of an often thickened interstitium (that is, these capillaries were separated by other cells and

connective tissue). This positioning indicated the presence of a double capillary network (see Figure 3.9A). The double capillary network remained until at least P70, after which, septa with a single capillary layer became more common. Initially, these capillary networks were often placed to one side of what appeared to be a now thickened septa, however, by P100, the single capillary network had become centrally positioned (Figure 3.9B). Type-I and –II AECs had taken on a completely mature phenotype and were the most common cells present, with less than 4% being undifferentiated or intermediate in nature. Despite this, the proportion of Type-I and –II AECs fluctuated between 70 and 100 days, with Type-I AECs being the predominant cell type at 70 days but decreasing in proportion by 100 days of postnatal life (Figure 3.11).

No secondary septal crests, characterised by the presence of tightly bundled elastin at the tip of the new protrusion from the primary septa (Figure 3.12), were observed in the lungs of neonatal dunnarts under P45; indicating that no alveolarisation is taking place prior to this time. At P45, the first secondary septal crests were seen (Figure 3.13), which interestingly corresponds to the time when the double capillary network was observed. The secondary septal crest density increased with postnatal age until a peak was reached at P100 (13.02 ± 2.37 %), suggestive that this as the most active time of alveolarisation. By P125, the period of bulk alveolarisation is assumed to be drawing to a close and alveoli are now being formed at a slower pace, with the septal crest density at 4.95 ± 2.16 % (Figure 3.13).

Figure 3.7 Contact of the phrenic nerve with the diaphragm in the P0 fat-tailed dunnart.

Shown is the diaphragm (D) separating the lungs (Lu) in the thoracic cavity from the liver (Li) in the abdominal cavity in the P0 fat-tailed dunnart. Immunohistochemistry confirms the presence of the phrenic nerve (Ph), which has made contact with the diaphragm in the characteristic bifurcated pattern.

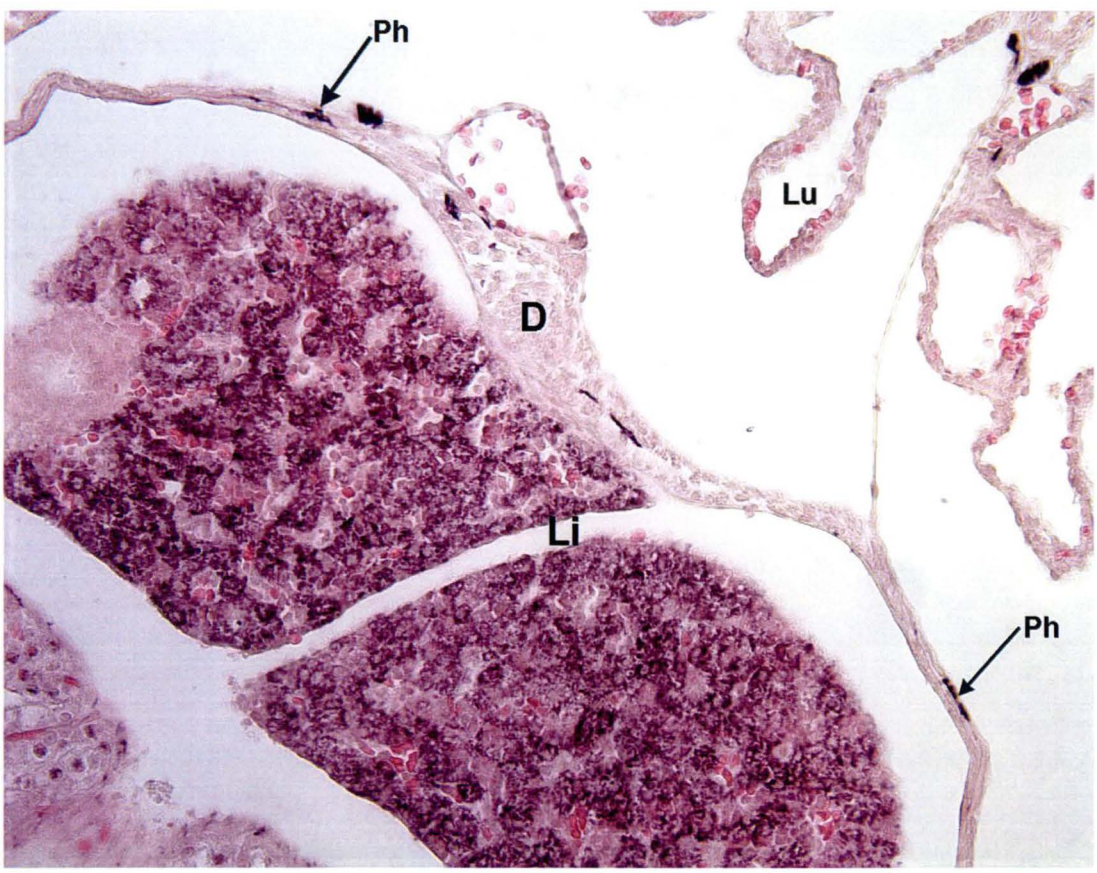
Ph
Lu
D
Li
Ph

Figure 3.8 Light micrographs demonstrate the changes in lung architecture during development in the fat tailed dunnart.

A reduction in the size of the saccules, and an increase in the surface area available for gas exchange is achieved by septation. Sections were stained for elastin (black/brown) using a modified Weigert's resorcin fuchsin method and counterstained with 0.25 % tartrazine in saturated picric acid.

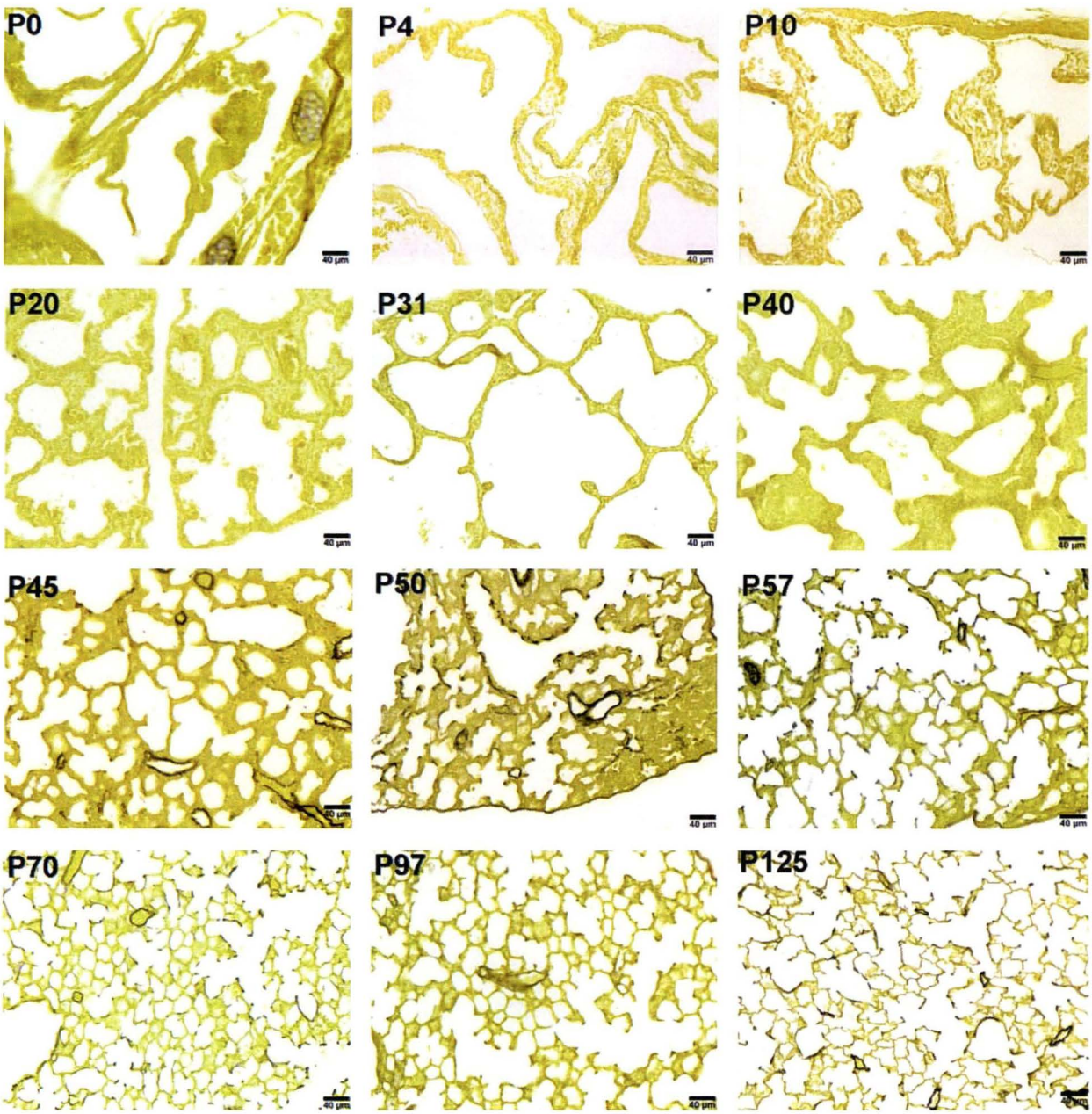
P0
P4
P10
P20
P31
P40
P45
P50
P57
P70
P97
P125

Figure 3.9 The transition from the double capillary to single capillary vasculature in the lung of the fat-tailed dunnart.

Up until at least P70 (shown in A) the capillaries (c) were observed on both sides of a thickened interstitium separated by other cells and connective tissue as a double capillary network. By P100 (B) the single capillary network had formed and was generally centrally positioned.

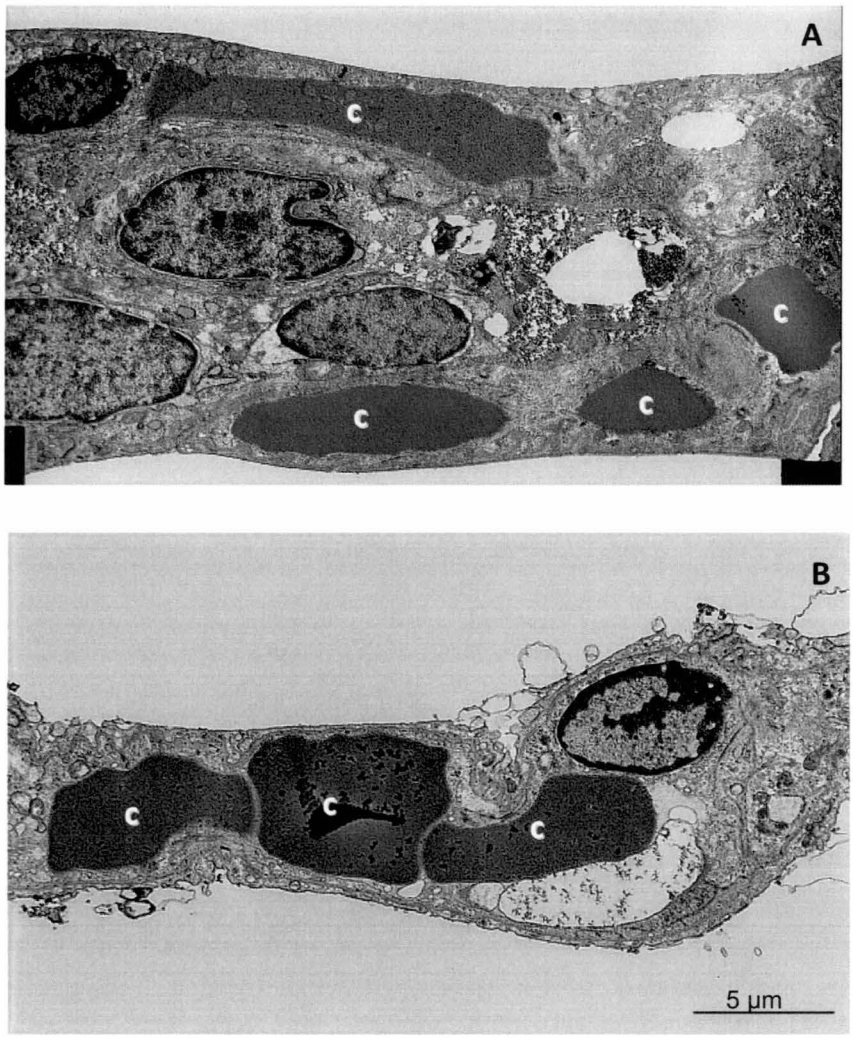
A
C
C
C
C
B
C
C
C
5 µm

Figure 3.10 Alveolar Epithelial Cells present on the day of birth in the fat-tailed dunnart.

Both Type-I AECs (TI) and Type-II AECs (TII) are present on the first day of life in the fat-tailed dunnart. The Type-I AEC is characterised by its lack of perinuclear cytoplasm and elongated cytoplasmic extension, seen over the top of a blood vessel (BV) here. The Type-II AEC is characterised by microvilli and lamellar bodies. Surfactant coils (S) can be seen in the airspaces (A) overlying each of the cell types.

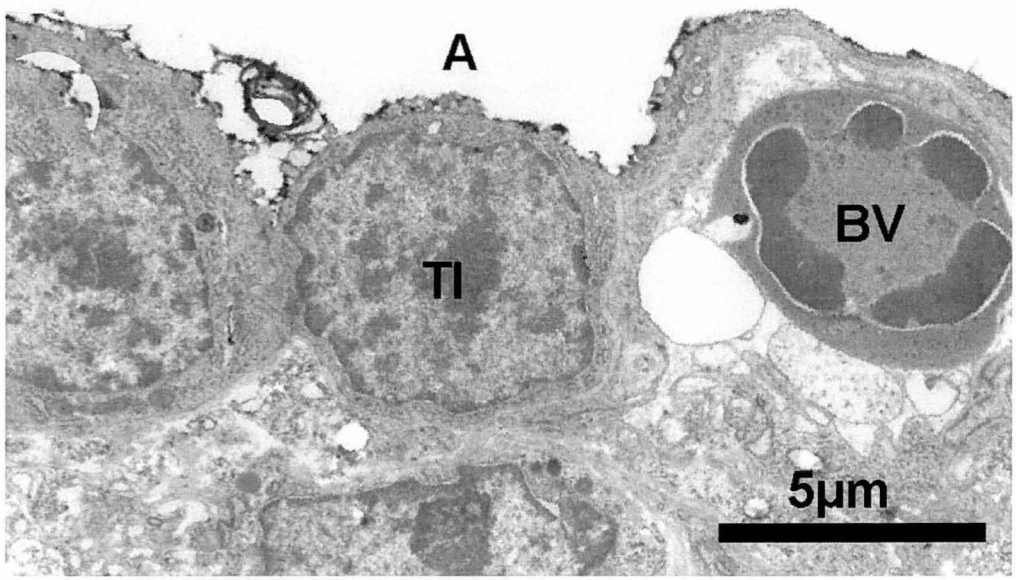
A
TI
BV
5µm

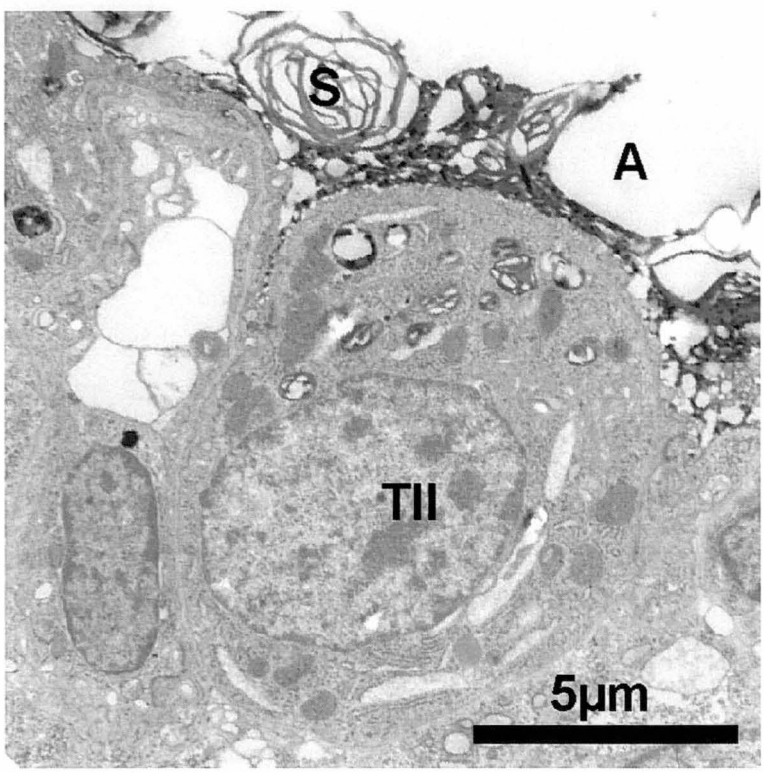
S
A
TII
5µm

Figure 3.11 Differentiation of Alveolar Epithelial Cells in the lung of the developing fat-tailed dunnart.

Shown are the postnatal changes to the proportion of alveolar epithelial cells. At birth, less than 7 % of the AECs are undifferentiated and 14 % are intermediate in appearance. The proportion of Type-II AECs decrease through development while the proportion of Type-I AECs increases. Despite this an interesting fluctuation occurs between P70 and P100. Symbol legend indicates cell type. Error bars represent 1 S.E.M. Values indicated by a different letter are significantly different from each other.

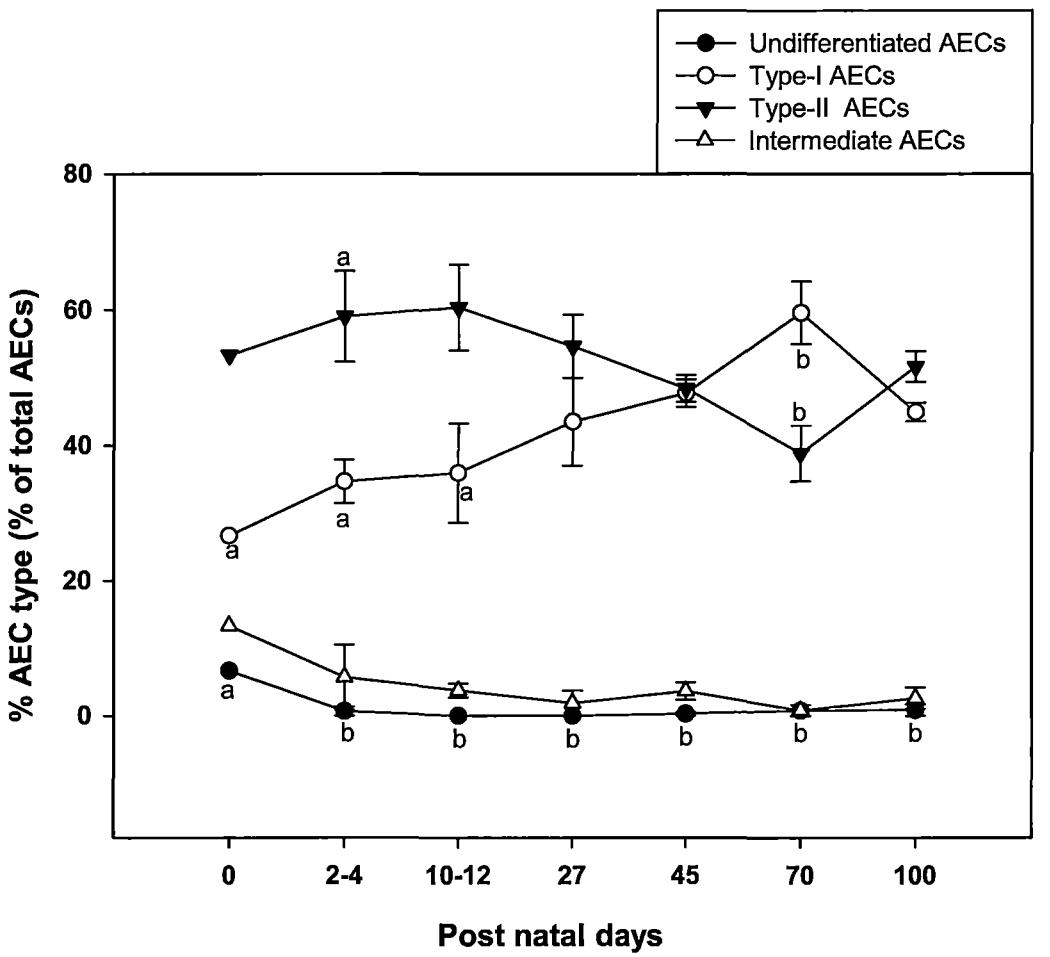
Undifferentiated AECs
Type-I AECs
Type-II AECs
Intermediate AECs
% AEC type (% of total AECs)
80
60
40
20
0
0
2-4
10-12
27
45
70
100
Post natal days

Figure 3.12 Secondary septa determined by elastin deposition.

Shown is a section stained for elastin (black/brown) using a modified Weigert's resorcin fuchsin method and counterstained with 0.25 % tartrazine in saturated picric acid. Secondary septa were determined by protrusions from the intersaccular walls with elastin deposition at the tip (black/brown).

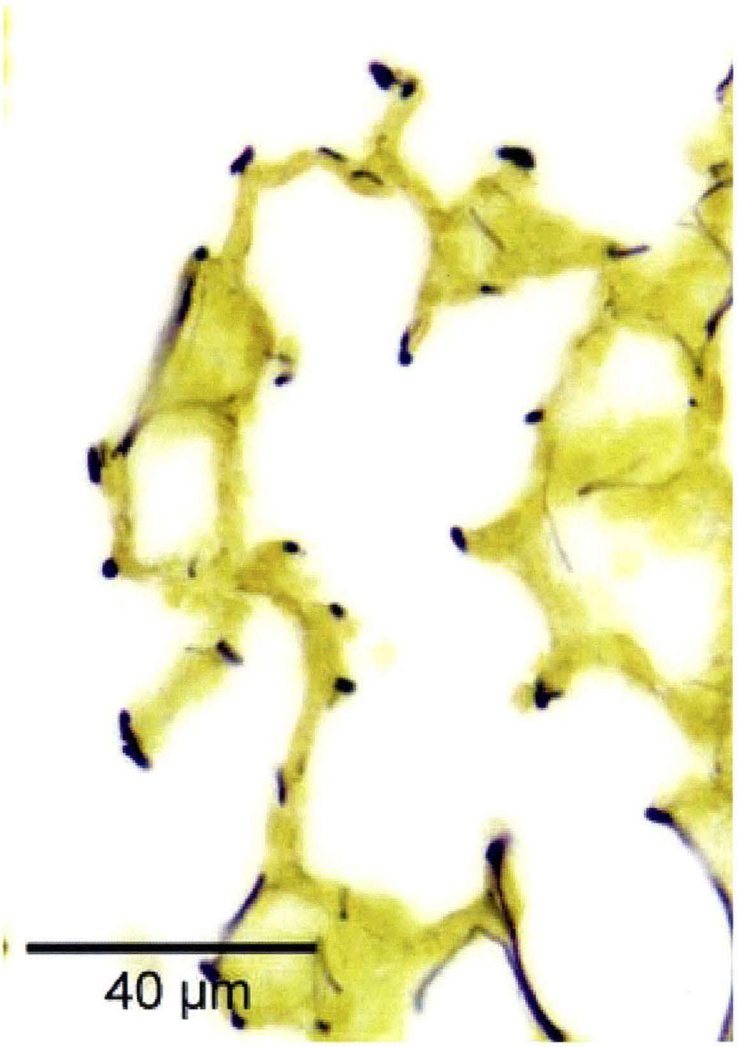
40 µm

Figure 3.13 Secondary septal crest development in the fat-tailed dunnart.

Shown is the volume density of secondary septa in the lung parenchyma plotted as a function of post natal days. The first secondary septa were not observed until P45, indicating that alveolarisation is not occurring prior to this time. A peak is reached between 70 and 100 post natal days suggesting that this is an important time in bulk alveolarisation. Values are means ± 1 S.E.M. Values indicated by a different letter are significantly different from each other.

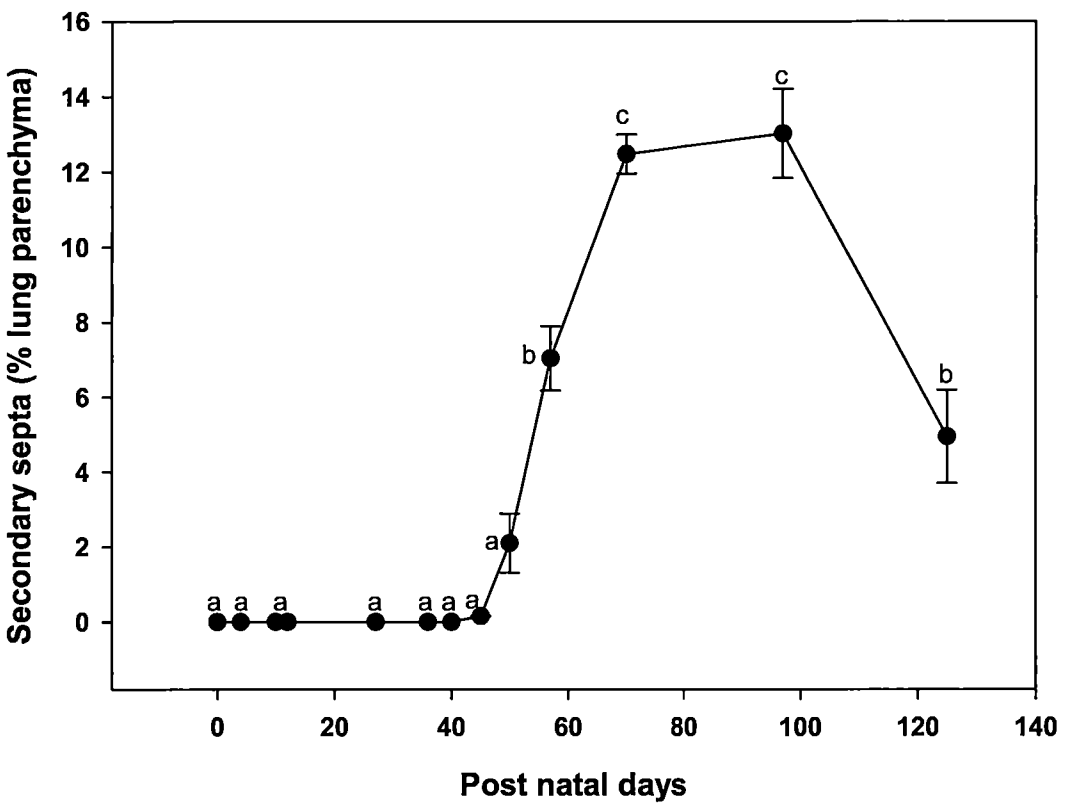
Secondary septa (% lung parenchyma)
16
14
12
10
8
6
4
2
0
a a a a a a a a
b
c
c
b
0
20
40
60
80
100
120
140
Post natal days

3.4 DISCUSSION

In most mammals, the respiratory system is required to be sufficiently developed at birth to take over as the organ of gas exchange. However, in the newborn fat-tailed dunnart, the skin is almost solely responsible for gas exchange, and less than 35 % of newborn dunnarts were observed to make any respiratory effort (despite maintaining pink skin and body movements) on the day of birth; possibly these animals were a few hours older than those in which no breathing was detected. "Breathing", if it occurred, would generally last for a couple of minutes, be accompanied by gross body movements, and be proceeded with a significant period of apnoea (such that some animals were not seen to breathe again for the rest of the measurement). Further, the observed tidal volumes were probably insufficient for reliable gas exchange.

We speculate that these small and inconsistent movements are used to prepare the muscles of respiration for the task ahead and therefore somewhat equivalent to the role of fetal breathing movements seen in mammals *in utero.* While indications are that a central rhythm generator exists to some degree; whether it is still developing, or the breaths are not being manifested, remains unknown.

Once ventilation was established, a held inspiration was observed at the end of each breath during the first weeks of life in the neonatal fat-tailed dunnart. This characteristic post-inspiratory pause has also been observed in the respiratory cycle of other neonatal marsupials (Sevcik et al., 1955; Farber et al., 1972; MacFarlane and Frappell, 2001) and serves to keep the lung elevated above functional residual capacity (FRC), presumably to

maximise gas exchange, minimise the cost associated with breathing and aid in the prevention of alveolar collapse. While far more pronounced in the neonatal marsupial, this strategy has been adopted by a number of other newborn mammals (Mortola, 1984) particularly in the first hours of life (Pask et al., 2000). Prevention of atelectasis and an increase in the time frame for gas exchange would be particularly important when the lung is structurally immature as in the case of the dunnart, comprising of branching airways which terminate in large simple sacs and hence provide a small surface area for gas exchange. The convective requirement of the neonatal fat-tailed dunnart is considerably below the expected value from allometric equations relating $\dot{V}_E$ to $\dot{V}_{O_2}$ (Figure 3.14) suggesting that blood O_2 would be low until between P23 and P35 when the expected convective requirement is established.

A delay in the onset of ventilation is also seen in the Julia Creek dunnart (Mortola et al., 1999; Frappell and Mortola, 2000). Both species have a similar gestation time (12-13 days), which raises the possibility that the short gestation time is insufficient to allow for complete development of the respiratory system. This was evidenced through our studies of septation as well as via our ultrastructural observations.

The respiratory system of the newborn dunnart is no more compliant than would be predicted from other larger newborn mammals, with the allometric relationship holding true for newborn marsupials (Figure 3.15). In newborn mammals, including marsupials, the compliance of the respiratory system (C_{rs}) is largely determined by the compliance of the lungs, rather than the chest wall (Mortola, 1987; Frappell and Mortola, 1989).

Figure 3.14 The establishment of convective requirement in newborn marsupials.

Very small newborn marsupials have a low convective requirement until several weeks after birth, when the skin no longer plays a pivotal role in gas exchange. Postnatal ages (days) are indicated for marsupial neonates.

● Adult eutherians and marsupials, newborn eutherians (Mortola and Tenney, 1986; Mortola et al., 1989; Frappell et al., 1992; Frappell and Baudinette, 1995; Mortola and Lanthier, 1996).

▣ Adult tammar wallaby (Frappell and Baudinette, 1995). □ Neonatal tammar wallaby (MacFarlane and Frappell, 2001).

◮ Adult Julia Creek Dunnart (Frappell et al., 1992). △ Neonatal Julia Creek dunnart (Frappell and Mortola, 2000).

▽ Adult fat-tailed dunnart (Frappell et al., 1992). ▽ Neonatal fat-tailed dunnarts from this study. ▽Fat-tailed dunnarts published in (Frappell and MacFarlane, 2006).

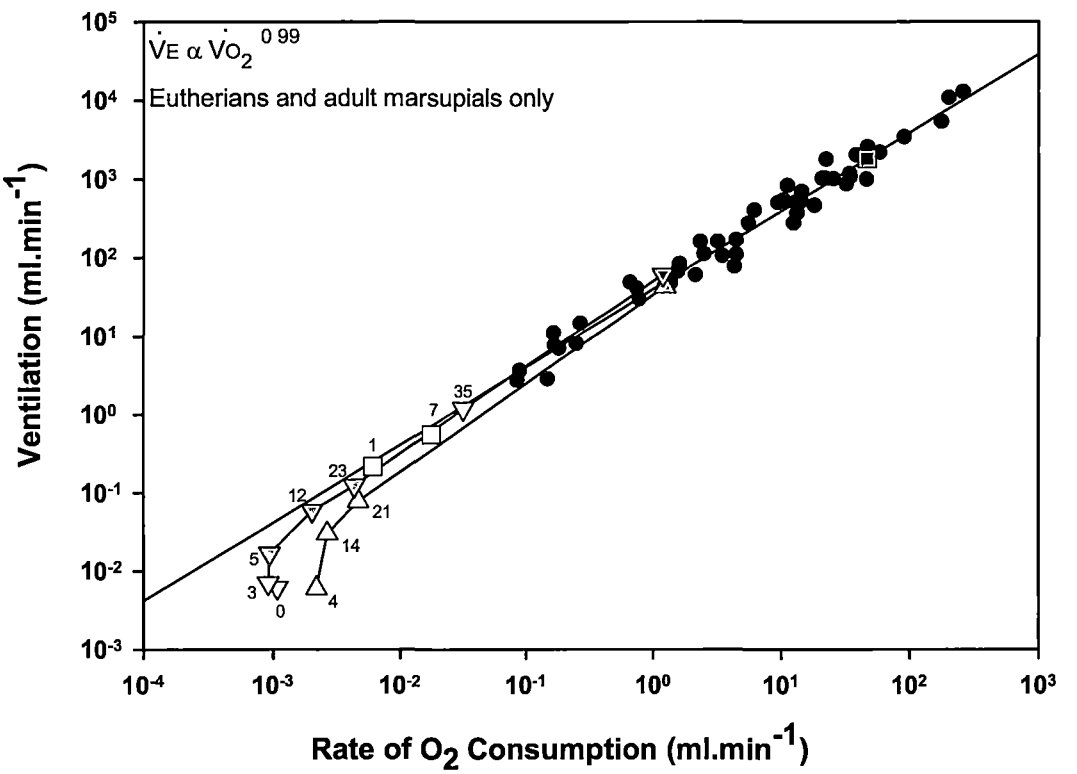
$\dot{V}_E \alpha \dot{V}O_2^{0.99}$
Eutherians and adult marsupials only
Ventilation (ml.min^{-1})
Rate of O_2 Consumption (ml.min^{-1})
10^5
10^4
10^3
10^2
10^1
10^0
10^{-1}
10^{-2}
10^{-3}
10^{-4}
10^{-3}
10^{-2}
10^{-1}
10^0
10^1
10^2
10^3
35
7
1
23
12
21
14
5
3
0
4

Figure 3.15 Respiratory system compliance (C_{rs}) as a function of body mass in newborn mammals.

Shown are mean values of respiratory system compliance for neonatal fat-tailed dunnarts (grey inverted triangle) with other newborn mammals and marsupials. Crs in the newborn fat-tailed dunnart is as predicted from other, larger, newborns. Postnatal age is indicated by the text. N=5 at each age. Comparative data taken from (Mortola, 2001; MacFarlane et al., 2002).

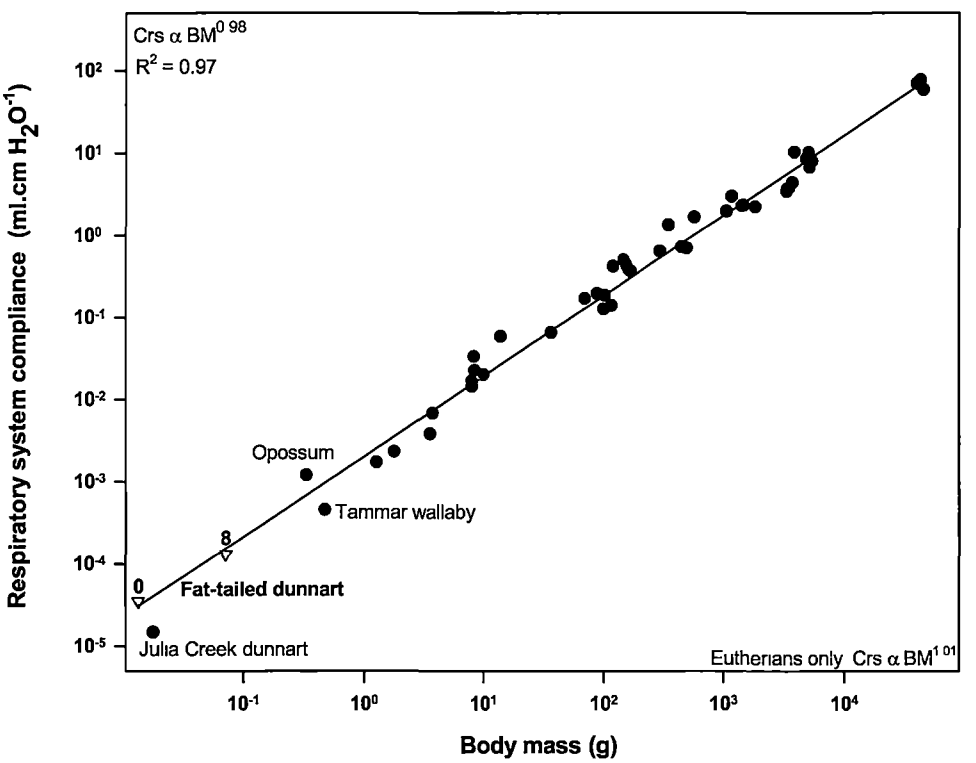
Crs α BM^0.98
R^2 = 0.97
Opossum
Tammar wallaby
8
0
Fat-tailed dunnart
Julia Creek dunnart
Eutherians only Crs α BM^1.01
Respiratory system compliance (ml.cm H2O-1)
Body mass (g)

The functional consequences of a highly compliant chest wall are a low resting lung volume as well as chest distortion, and the associated volume loss during inspiration (Mortola et al., 1985b). Chest distortion was observed in the newborn tammar wallaby (MacFarlane et al., 2002), and while not measured in this study, is likely to be a factor with the highly compliant lung of the neonatal fat-tailed dunnart once breathing commences.

Lack of neuromuscular development may also contribute to the delay in the onset of breathing. While the phrenic nerve was shown to have contacted the diaphragm in the P0 animals, it is not yet known when the inception of respiration occurs. In embryonic rats, initial contact by the phrenic nerve to the primordial diaphragm, or pleuroperitoneal fold (PPF), occurs on embryonic day 13 (E13) (Allan and Greer, 1997b). Phrenic nerve intramuscular branching commences 24 hours after initial contact with the diaphragm (Greer et al., 1999), and continues, along with subsequent diaphragmatic myotubule formation, until age E17.5. At this time the mature pattern of innervation and muscle architecture are approximated, and interestingly, coincides with the inception of respiratory drive (E17) (Greer et al., 1999). This is a greater time period than the 13 day gestation of the fat-tailed dunnart and may therefore contribute to the lack of coordinated breathing in the first days of life.

The lung architecture of the mature marsupial compares to that of eutherian mammals (Gemmell, 1986). However, at birth, the lung of the fat-tailed dunnart is nothing more than a few tubular like structures, with thick septal walls and a double capillary network, indicative of a lung at the canalicular stage of lung development. The placement of the

vessels in the tubular epithelium leads to a high diffusion distance, as does the relatively thickened cytoplasmic extensions. The singular cytoplasmic extension we observed may also lead to a decrease in the surface area available for gas exchange, but more importantly indicates that the development of Type-I AECs is occurring directly from undifferentiated cell types (Flecknoe et al., 2003). The decrease in diffusing capacity due to capillary placement has also been observed in the newborn quokka (Makanya et al., 2001; Makanya et al., 2007), which until now has been the only newborn documented to be in the canalicular stage of lung development at birth.

By P45 (~1.2 gram) a sufficiently developed double capillary network was in place, with the capillaries in close proximity to the overlying epithelial cells; indicative of a fully functioning gas exchange surface. Interestingly, this age also corresponds to the detection of the first secondary septal crests, determined by the presence of secondary septa with tightly bundled elastin at the tip, and therefore the commencement of the alveolarisation phase of lung development. While the first secondary septa were detected in P45 pouch young, a peak was not reached until P70-100, implicating this as the time of bulk alveolarisation. At P40 the fat-tailed dunnart relinquishes permanent attachment from the teat and between P60 and P70, the young leave the nest for the first time and are subsequently weaned (Renfree and Lewis, 1996), presumably now capable of sustained thermogenesis. The associated increase in metabolic rate accompanying endothermy requires an increase in the internal partitioning of the lung (Tenney and Remmers, 1963) and therefore an increase in the number of alveoli at this time. Alveolarisation in the tammar wallaby also occurs over an extended period of time

with well developed alveoli present at the time of pouch vacation (Runciman et al., 1998a), which corresponds to the attainment of endothermy and the associated increase in demand for oxygen (Sevcik et al., 1955). The development of pulmonary circulation lags behind the development of the airways (Renfree, 1995) and as such the single capillary network was first detected after 70 postnatal days, but not centrally located until 100 postnatal days; the central location of the capillary is likely due to a thinning of the interstitium.

Despite the primitive appearance of the general lung structure, some secreted surfactant coils were detected in the airways of the fat-tailed dunnart on the first day of life, and secreted surfactant was abundant in the airways by 4 postnatal days. The presence of surfactant is not particularly surprising given the detection of the surfactant proteins in the newborn tammar wallaby (Miller et al., 2001), the similarities (to eutherians) in distribution and abundance of phospholipid classes in the surfactant of the tammar wallaby through development (Ribbons et al., 1989) and the fact that the compliance of the respiratory system is close to the value expected from the allometric relationship.

The development of a normal alveolar epithelium is crucial in the preparation for the onset of air-breathing, and the proportion of AECs is critical for maintaining normal lung function. In the newborn dunnart, less than 7 % of the AECs were undifferentiated at birth (although the presence of glycogen indicates a very recent differentiation), indicating that the epithelial cells appear sufficiently differentiated to allow respiration. The vast number of differentiated AECs at the time of birth was surprising. Indeed, AEC differentiation appears to be very much accelerated in these animals with respect to the

rest of their gross lung development. The epithelium is however, less developed than other newborn mammals (*e.g.* sheep and mice) where no undifferentiated cells are seen (Renfree and Fox, 1975).

The epithelium of the dunnart increases in proportion of both Type-I and Type-II AECs in the period from birth to 12 postnatal days, due the concurrent decline in the proportion of undifferentiated and intermediate cell types, suggesting that the epithelium continues to develop after birth. The Type-II AEC is considered the progenitor cell type for both Type-I and -II AECs (Renfree, 1973) so the reduction in the proportion of Type-II AECs (60.4 ± 6.3 % to 38.8 ± 4.1 %) and concurrent increase in Type-I AECs (35.9 ± 7.3 % to 59.6 ± 4.6 %) in the period from P10 to P70 is perhaps indicative of this differentiation, however a concurrent increase in cells of an intermediate phenotype was not evident. It is known that sustained increases in fetal lung expansion (stretch) induce Type-II AECs to trans-differentiate into Type-I AECs via an intermediate cell type, as well as influence the three-dimensional tissue structure of the lung (Carroll and Fitzgerald, 1993; Harding and Hooper, 1996; Flecknoe et al., 2000; Hooper and Wallace, 2006). With the onset, and subsequent increase in ventilation, commencing after an extended period of time from birth, in addition to the frequent sighs (several per minute in the P5 and P12 neonates) observed during this time, it could be speculated that the associated mechanical factors are sufficient to alter the AEC proportion.

The morphological features required at birth for a functioning lung are a large surface area for gas exchange, a thin air-blood barrier, a surfactant system, a conductive airway tree and appropriately developed vasculature (Pask et al., 2007). While we detect

surfactant coils in the airways of newborn fat-tailed dunnarts, it is likely that low diffusion capability, resulting from the high diffusion distance caused by underdeveloped vasculature, small surface area available for gas exchange, and thickened singular cytoplasmic extensions of Type-I AECs, contributes to the functional inadequacy of the lungs in the newborn. In addition, it is likely that poor muscle co-ordination, chest wall distortion and lack of respiratory drive impede efficient breathing in the newborn and force the neonatal fat-tailed dunnart to rely predominately on its skin for gas exchange; made possible by its low metabolic rate and small size. The fat-tailed dunnart provides an excellent model for the study of lung development as it is born at a comparatively primitive stage of lung development (human infant 17-26 weeks gestation), with lungs that are not yet functional.

4 PHASE CONTRAST IMAGING OF NEONATAL MARSUPIAL LUNGS USING A SYNCHROTRON RADIATION SOURCE

4.1 INTRODUCTION

Marsupials are born prematurely by eutherian standards with respect to their lungs. While surfactant is present (Ribbons et al., 1989; Miller et al., 2001, Simpson, chapter 3), the lungs of the neonatal marsupial are at a very early stage of development. In the case of the fat-tailed dunnart *(Sminthopsis crassicaudata)* (Chapter 3) and quokka wallaby (*Setonix brachyurus)* (Makanya et al., 2007), the lungs are at the canalicular stage; though more commonly marsupials are born with lungs at the saccular stage, as is the case with the tammar wallaby (*Macropus eugenii*) (Runciman et al., 1996). In marsupials the majority of lung development occurs in the air-breathing extra-uterine environment.

Traditional morphometric techniques have established that lung volume scales isometrically, and identically, in marsupials and eutherians, throughout development. On a mass-specific basis, however, the quokka appears to have a relatively small lung volume at birth, perhaps related to the fact that it is born with a lung at the canalicular stage. In contrast, it would seem that the tammar wallaby and the North American Opossum (*Didelphis virginiana*) have larger than predicted mass-specific lung volumes (Frappell and MacFarlane, 2006).

Despite making the transition to the saccular stage of lung development just 3 days before birth (Runciman et al., 1996; Runciman et al., 1998b), the lung of the tammar wallaby is largely functional as a gas exchanger, contributing 60-70 % of the gas exchange required to meet the total metabolic demands of the newborn (MacFarlane and Frappell, 2001). The remaining 30-40 % of gas exchange is attributed to the skin. The skin

continues to play a role in meeting metabolic demands until four days postpartum (P4) in the tammar wallaby (MacFarlane and Frappell, 2001).

This period of reliance on the skin for respiration is much longer, and the initial reliance of the skin much higher (approaching 100 %), in a smaller newborn marsupial species, the Julia Creek dunnart (*Sminthopsis douglasi*) (Mortola et al., 1999; Frappell and Mortola, 2000)) . Similarly, in the fat-tailed dunnart, the skin is responsible for almost all gas exchange at birth, and continues to play a role in respiration until P40 (Chapter 3). In part, this is enabled by the large surface area to volume ratio associated with a very small body size and low metabolic rate, and also attributed to possible neural and/or mechanical constraints to pulmonary ventilation, as well as the presence of cardiac shunts in these immature newborns (Frappell and MacFarlane, 2006).

Phase contrast imaging enhances edges of material boundaries, where differences in refractive index occur, for example the boundaries between different tissue types (Lewis et al., 2003). A marked phase contrast exists between the air in the lungs and the surrounding tissues, allowing for high definition imaging of the airways.

Phase contrast imaging with a synchrotron radiation source has been used to elucidate the biomechanical mechanisms of tracheal compression, and the role of convective respiratory mechanisms in a range of insects (Westneat et al., 2003; Kaiser et al., 2007; Socha et al., 2008; Greenlee et al., 2009). Synchrotron imaging has also been used to provide further insight into the alveolarisation of mouse lungs (Mund et al., 2008; Schittny et al., 2008) and the first breathes in the rabbit pup (Hooper et al., 2007; Hooper

et al., 2009). Until recently, synchrotron imaging studies of the lung often focused on methodology (Yagi et al., 1999; Kitchen et al., 2004; Porra et al., 2004; Lewis et al., 2005; Sera et al., 2005), and have always been undertaken in mammals which have comparatively more mature lungs than the newborn marsupial.

High resolution images of the lungs in the tammar wallaby and fat-tailed dunnart were obtained during the first weeks of life using phase contrast imaging with a synchrotron radiation source, allowing visualisation of lung development in these neonates. In addition, three-dimensional (3-D) reconstructions of computed tomography (CT) data sets permitted a new method for the calculation of functional lung volumes and surface areas for these stages of development.

4.2 MATERIALS AND METHODS

4.2.1 Animal collection

Reactivation of a diapaused blastocyst occurs following the removal of a tammar wallaby pouch young with birth expected 26 days later (Hinds et al., 1990). Tammar wallabies and fat-tailed dunnarts approaching full-term (26-28 days and 13-14 days (Bennett et al., 1990) respectively) were continuously monitored for signs of giving birth, and/or underwent regular pouch checks. Young at several ages ranging from birth to several weeks were collected and euthanized by anaesthetic overdose under La Trobe University ethics permit LTU AEC 04/37(L).

4.2.2 Sample preparation

Once killed, animals had their nasal nares blocked with a quick setting polyether compound (Impregum F, ESPE) and were quickly frozen at -20 °C in an evacuated zip lock bag with moist gauze to prevent desiccation. Specimens were maintained at -20 °C until they were put on dry ice for air-transport to the SPring-8 synchrotron facility, Hyogo, Japan, were they were kept frozen until preparation for imaging began. For imaging, pouch young were placed into a snug fitting plastic tube and held in place with a plastic pin that prevented movement during imaging if required. A cryostat was placed in the experimental hutch and directed a cold stream of air over the specimen to ensure the sample was kept just above the freezing point, ensuring that ice crystals did not interfere with the imaging.

4.2.3 Phase contrast imaging

Phase contrast enhanced single images and computed tomography data sets were acquired at the Biomedical Imaging Centre, SPring-8 synchrotron, Hyogo, Japan. To provide maximum edge enhancement to elucidate the lung structure, single images were acquired on the high coherence 20XU beamline, using a propagation distance of approximately 3.7 m and an X-ray energy of 17.7 keV. Images were recorded using a Hamamatsu phosphor charged-coupled device with pixel size of approximately 3x3 μm^2. Since the beam size is limited (approximately 3 mm vertically and 6mm horizontally) on the 20XU beamline, several images were taken in a raster scan and then tiled together to create the final image in animals that were larger than these dimensions. Images were

conventionally corrected for dark current offset and full field non-uniformities before tiling (if required). A larger beam size is available on Beamline 20B2 (approximately 25 mm vertically and > 300 mm horizontally) and this beamline was used to acquire computed tomography data at 20 or 25 keV. A shorter propagation distance of 15-60 cm and higher X-ray energy was used to avoid tomography reconstruction artefacts. Between 1296 and 3772 projections were taken over 180° around the axis of rotation, depending on the step size. The exposure time was 1000 or 1500 ms for each projection. Since the synchrotron beam is essentially parallel, computed tomography reconstructions were carried out using a first generation CT geometry on a slice by slice basis, leading to over 1000 transverse slices being reconstructed.

4.2.4 Lung surface area and volume calculations

Lung surface areas and volumes were calculated using ImageJ (National Institutes of Health). The reconstructed images were first thresholded to create a binary image that could be easily segmented to highlight lung regions only. The images were then inverted so as the lungs appear white, and non-air filled structures are black, which is necessary for the morphological filters to run. These filters reduce any noise in the images. Volumes and surface areas were then calculated for each CT slice by using the "analyse particle" function which finds regions in the binary images between certain sizes (>30 and < 3500 pixels) and counts their number, area and perimeter. Surface areas were calculated by summing the perimeter for each slice and the volume determined by summing the area, knowing the thickness of each slice was 1 pixel.

4.2.5 Allometry

Where appropriate, least-squares regressions were fitted to log-log transformed data for allometric analysis.

4.3 RESULTS

Phase contrast imaging has great potential in biomedical imaging, as demonstrated in this study, with the high resolution images obtained for lung development in neonatal marsupials. At 36 hours after birth, the lung of the tammar wallaby is a simple saccular structure (Figure 4.1), which increases markedly in complexity by P10 and further again by P20. This increase in complexity is concurrent with a decrease in the size of air sacs, and at these ages the inflated lung tissue was seen as a speckled intensity pattern, similar to that seen in more developed eutherian species (Kitchen et al., 2004; Kitchen et al., 2005).

The lungs of the newborn fat-tailed dunnart are more immature than those of the tammar wallaby. The plane radiographs of the developing fat-tailed dunnart (Figure 4.2) indicate that within the first hour of life, just two lung sacs contain air. Within 36 hours, the dunnart has doubled in body mass, and undergone an increase in the complexity of the lung. It is at this age that air is first observed in the trachea, though not in all animals imaged. Further compartmentalisation occurred in the lung between 6 and 10 postnatal days, however, the lung was still observed as large circular air sacs at the end of this period, the shape of which can be better observed in the 3-D rendering (Figure 4.3). Between 10 and 40 postnatal days, substantial changes were seen in the architecture of

the lung (Figures 4.2 and 4.3). The air sacs were no longer large circular sacs, and lung volume and surface area were improved through extensive increases in air sac number, as well as architectural complexity.

The neonatal tammar wallaby and fat-tailed dunnart displayed lower lung volumes (Figure 4.4) and parenchymal surface areas (Figure 4.5) than were expected from equations relating these variables to body mass. The slopes for both lung volume and surface area in the newborn marsupials using synchrotron imaging were significantly different from that of the eutherians determined by traditional morphometric techniques ($P < 0.001$). However, lung volume is predicted to scale with mass as expected after the neonatal marsupial reaches a body mass of 1 g and no longer relies on the skin for gas exchange.

4.4 DISCUSSION

It is generally accepted that the newborn mammal must rapidly adapt to air breathing through clearance of fetal lung liquid, the onset of a rhythmic breathing pattern and establishment of a functional residual capacity (Mortola, 1987). In fact, viability of the eutherian neonate depends on an adequately developed respiratory system. However, the increasing evidence that newborn marsupials rely to varying degrees on their skin for gas exchange (Frappell and Mortola, 2000; MacFarlane and Frappell, 2001); Chapter 3) raises questions regarding whether the short gestation common in marsupials is sufficient to allow adequate development of the respiratory system prior to birth.

Figure 4.1 Phase contrast X-ray imaging of the developing tammar wallaby.

Shown are phase contrast images of the developing tammar wallaby using a synchrotron radiation source. 36 hours after birth the lungs of the tammar wallaby are simple and saccular in structure. The lung increases in complexity by P10 and further again by P20 with an increase in the number of air sacs and a decrease in the size of these air sacs. Anterior-posterior view (top) and lateral view (bottom). Scale bar represents 1 mm.

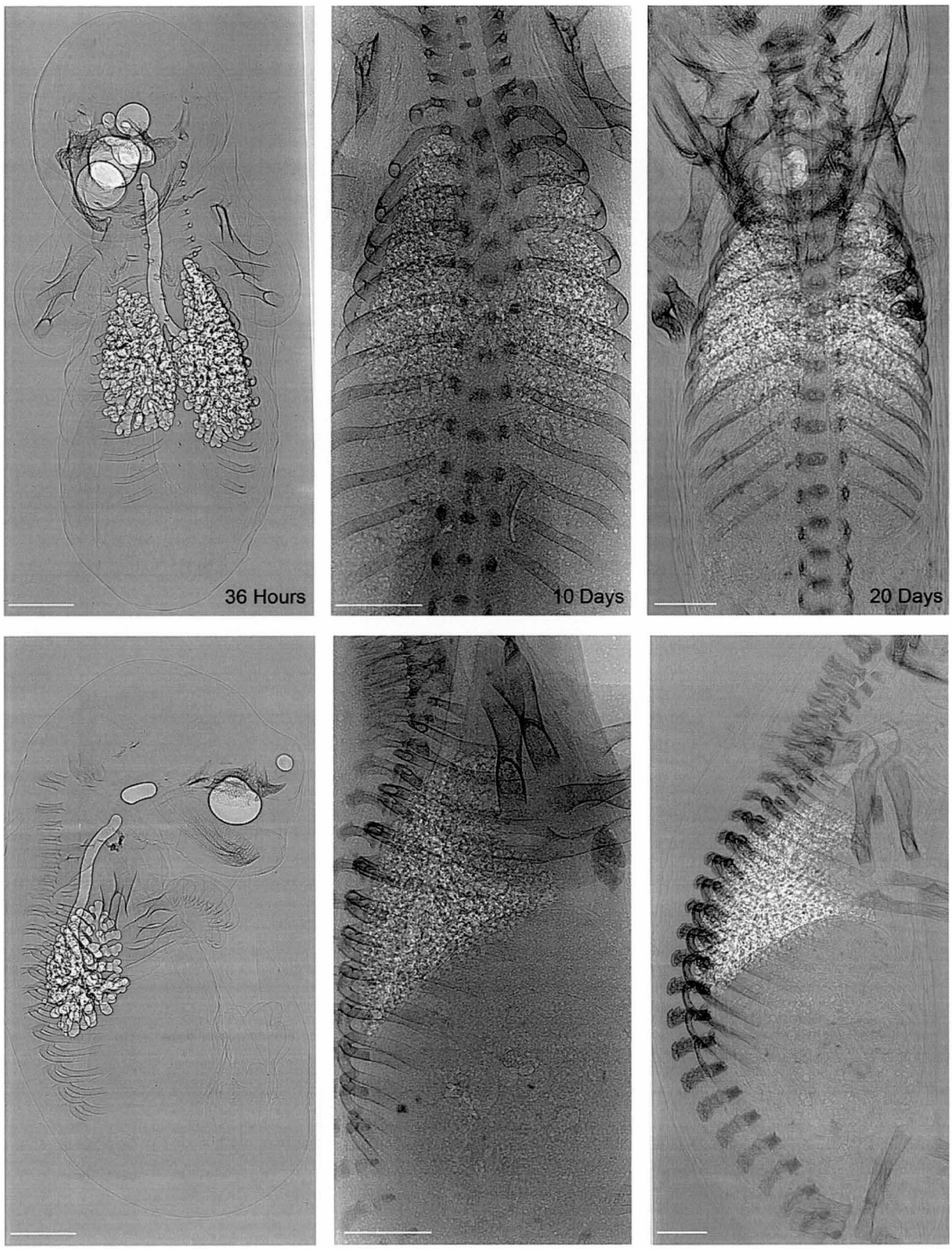
36 Hours
10 Days
20 Days

Figure 4.2 Phase contrast X-ray imaging of the developing fat-tailed dunnart.

Shown are phase contrast images of the developing fat-tailed dunnart using a synchrotron radiation source. With just 2 air bubbles visible after parturition, the dunnart undergoes a substantial degree of extrauterine lung development. At P10, the lungs are still characterised by large open circular sacs. By P20 the size, shape and number of air sacs have changed. Anterior-posterior view (top) and lateral view (bottom). Scale bar represents 1 mm.

40 days
20 days
10 days
6 days
36 hours
<1 hour

Figure 4.3 3-Dimensional volume rendering from fat-tailed dunnart computed tomography data sets.

Shown are three frames captured over 90 degrees of lung rotation, further demonstrating the increase in air sac number, and changes to air sac shape throughout the first weeks of lung development in the fat-tailed dunnart. Scale bar represents 200 μm.

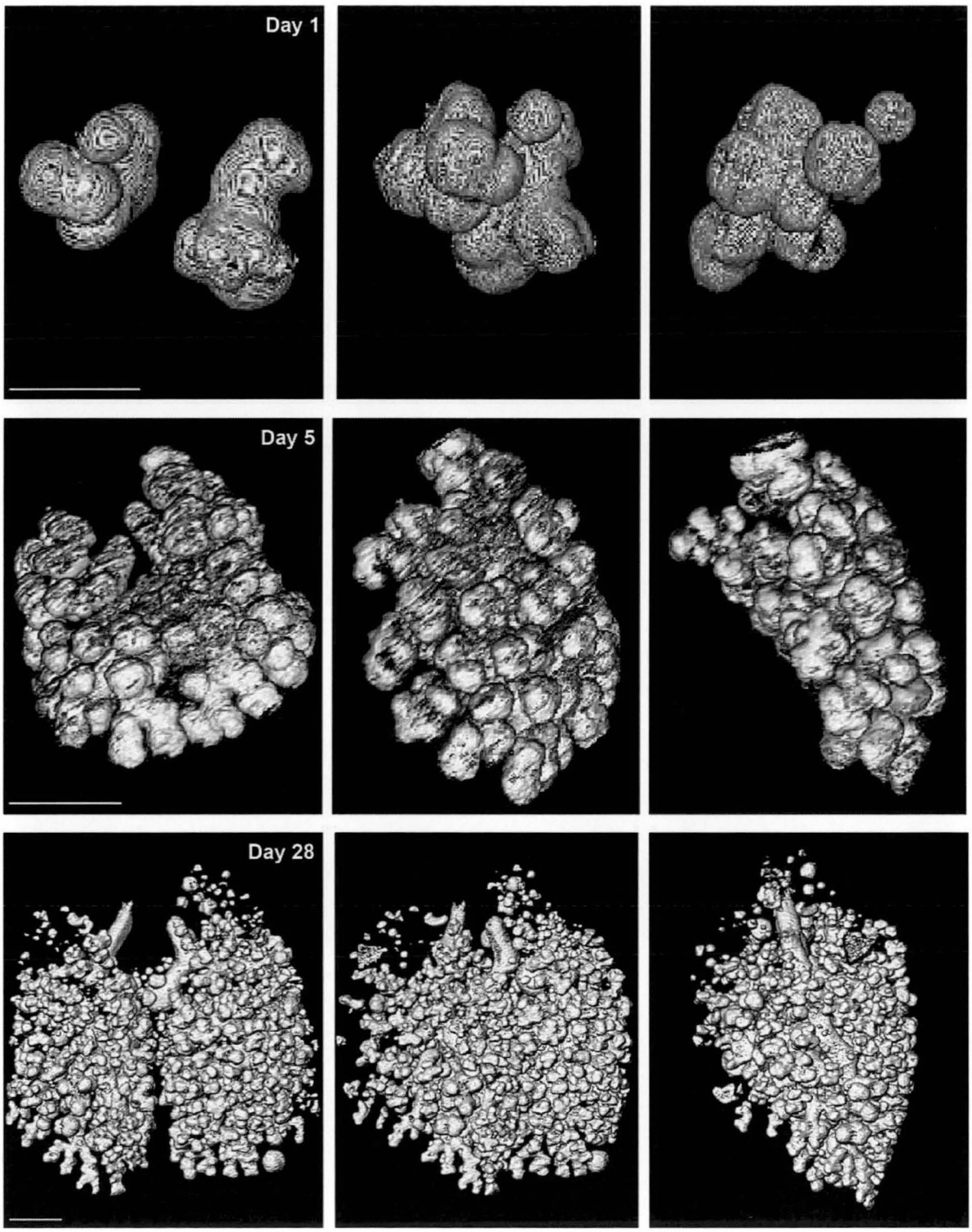
Day 1
Day 5
Day 28

Figure 4.4 Lung volume (A) and mass specific lung volume (B) as a function of body mass during postnatal development.

Grey circles represent both adult and newborn eutherian mammals. Black circles represent newborn and adult marsupials. Dark blue circles represent tammar wallaby joeys measured in this study aged from birth to P30. Light blue circles represent fat-tailed dunnart pouch young measured in this study from P1 – P20. The newborn marsupials measured in this study (with synchrotron imaging) show a lower than expected lung volume, until a body mass greater than 1 g, when the lungs become the main (only) source of gas exchange. Data taken from (Burri et al., 1974; Bartlett and Areson, 1977; Lechner and Banchero, 1982; Zeltner and Burri, 1987; Davies et al., 1988; Frappell and Mortola, 1989; Castleman and Lay, 1990; Runciman et al., 1998a; Runciman et al., 1999; Makanya et al., 2003; Makanya et al., 2007).

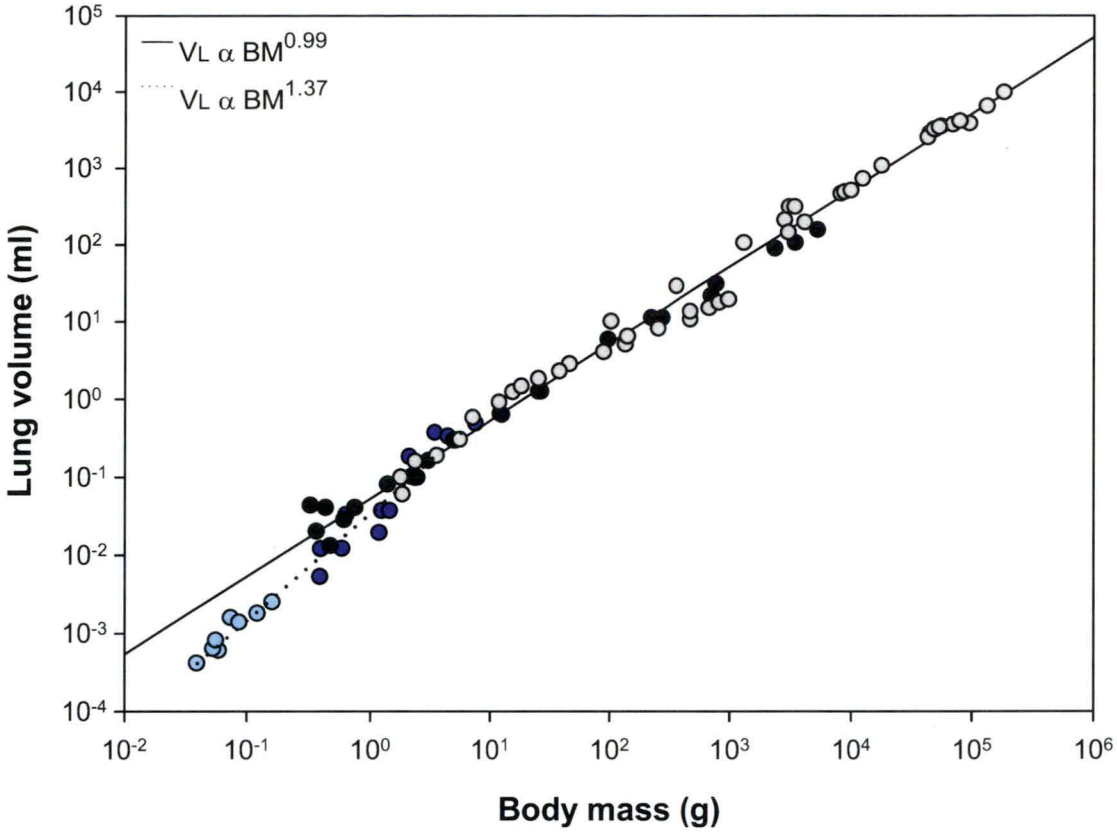
VL α BM0.99
VL α BM1.37
Lung volume (ml)
Body mass (g)

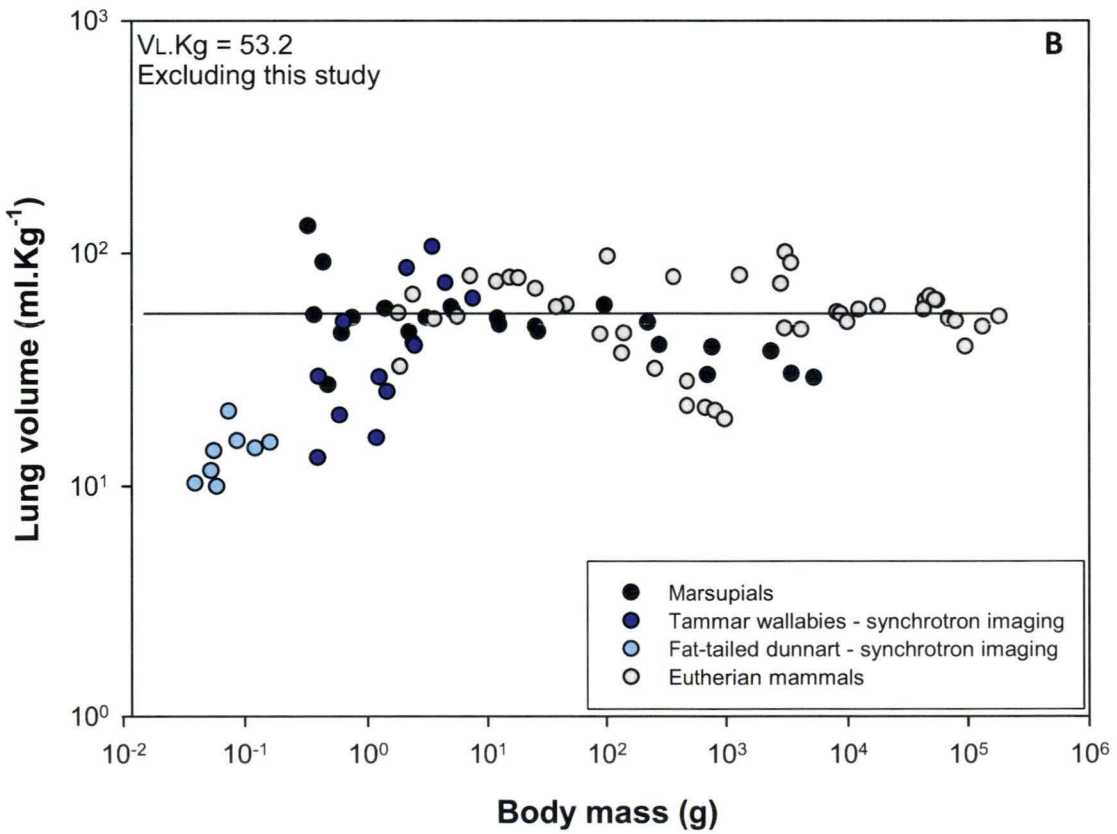
VL.Kg = 53.2
Excluding this study
B
Lung volume (ml.Kg-1)
Marsupials
Tammar wallabies - synchrotron imaging
Fat-tailed dunnart - synchrotron imaging
Eutherian mammals
Body mass (g)

Figure 4.5 Surface area of the lung as a function of body mass during postnatal development.

Shown is the surface area of the lung during postnatal development. As with other marsupials, the animals measured in this study display a surface area less that that predicted from the allometric equation, most likely due to the fact that alveolarisation and the subsequent increase in surface area by septation does not commence until after P70 in the tammar wallaby and P45 in the fat-tailed dunnart. Symbols and references as in Figure 4.4.

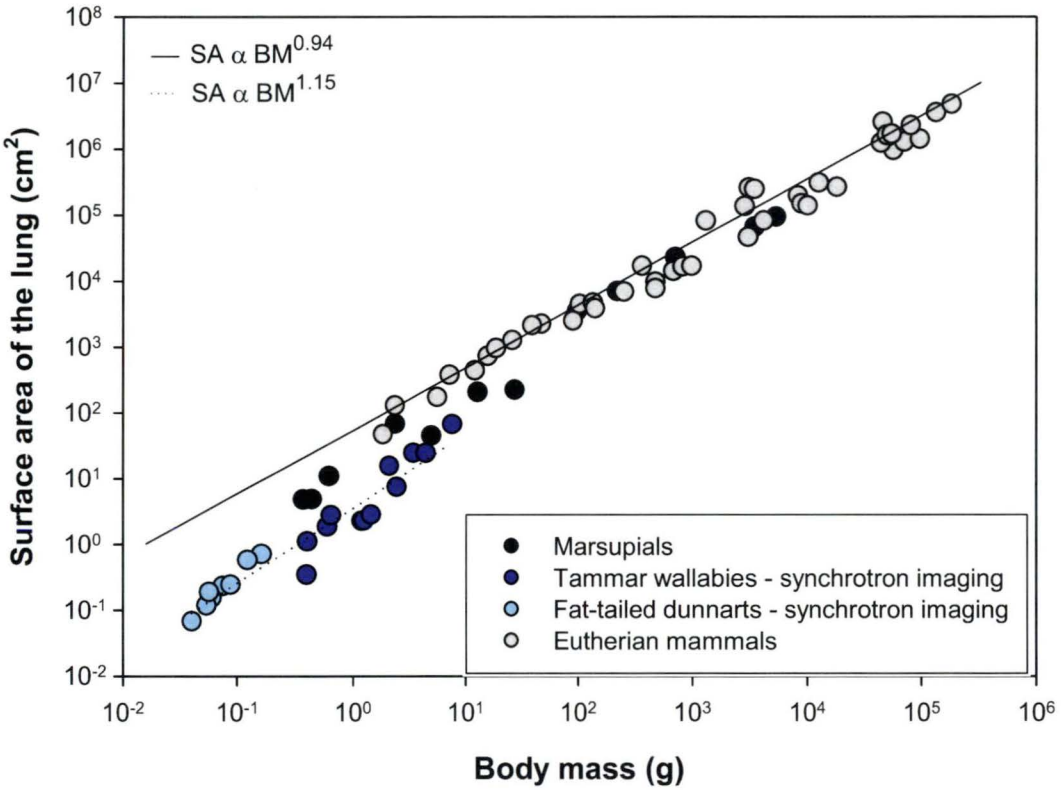
SA α BM^0.94
SA α BM^1.15
Surface area of the lung (cm²)
Body mass (g)
Marsupials
Tammar wallabies - synchrotron imaging
Fat-tailed dunnarts - synchrotron imaging
Eutherian mammals

The two air bubbles seen in the thorax of the 1 hour old dunnart may be an indication that the lung is grossly under-developed and comprises of only two simple sacs. Alternatively, the architecture of the lung may be slightly more developed than this, but the airspace not completely cleared of fetal lung liquid, rendering the phase contrast non-existent in these fluid filled areas of the lung. In fact, this explanation is more likely given that light and electron microscopy demonstrated a couple of thick septal walls within the primitive tubular structures and an over-abundance of thick material in the airspaces (Chapter 3). Also, the predominant driver for airway liquid clearance is trans-pulmonary hydrostatic pressure, generated by inspiratory activity (Hooper et al., 2007), and since the newborn fat-tailed dunnart rarely demonstrates inspiratory activity (Chapter 3) it could be argued that clearance takes place over an extended period of time, once a reliable respiratory rhythm is established.

The implications of this potential delay in lung liquid clearance, combined with the primitive architecture of the airways, are that low lung volumes and decreased surface area are expected leading to inefficient gas exchange. Higher than predicted mass specific lung volumes have previously been reported for the newborn opossum (Frappell and Mortola, 1989) and tammar wallaby (Runciman et al., 1998a), while lower than predicted lung volumes have been reported in the newborn quokka (Makanya et al., 2007). The lung volumes determined in the present study represent functional or physiological lung volumes, in that they represent the air filled, hence gas exchanging, regions of the lungs, not the morphological volumes determined with traditional microscopic techniques. As the physiological lung volume in the newborn marsupial is

less than allometrically predicted from other species that rely entirely on the lungs from birth (Figure 4.4), it is perhaps not surprising that marsupial neonates are reliant on their skin to varying extents for gas exchange. The lung volume of the tammar wallaby reaches values expected for an animal of its size at around a body mass of 1 g, which coincidently is the time when the lung is responsible for 100 % of gas exchange (MacFarlane and Frappell, 2001). Unfortunately, we have no data for dunnarts above 20 days of age (0.18 grams) but expect that their lung volume would reach predicted values by the time they weigh ~1 g and no longer rely on cutaneous gas exchange.

The low lung volume may relate to the stage of lung development; the earlier the stage, the lower the lung volume at birth, as well as the extent to which the newborn relies on its lungs for gas exchange. Microscopic morphology has determined that lung volume increases ~23 fold through development in humans and rats, (Zeltner and Burri, 1987; Zeltner et al., 1987), with marsupials demonstrating a much greater increase in lung volume; a 3,800 fold increase in the case of the tammar wallaby (Runciman et al., 1998b) and a staggering 8,000 fold increase in the quokka (Makanya et al., 2003). In the quokka, dramatic increases in lung volume were observed during the first 5 postnatal days as the lung changed from the canalicular to saccular stage of lung development. This increase was predominantly due to airspace expansion rather than septal development (Makanya et al., 2003) as septal development occurs later. The presence of a well organised capillary bi-layer is indicative of transition to the saccular stage of lung development (Burri, 1984); a feature which is not observed in the fat-tailed dunnart until between P27

and P45, around the same time that cutaneous exchange ceases to be important (see chapter 3).

There are numerous consequences to low lung volumes in newborns, including the fact that the alveoli (or air sacs) have a much greater tendency to collapse. Newborns often minimise this potential problem by maintaining a dynamic elevation of FRC above resting lung volume. In many newborns, this is achieved by a slowing of expiratory emptying (by braking action of the inspiratory muscles), coupled with narrowing of the glottis during expiration, to prolong the expiratory time constant (Mortola et al., 1982; Kosch and Stark, 1984). This strategy is particularly pronounced in the newborn marsupial, where a characteristic post-inspiratory pause has been reported in the breathing trace of all marsupial neonates studied to date (Farber, 1972; Farber, 1978; MacFarlane and Frappell, 2001; Frappell and MacFarlane, 2006); the breath-hold resulting from the closure of the glottis at the end of inspiration. Presumably this serves to overcome lung collapse, increase the opportunity for gas exchange and minimise the energetic cost of breathing when the mechanical properties of the respiratory system do not favour efficient ventilation (Frappell and Mortola, 2000). It is possible that the lung volumes reported in this study are lower than the functional lung volumes in living neonates due to the lungs deflating below FRC, though the same would also be true of neonatal lungs examined morphometrically.

Similarly to lung volume, the surface area available for gas exchange in the newborn wallaby and dunnart lung is also below values predicted from allometry (Figure 4.5). A lower than expected surface area has also been reported in neonatal marsupials using

traditional morphometric techniques. Presumably, this is related to the fact that newborn marsupials are born with lungs pre-alveolarisation, and it is not until this phase of lung development that we would anticipate significant increases in alveolar surface area as a result of secondary septation. From birth to P70, the lungs of the tammar wallaby are in the saccular stage of lung development (Runciman et al., 1999), while the fat-tailed dunnart does not commence alveolarisation until at least P45 (Chapter 3). The mere presence of septation is not indicative of an increase in functional surface area for gas exchange. In fact, it is estimated that only about 50 % of the surface area of the terminal air sac in the newborn tammar wallaby, which is well developed when compared to the quokka and fat-tailed dunnart, is actually available to exchange gas due to placement of the blood vessels (Runciman et al., 1999).

While quantification of surface area and lung volume using traditional morphometric techniques in comparison to the functional surface areas and volumes obtained in this study would have been beneficial, pressure fixation was not possible in these minute newborns. Morphological determination of the capillary density and thickness of the air-blood barrier over development would also have been of benefit, aiding in assessment of diffusing capacity, however such measurements also require pressure fixation.

The enormous amount of lung development observed in the weeks after birth is not surprising given an increasing reliance on the lung for gas exchange as the general surface area with respect to body size decreases and the demand for oxygen increases, particularly as the capability for thermogenesis develops (Frappell, 2008). The finding of a low lung volume in the marsupial neonate further supports the maxim that cutaneous

gas exchange occurs in the marsupial neonate because the respiratory apparatus is not yet capable of meeting the gas exchange requirements of the newborn. Low lung volumes, delayed fluid clearance from the airways and mechanical distortion, together with the absence of a continuous breathing pattern at birth in the smallest of the newborns all point towards constraints on the respiratory system. It remains to be demonstrated whether the neuromuscular machinery required to drive ventilation is present in the smallest marsupial newborns.

5 THE EFFECTS OF HYPOXIA AND HYPERCAPNIA ON VENTILATION AND METABOLISM DURING DEVELOPMENT IN THE FAT-TAILED DUNNART

5.1 INTRODUCTION

Co-ordinated ventilation at birth is reliant on a central rhythm generator, as well as sufficiently mature respiratory motoneurones and muscles (Feldman et al., 2003). While afferent information to the respiratory centres from lung and airway mechanoreceptors, and peripheral and central chemoreceptors, is not essential for neuronal rhythmicity, it is important for the modulation of the depth, timing and pattern of respiration (Milsom, 1990). The interplay of these factors is subject to maturational changes, and neonatal breathing is inherently variable due to the immature state of integration between these components. While the neural and muscular components of the mammalian respiratory system mature postnatally, they must be sufficiently developed to function at birth, and allow generation of a rhythm that enables ventilation in a highly compliant thorax (Greer et al., 2006).

Respiratory activity in response to changes in O_2 (hypoxia) or CO_2 (hypercapnia) is dependent on the relative size and maturity of the species at birth, and generally increases with postnatal age (Bonora et al., 1994). The peripheral chemoreceptors, the carotid and aortic bodies, detect arterial hypoxia (and also hypercapnia, *see below).* There also exists a multiplicative interaction between O_2 and CO_2 such that at higher P_{CO_2} the response to falling O_2 becomes greater. In this way, the carotid body provides significant respiratory drive during asphyxic conditions when P_{O_2} is low and P_{CO_2} is high. Given the relative insensitivity of the carotid body to O_2 fluctuation under normal conditions (*i.e.* in the absence of pathological conditions), it does not contribute to O_2-

dependent respiratory drive, although it does provide tonic inputs to maintain respiratory stability (Nattie, 2006). The response to hypoxia increases with age, probably as the sensitivity of the carotid body glomus cells, the primary mediators of the increase in ventilation (hyperpnoea) during acute hypoxia, resets to the relatively hyperoxic conditions of the extra-uterine environment (Hanson et al., 1989).

In contrast to the adult, the newborn is does not sustain a hyperpnoea in response to hypoxia, and the ventilatory response is often biphasic, with an initial increase in minute ventilation followed by a decline, in some cases to below the pre-hypoxic levels (Neubauer et al., 1990). In general, reductions in $\dot{V}_E$ are attributed to decreases in either the mean inspiratory flow (V_T/T_I), which correlates with measurements of respiratory drive and represents a mechanical translation of neuronal output in neonates due to the linearity of the volume-time profile; or inspiratory duty cycle (T_I/T_{TOT}), which is primarily determined by the timing characteristics of the respiratory pattern generators (Milic-Emili and Grunstein, 1976). Hypometabolism plays an important role in neonates for mitigating hypoxia (Mortola, 1993). Despite the reduced breathing in newborns subjected to acute hypoxia, a hyperventilation (*i.e.* increase in the convective requirement) is still observed because of a disproportionate drop in the rate of oxygen consumption ($\dot{V}_{O_2}$).

Both the carotid bodies and the central brainstem chemoreceptors detect changes in CO_2/pH and affect breathing. The carotid bodies detect P_{aCO_2}, leading to a rapid ventilatory response, while the central chemoreceptors detect interstitial fluid pH and monitor the balance of arterial CO_2, cerebral blood flow, and cerebral metabolism to

provide most of the steady-state response and the needed tonic drive under normal CO_2/pH conditions (Nattie, 2006). Further, given the ability of the carotid bodies to respond quickly to increasing PCO_2, they provide a detection system which is able to operate on a breath by breath basis (Nattie, 2006; Smith et al., 2006). Similarly to the hypoxic response, newborns also show an attenuated ventilatory response to hypercapnia when compared to adults (Carroll et al., 1993; Carroll and Fitzgerald, 1993; Davis et al., 2006). In general, newborn mammals respond to CO_2 with a sustained hyperventilation (Saetta and Mortola, 1987), with little or no hypometabolic response (Mortola and Lanthier, 1996; Saiki and Mortola, 1996). Increases in both VT and f contribute to the initial hyperventilation in response to increasing CO_2 (Cummings and Frappell, 2009). With time, f returns to baseline and the hyperventilation is sustained solely by the increase in VT (Bonora et al., 1994; Cummings and Frappell, 2009). While adults and the neonates of various species increase both VT and f in response to hypercapnia, there is evidence that preterm infants only increase VT (Martin et al., 1985; Eichenwald et al., 1993). This may be a result of both mechanical and neuronal factors (Krauss et al., 1965).

There are, however, exceptions to these 'rules', with the opossum neonate providing a good example. First, they have an unusually large ventilatory response to hypoxia during the early neonatal period which attenuates with age (Farber et al., 1972). Second, unlike most neonatal mammals, the opossum has an unusually large hypometabolic response to hypercapnia (Farber, 1972). The *in vitro* brain stem preparation has demonstrated that the newborn opossum possesses neurons capable of rhythmic respiration (Eugenin and

Nicholls, 2000), despite having a similar gestation period to the fat-tailed dunnart (a mere 13 days), and that the firing rates do not present a limitation to breathing (Farber, 1993). We have evidence that the phrenic axons have made contact with the diaphragm of the newborn fat-tailed dunnart (Figure 3.7). Despite this, continuous breathing is not expressed in the newborn dunnart until around 3 postpartum days (P3) (Frappell and MacFarlane, 2006), suggesting that either descending inspiratory drive is inadequate or that some afferent signal is suppressing the respiratory rhythm centrally. The purpose of this study was to characterise the ventilatory and metabolic response to hypoxia and hypercapnia in the fat-tailed dunnart, one of the smallest and most immature newborn mammals, to determine whether low chemosensitivity may prevent the expression of normal breathing. The postnatal development of chemoresponses was also of interest.

5.2 METHODS

Ventilatory and metabolic responses to inspired gases (Air, 5 % CO_2, 10 % O_2) were measured in fat-tailed dunnart pouch young at P0 (the day of birth), P5, P12 and P23 using a closed respirometry system similar to that used in Chapter 3 and modified from (Frappell et al., 1989; MacFarlane and Frappell, 2001).

5.2.1 Metabolic rate

A tiny mask was constructed from a short piece of polyethylene tubing that enclosed the nostrils and mouth and was sealed to the skin using a non-toxic polyether material (Impregum, 3M ESPE) prior to being inserted through a 10 ml syringe thermoplastic elastomer gasket (Terumo Medical, Japan). The masked animal and gasket were inserted

into a water-jacketed chamber maintained at a constant temperature of 36 °C (pouch temperature) and 100 % relative humidity, with the gasket effectively dividing the chamber into two. Each compartment was sealed by a similar gasket at either end of the chamber. After an equilibration time, the compartments were sealed for a known period of time depending on the mass, and hence, metabolic rate of the animal (5 – 15 minutes). Subsequently, the compartments were flushed individually with a known flow (21 ml.min^{-1}), and the gas from each compartment passed through Nafion® tubing (dead space 0.6 ml) surrounded by a molecular sieve desiccant (crystalline metal aluminosilicate zeolite) prior to being analysed for fractional concentrations of O_2 and CO_2 by gas analysers (ADInstruments, ML205). The output of each gas analyser was recorded at 200 Hz (Chart 4.2 and PowerLab, ADInstruments, Colorado Springs). The rates of oxygen consumption ($\dot{V}_{O_2}$) and carbon dioxide production ($\dot{V}_{CO_2}$) were calculated from the time integral of the gas concentration curves multiplied by the flow and the reciprocal of the time for which each compartment was sealed (Frappell and Mortola, 2000). Total rate of oxygen consumption is reported throughout and was obtained by summing $\dot{V}_{O_2}$ from the lung and skin compartments.

5.2.2 Ventilation

Ventilation ($\dot{V}_E$) was measured when the chamber was sealed via a pressure transducer (Spirometer ML141, ADInstruments) connected to the head compartment, and the pressure oscillations were acquired at 200 Hz (Chart 4.2 and PowerLab, ADInstruments). The pressure oscillations associated with breathing were calibrated for volume by the injection and withdrawal of 2 µl of air, the stability of the pressure change with each

injection was also used to indicate the integrity of the seal for the chamber When analysing ventilation, at least 50 consecutive breaths were analysed for tidal volume (V_T), inspiratory time (T_I), expiratory time (T_E), post-inspiratory pause (T_P; note that T_P is fractional to T_E because it represents the passive-static component of T_E, achieved with closed glottis), total breath time ($T_{TOT} = T_I + T_E$), frequency ($f = 60/T_{TOT}$), respiratory drive (V_T/T_I), duty cycle (T_I/T_{TOT}) and minute ventilation ($\dot{V}_E = V_T \times f$). Ventilation in P0 animals displayed marked instability with prolonged apnea (Chapter 3); therefore, all recorded breaths were analysed in these animals. Animals in which ventilation was not discernable were not included in the analysis. Gaseous metabolism is expressed at standard temperature, pressure and humidity (STPD: 1 mL O_2 = 0.0446 mmol O_2) and volume at body temperature, pressure and humidity (BTPS).

5.2.3 Gas challenges

Measurements of ventilation and metabolism were first conducted in room air (~21 % O_2, 0.03 % CO_2), followed by a 5 -10 minute recovery. Animals were then subjected to either hypoxia (10 % O_2) or hypercapnia (21 % O_2, 5 % CO_2, N_2 balance) supplied by a Wosthoff gas mixing pump. In the case of hypercapnia, the animals were exposed to the 5 % CO_2 for 5 minutes prior to sealing the chamber for measurement, and analysis performed within the first minute (*i.e.* at 5-6 min CO_2 exposure, allowing examination of the central chemoresponse). When exposed to hypoxia, the chamber was sealed as soon as the gas mix had washed in and oxygen levels stabilised at 10 % O_2 so as to allow for the analysis of ventilation at 1 minute and 6 minutes post-hypoxic exposure; enabling examination of the biphasic response which newborns generally exhibit in response to

hypoxia. The difference in the time domains, account for the relatively fast carotid body response when compared to the slower central (CO_2) chemoreflex. After measurement of the ventilatory and metabolic responses to the inspired gas, the chamber was flushed for 10 min with room air, prior to a second air measurement. Details about animals measured can be found in Table 5.1.

5.2.4 Statistics

Student T-tests were used to determine whether the value obtained during a particular gas challenge was different from the value in normal room air using GraphPad Prism. Significance was considered at $P < 0.05$.

5.3 RESULTS

No discernable ventilatory pattern was observed in 2/3 of neonates at P0 (Chapter 3). In the P0 neonates where a ventilatory pattern was detected, this was often accompanied by extended periods of apnoea, occasionally in excess of 15 minutes (note the small V_T and low f; Figure 5.1). By P5, the breathing pattern was more fully established; each breath characterised by a post-inspiratory pause (Figure 5.1), together with frequent augmented breaths, or sighs, with periods of instability. P12 appeared to be a period of transition from the immature breathing pattern (with post-inspiratory pause), to the adult breathing pattern (without post-inspiratory pause as detected in some P12, and all P23 neonates). The presence of large numbers of augmented breaths in the P12 animals with an immature breathing pattern leads to variability in the respiratory parameters. The transition to the adult breathing pattern occurs primarily as a result of the

shortening of the post-inspiratory pause (Figure 5.1). A lengthening in TI and a shortening in TE are also evident through development (Figure 5.1). A significant increase in $\dot{V}_E/\dot{V}_{O_2}$ through development should also be noted, which presumably occurs as the skin contributes less to gas exchange and the lungs are established as the sole organ of respiration (Also see Chapter 3).

5.3.1 The effects of hypercapnia on fat-tailed dunnart neonates

While there was a tendency for convective requirement ($\dot{V}_E/\dot{V}_{O_2}$) to increase at all ages in response to 5 % CO_2, a significant change was only observed at P0, owing to an unexpected but significant decrease in $\dot{V}_{O_2}$ (Figure 5.2A & C). Exposure to 5 % CO_2 led to significant decrease in $\dot{V}_{O_2}$ at P0 ($P < 0.05$), but no change in $\dot{V}_{O_2}$ at older ages (Figure 5.2C). There was no significant hypercapnic ventilatory response at P0; the response approached significance in the other neonates ($P < 0.075$) (Figure 5.2B). The hyperpnoeic response observed in P5 animals exposed to 5 % CO_2 is due mainly to a significant increase in f, while at P23 the response is dominated by a significant increase in VT (Figure 5.3). The decrease in f experienced by P23 animals, however, negates any increase in $\dot{V}_E$. There was no significant change in duty cycle in response to 5 % CO_2 exposure (Figure 5.4A). A significant increase in respiratory drive was evident in P12 neonates, with the CO_2 induced increase in VT/TI approaching significance in the P23 neonates ($P = 0.06$) (Figure 5.4B).

In summary, fat-tailed dunnarts increase their $\dot{V}_E/\dot{V}_{O_2}$ in room air over development. Their response to CO_2 is limited; only at P0 is there a significant increase in $\dot{V}_E/\dot{V}_{O_2}$,

owing to a decrease in $\dot{V}_{O_2}$. Although there was no significant effect of CO_2 on $\dot{V}_E$ across any age, P12 animals tended to have a response. Further, at P12 there was a significant effect of CO_2 on respiratory drive. Given the between-animal variability, more animals are probably required to be studied at P12, and perhaps other ages, to determine if there is a true effect of CO_2 on ventilation.

5.3.2 The effects of hypoxia through development in the fat-tailed dunnart

Across all ages except P12, there was a significant increase in $\dot{V}_E/\dot{V}_{O_2}$ after 1 min of hypoxia ($P < 0.05$; Fig. 5.5A). This effect was achieved predominantly by a decrease in $\dot{V}_{O_2}$ ($P < 0.05$, Figure. 5.5C). There was no increase in ventilation in response to hypoxia, regardless of the duration of exposure (Fig. 5.5B). In fact, in P5 and P12 animals, hypoxia significantly suppressed $\dot{V}_E$ at 6 min, with $\dot{V}_E$ being immediately suppressed in the P12 neonates. Thus, a biphasic hypoxic ventilatory response, as has been described in other neonatal mammals, was not observed. There was no increase in tidal volume at any age in response to hypoxia; reflecting the decrease in $\dot{V}_E$, tidal volume actually fell in both P5 and P12 animals (Figure 5.6). Despite no effect on overall $\dot{V}_E$, there was an increase in f at P0 in response to hypoxia which was mirrored by an increase in T_I/T_{TOT} (Figure 5.7A). The absence of a ventilatory response at any age precluded any increase in respiratory drive (V_T/T_I) (Figure 5.7B).

In summary, much like hypercapnia, hypoxia had little effect on ventilation at any age. In fact, hypoxia, if anything, had a suppressive effect on $\dot{V}_E$. Regardless, owing to its suppressive effects on $\dot{V}_{O_2}$, hypoxia still led to a hyperventilatory response.

Table 5-1 Experimental animals for gas challenges.

Numbers (N) and masses of fat-tailed dunnart neonates for whom metabolic and ventilatory variables were analysed in air, hypercapnia and hypoxia.. Note for P0 that 2/6 indicates that an episode of ventilation was detected in 2 of the 6 animals studied at this age. Masses are presented as means ± 1SD.

Age	Mass (mg)	Control (Air)	N 5 % CO_2	N 10 % 0_2
P0	18±8	12	2/6	2/4
P5	57±6	7	4	4
P12	101±20	9	6	5
P23	223±30	9	4	5

Figure 5.1 Spirogram demonstrating a characteristic breath for P0, 5, 12 and 23 fat-tailed dunnarts.

Shown are respiratory timing and tidal volumes for neonatal fat-tailed dunnarts at P5, 12 and 23 in black as indicated by the text. Data for P0 (grey) include all measurable breaths. Note the increase in frequency, tidal volume and inspiratory time with increasing age and the decrease in the post-inspiratory pause and expiratory time over development.

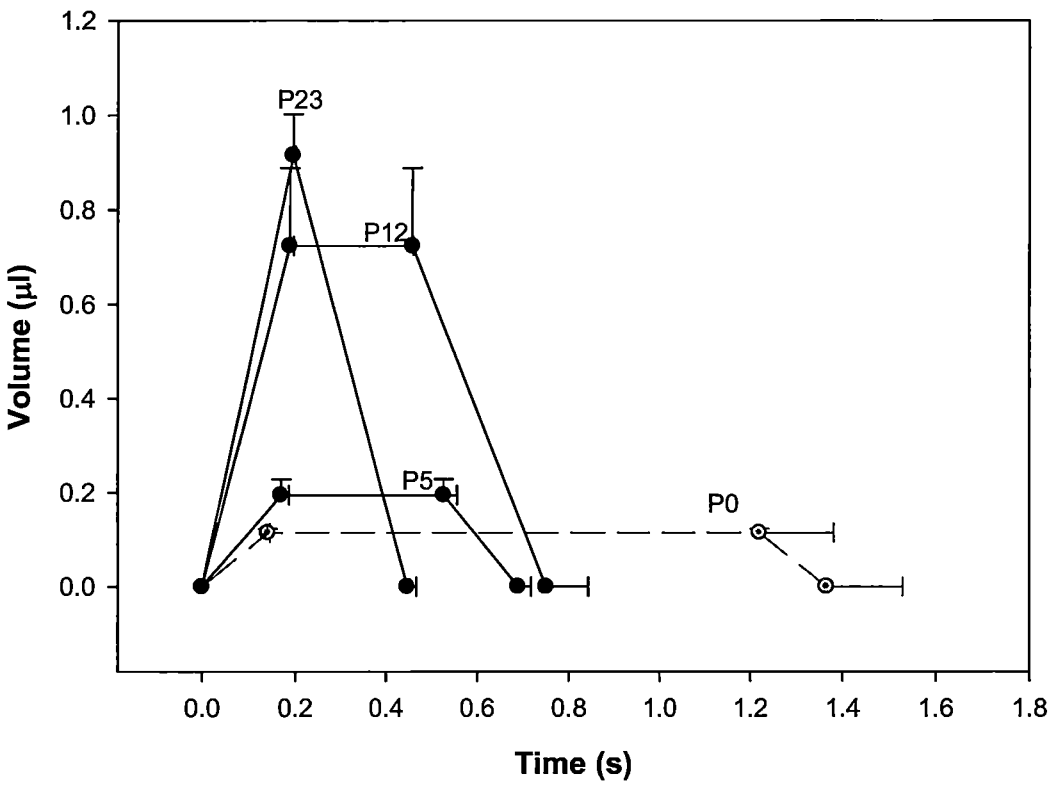
1.2
1.0
0.8
0.6
0.4
0.2
0.0
Volume (µl)
P23
P12
P5
P0
0.0
0.2
0.4
0.6
0.8
1.0
1.2
1.4
1.6
1.8
Time (s)

Figure 5.2 The effects of hypercapnia on breathing and metabolism in the neonatal fat-tailed dunnart.

Shown are convective requirement ($\dot{V}_E/\dot{V}_{O_2}$) (A), mass specific minute ventilation ($\dot{V}_E$) (B) and total mass specific rate of oxygen consumption ($\dot{V}_{O_2}$) (C), in room air and after 5 min exposure to 5 % CO_2 in P0, 5, 12 and 23 fat-tailed dunnarts. Data are presented as means ± 1 S.E.M. * indicates significant difference from air.

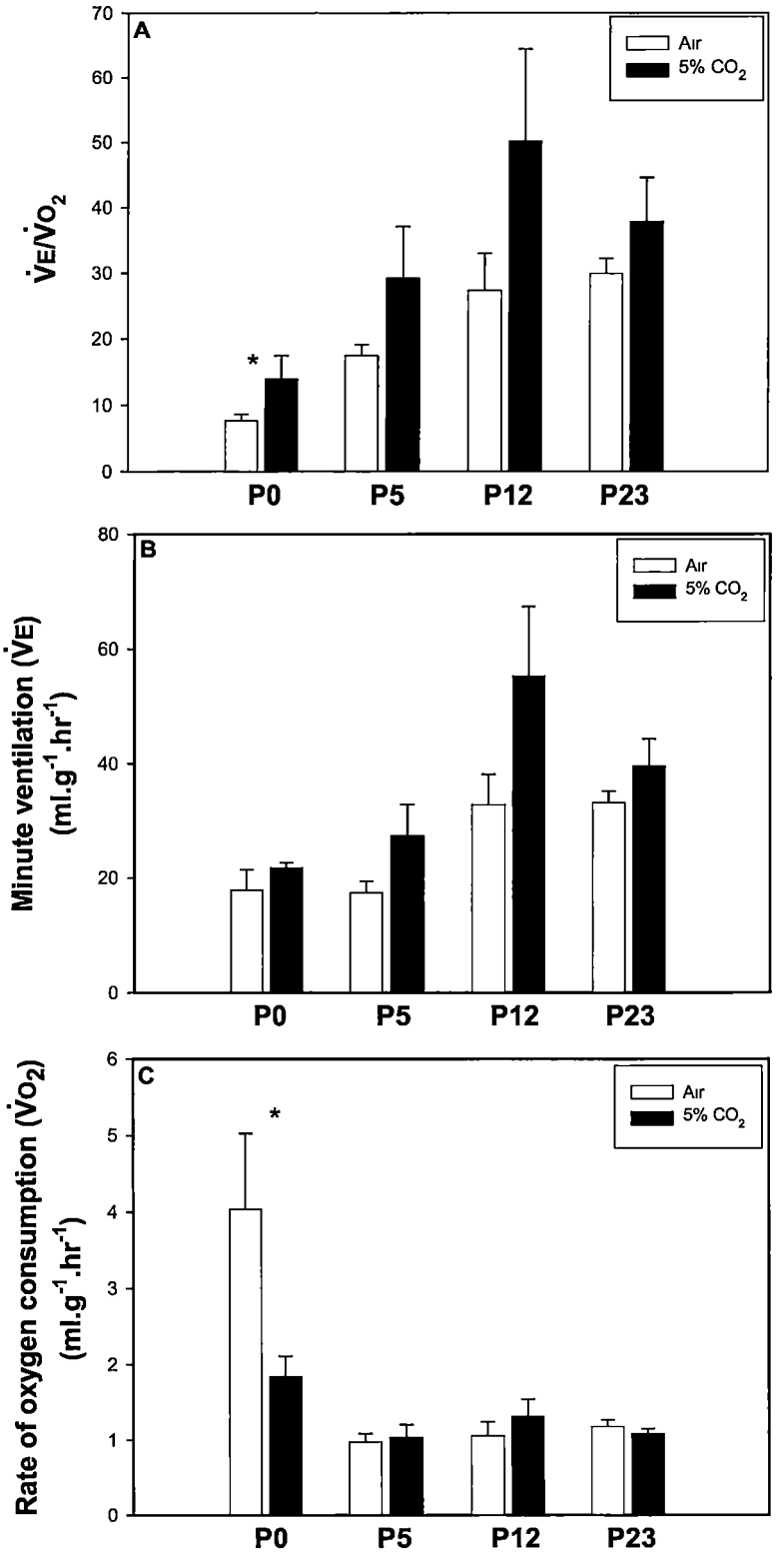
A
Air
5% CO2
V̇E/V̇O2
70
60
50
40
30
20
10
0
*
P0
P5
P12
P23
B
Air
5% CO2
Minute ventilation (V̇E)
(ml.g-1.hr-1)
80
60
40
20
0
P0
P5
P12
P23
C
Air
5% CO2
Rate of oxygen consumption (V̇O2)
(ml.g-1.hr-1)
6
5
4
3
2
1
0
*
P0
P5
P12
P23

Figure 5.3 The effects of hypercapnia exposure on the components of ventilation.

Shown are tidal volume (V_T) (A) and respiratory frequency (B) in room air and after 5 minutes of 5 % CO_2 exposure in the P5, P12 and P23 neonates. Note the significant frequency response at P5, and the tidal volume response at P23. Values are means ± 1 S.E.M. * indicates significant difference from air.

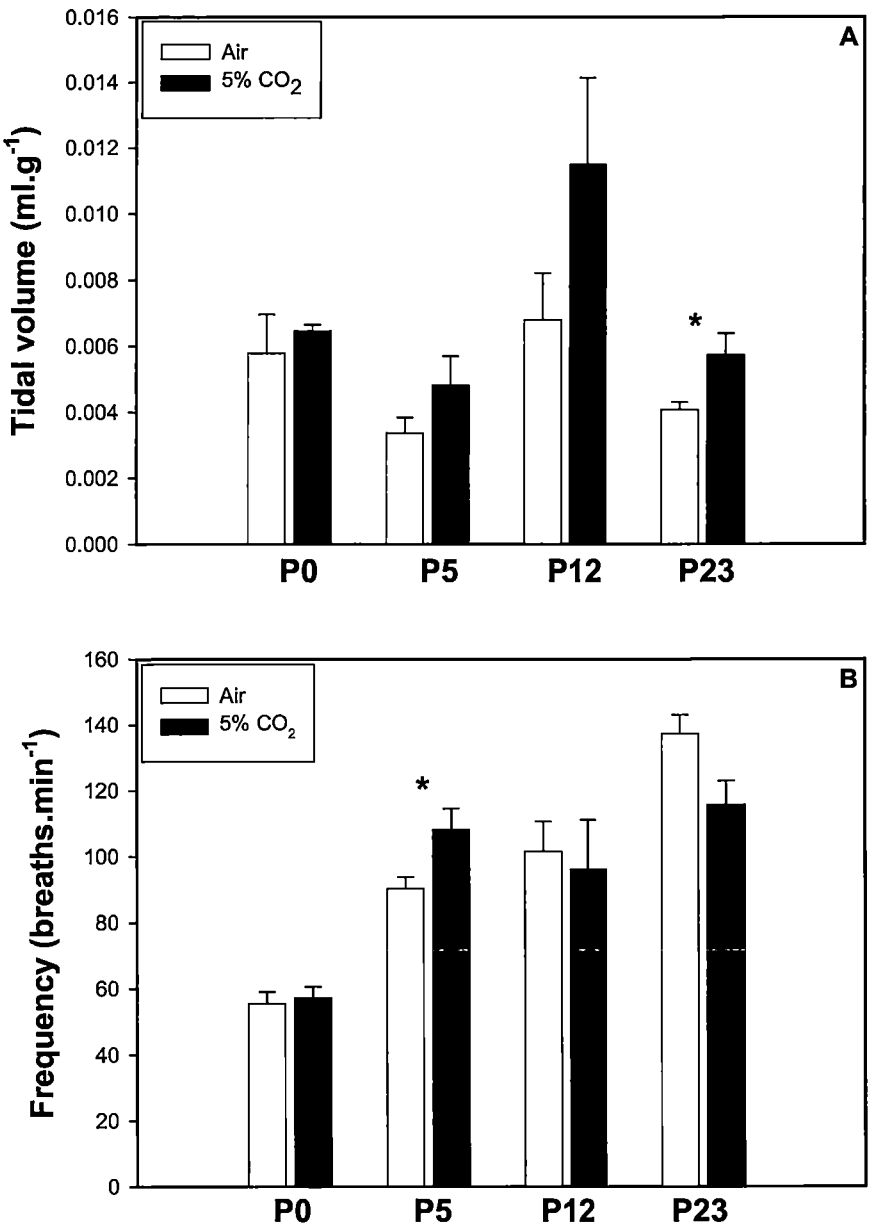
A
Air
5% CO_2
Tidal volume (ml.g^{-1})
0.016
0.014
0.012
0.010
0.008
0.006
0.004
0.002
0.000
*
P0
P5
P12
P23
B
Air
5% CO_2
Frequency (breaths.min^{-1})
160
140
120
100
80
60
40
20
0
*
P0
P5
P12
P23

Figure 5.4 The effects of hypercapnia on respiratory drive and the duty cycle in the neonatal fat-tailed dunnart.

Shown are duty cycle (A) and respiratory drive (B) in room air and after 5 min of 5 % CO_2 in P0, 5, 12 and 23 fat-tailed dunnarts. No significant change in the duty cycle was evident at any age. Respiratory drive was significantly increased upon exposure to 5 % CO_2 in P12 neonates and approached a statistically significant response in P23 neonates (P=0.06). Values are means ± 1 S.E.M. * indicates significant difference from air.

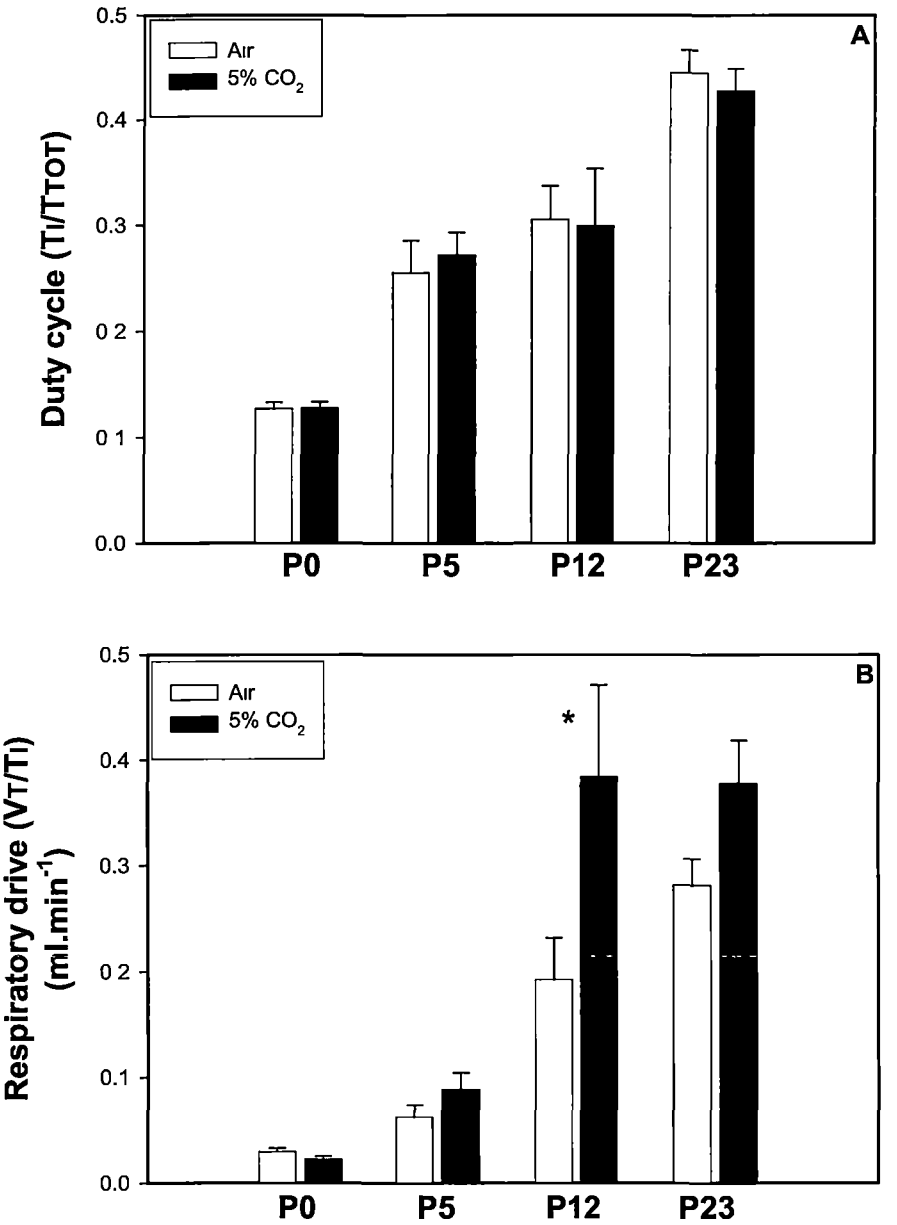
A
Air
5% CO_2
Duty cycle (T_I/T_{TOT})
0.5
0.4
0.3
0.2
0.1
0.0
P0
P5
P12
P23
B
Air
5% CO_2
*
Respiratory drive (V_T/T_I) ($ml.min^{-1}$)
0.5
0.4
0.3
0.2
0.1
0.0
P0
P5
P12
P23

Figure 5.5 The effects of hypoxia on breathing and metabolism in the neonatal fat tailed dunnart.

Shown are the convective requirement (A), minute ventilation (B) and total mass specific rate of oxygen consumption (C) in room air and 10 % O_2 for P0, 5 12 and 23 fat-tailed dunnarts. Ventilation and its components were analysed at 1 and 6 minutes after the onset of exposure. Data are presented as means ± 1 S.E.M. * indicates significant difference from normoxia.

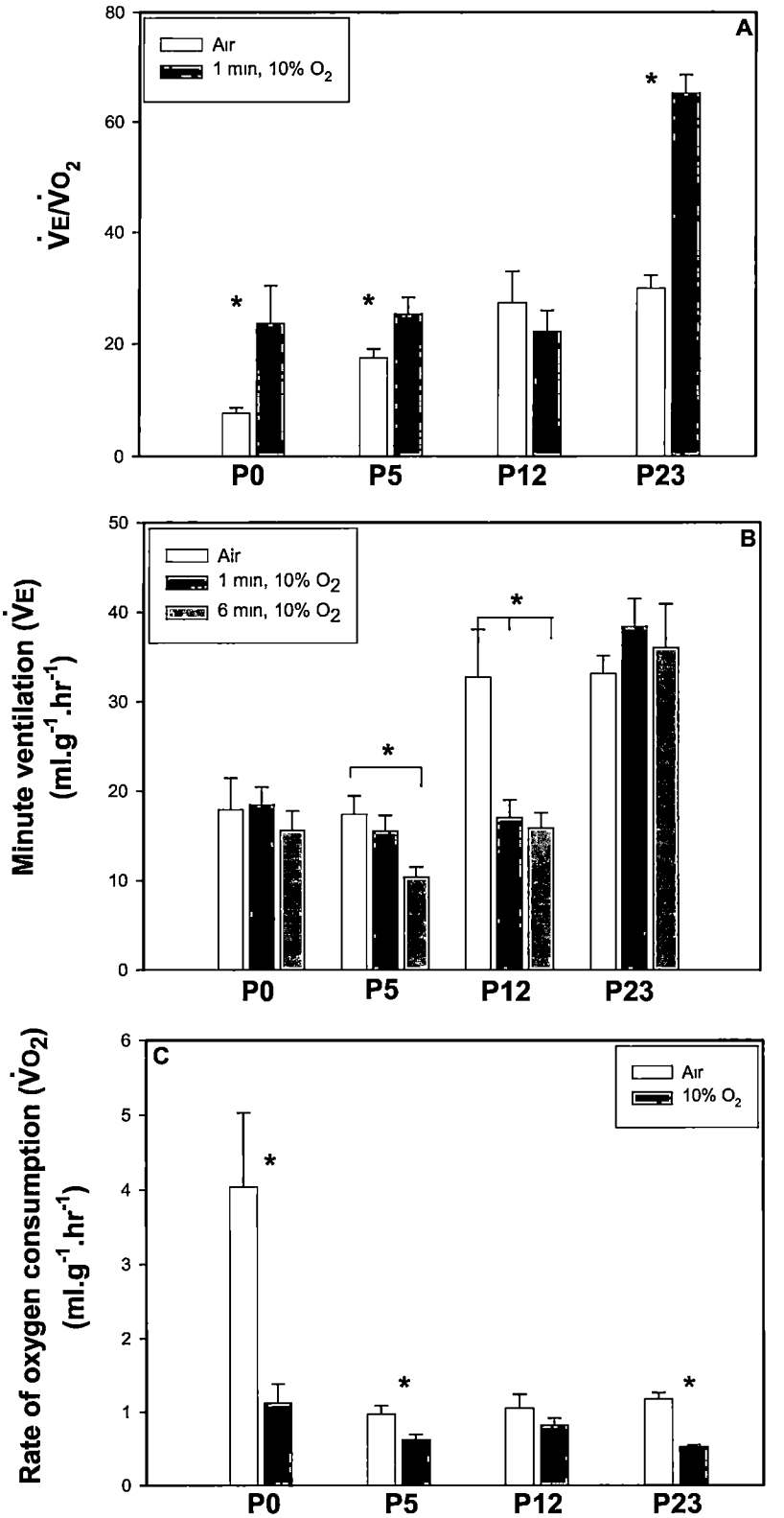
A
Air
1 min, 10% O2
V̇E/V̇O2
80
60
40
20
0
*
*
*
P0
P5
P12
P23
B
Air
1 min, 10% O2
6 min, 10% O2
Minute ventilation (V̇E)
(ml.g-1.hr-1)
50
40
30
20
10
0
*
*
P0
P5
P12
P23
C
Air
10% O2
Rate of oxygen consumption (V̇O2)
(ml.g-1.hr-1)
6
5
4
3
2
1
0
*
*
*
P0
P5
P12
P23

Figure 5.6 The effects of hypoxia on the components of ventilation.

Shown are tidal volume (A) and breathing frequency (B) in response to 10 % O_2 at 1 minute (dark grey) and 6 minutes (light grey) post exposure. No biphasic response to hypoxia was evident. Values are means ± 1 S.E.M. * indicates significant difference from normoxia.

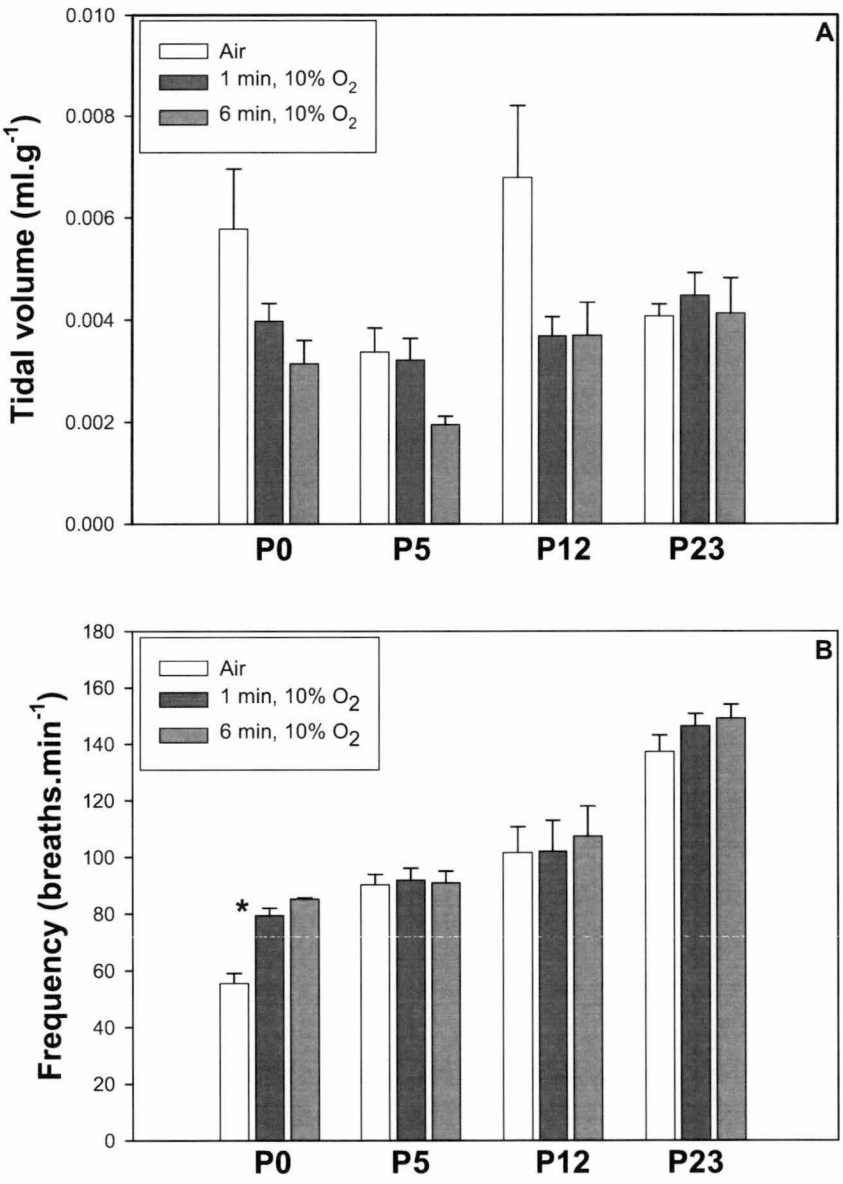
A
Air
1 min, 10% O2
6 min, 10% O2
Tidal volume (ml.g-1)
0.010
0.008
0.006
0.004
0.002
0.000
P0
P5
P12
P23
B
Air
1 min, 10% O2
6 min, 10% O2
Frequency (breaths.min-1)
180
160
140
120
100
80
60
40
20
0
*
P0
P5
P12
P23

Figure 5.7 The effects of hypoxia on respiratory drive and the duty cycle in the neonatal fat-tailed dunnart

Shown are duty cycle (A) and respiratory drive (B) at 1 (dark grey) and 6 (light grey) minutes post exposure to 10 % O_2 in P0, 5, 12 and 23 fat-tailed dunnarts. Presented as means ± 1 S.E.M. * indicates significant difference from normoxia.

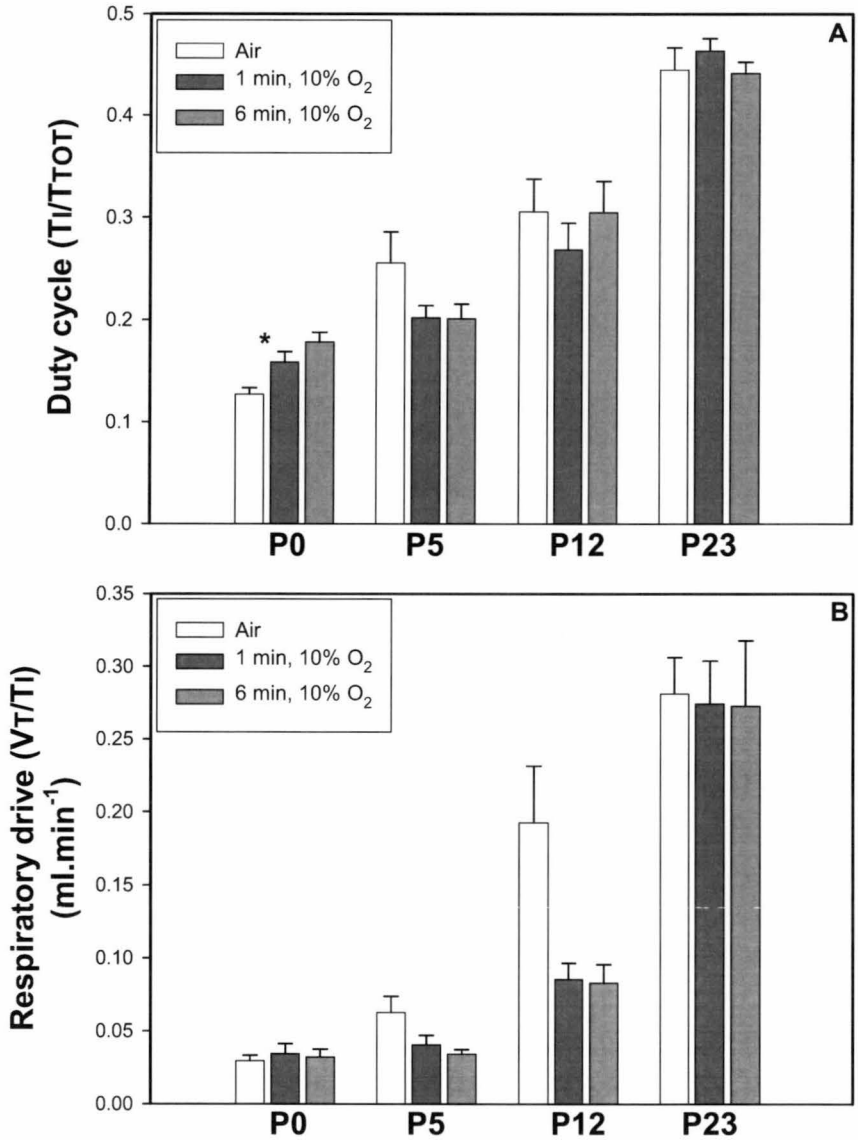
A
Air
1 min, 10% O2
6 min, 10% O2
Duty cycle (TI/TTOT)
0.5
0.4
0.3
0.2
0.1
0.0
*
P0
P5
P12
P23
B
Air
1 min, 10% O2
6 min, 10% O2
Respiratory drive (VT/TI) (ml.min-1)
0.35
0.30
0.25
0.20
0.15
0.10
0.05
0.00
P0
P5
P12
P23

Figure 5.8 Spirograms demonstrating the change in breath-timing and volume in response to hypoxia and hypercapnia in developing fat-tailed dunnart neonates.

Shown are mean control values (air) at P0, 5, 12 and 23 in grey, the effects of hypercapnia (solid black) at 5 minutes and hypoxia at 1 minute (dash black) and 6 minutes (dash-dot black). Error bars represent 1 S.E.M.

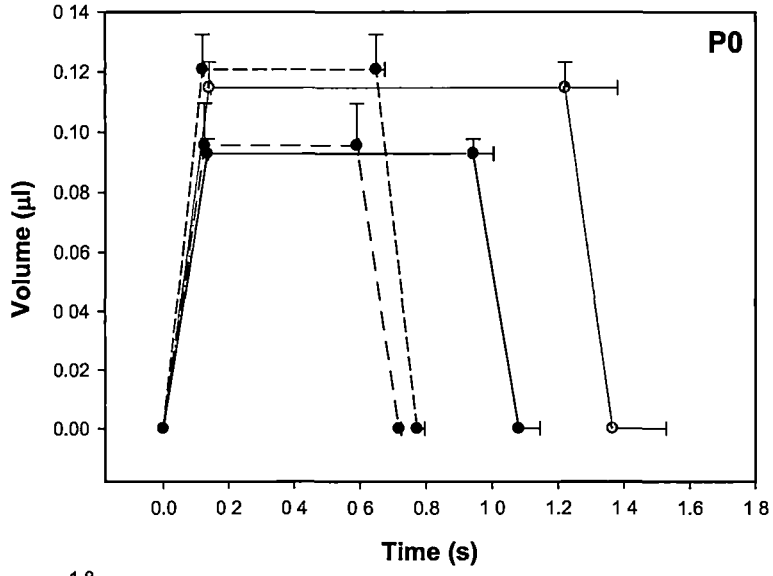
P0
Volume (µl)
Time (s)
0.00
0.02
0.04
0.06
0.08
0.10
0.12
0.14
0.0
0.2
0.4
0.6
0.8
1.0
1.2
1.4
1.6
1.8

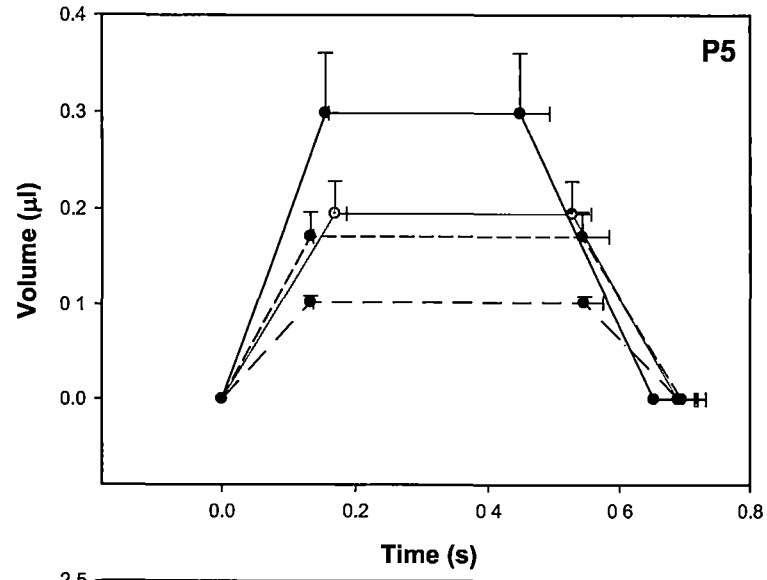
P5
Volume (µl)
Time (s)
0.0
0.1
0.2
0.3
0.4
0.0
0.2
0.4
0.6
0.8

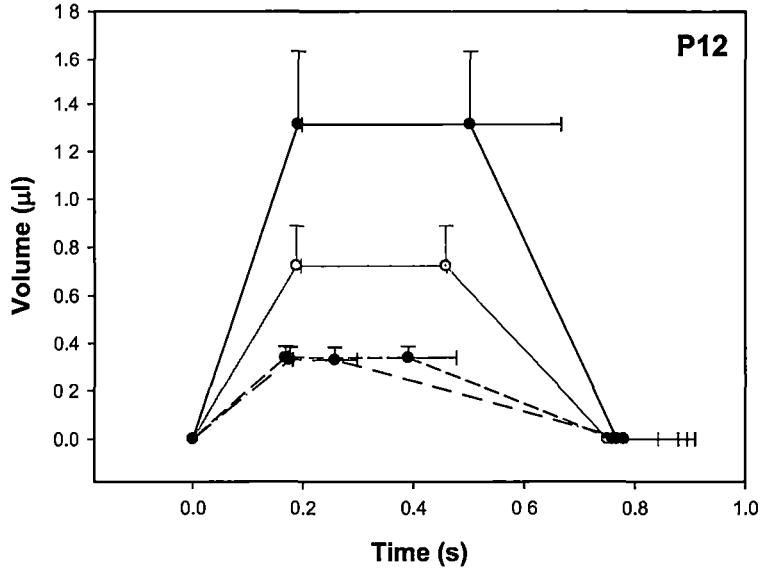
P12
Volume (µl)
Time (s)
0.0
0.2
0.4
0.6
0.8
1.0
1.2
1.4
1.6
1.8
0.0
0.2
0.4
0.6
0.8
1.0

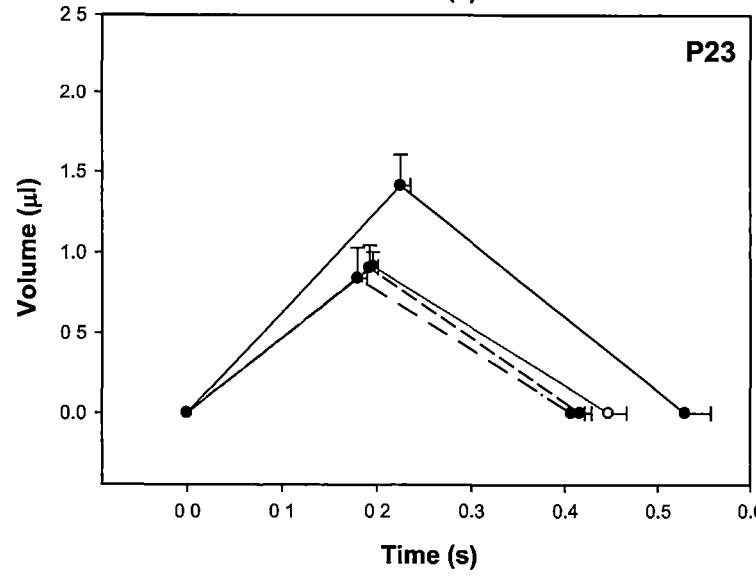
P23
Volume (µl)
Time (s)
0.0
0.5
1.0
1.5
2.0
2.5
0.0
0.1
0.2
0.3
0.4
0.5
0.6

5.4 DISCUSSION:

5.4.1 Development of the breathing pattern

The breathing pattern of the fat-tailed dunnart undergoes change with postnatal development. For example, the post-inspiratory pause diminishes, and the inspiratory time (T_I) is lengthened; with the progressive lengthening of T_I reported in neonates of several species, including the opossum (Farber, 1988), mice and rabbits (Mortola, 1984). The neonatal dunnart also undergoes an increase in tidal volume and breathing frequency, with the latter largely due to the decrease of the post-inspiratory pause; presumably as the breath hold is no longer required to aid in maximising gas exchange across an immature lung parenchyma. With the inconsistencies of breathing in the P0 neonates, along with low frequencies we have previously postulated that these movements are more likely to be preparing the musculature for breathing, as is the case with fetal breathing movements, rather than participating in alveolar gas exchange. DiPasquale et al., (1996) demonstrated that the firing frequency and stability of medullary respiratory neurons increases markedly in rats from E18 to birth (reviewed in Hiliare and Duron, 1999) with fetal networks oscillating at a slower rate than neonatal networks because of age dependent differences in the rhythmogenic neurones/network, fetal network activity being suppressed by endogenous inhibitory modulators, or under developed modulatory systems that provide excitatory drive to the respiratory networks (Greer et al., 2006). It is possible that the short gestation of 13 days has not allowed for complete development of the rhythmogenic neurons/network or modulators of respiration including the chemoreceptors. The ability to exchange gas across the skin

perhaps renders this lack of development inconsequential. Lower than expected $\dot{V}_E / \dot{V}_{O_2}$ in the early neonatal period, and the subsequent increase over development, is indicative that the pulmonary ventilation is not meeting the metabolic needs of the newborn at a time when cutaneous gas exchange plays an important role in providing O_2 and removing CO_2.

5.4.2 The effects of hypercapnia on breathing and metabolism

Newborns generally exhibit an attenuated ventilatory response to hypercapnia (and hypoxia) in comparison to adults; a phenomenon attributable to the immaturity of the chemoreceptors (Carroll et al., 1993; Green et al., 2008). The response to CO_2 is limited in the neonatal fat-tailed dunnart with only P0 animals exhibiting a significant increase in $\dot{V}_E / \dot{V}_{O_2}$ with inhalation of 5 % CO_2, which is the result of a significant decrease in $\dot{V}_{O_2}$. Although there was no significant effect of CO_2 on $\dot{V}_E$ across any age, P5, P12 and P23 animals tended to have a response. Indeed, at P12 there was a significant effect of CO_2 on respiratory drive, a significant effect on f at P5 and a significant increase in V_T in P23 dunnarts, all of which are components of $\dot{V}_E$.

In some species, including the fat-tailed dunnart, the ventilatory response to hypoxia is absent in the newborn (see Figure 5.5B), however a ventilatory response is still present in response to CO_2 (Mortola and Lanthier, 1996b; Watanabe et al., 1996) with hypercapnia promoting deep breathing (Brady and Dunn, 1970; Guthrie et al., 1985; Saetta and Mortola, 1987) with little effect on metabolism (Mortola and Lanthier, 1996). The hypercapnic induced hypometabolism observed in the P0 dunnart has also been

reported in another marsupial, the P5 opossum, though in the opossum the hypometabolism was in conjunction with a hyperpnoea (Farber et al., 1972). This hypometabolism is employed as a strategy to hyperventilate (*i.e.* increase $\dot{V}_E/\dot{V}_{O_2}$) in these very small and underdeveloped newborns; possibly because the mechanical constraints to breathe (MacFarlane et al., 2002) lead to an inability to sufficiently increase $\dot{V}_E$. Similarly for human infants born preterm, CO_2 responsiveness appears to increase progressively after birth (Rigatto et al., 1991), although whether this is actually due to an increase in CO_2 sensitivity or to improved lung function and rib caged stability remains uncertain. Indeed, a significant increase in tidal volume in response to CO_2 was not evident in the dunnart until P23 adding further weight to the idea that mechanical constraint, particularly chest wall distortion, may be responsible for the attenuation of the $\dot{V}_E$ response to hypercapnia. By P12, the CO_2 induced hyperpnoea was largely the result of increased V_T and a resultant increase in respiratory drive (V_T/T_I) was present, with no change in timing (T_I/T_{TOT}) which is suggestive of an increase in respiratory centre output caused by central, rather than peripheral, stimulation of the CO_2 receptors (Rigatto et al., 1981).

Interestingly, adult marsupials demonstrate a blunted response to inspired CO_2, with the response presumably further attenuated in neonates, possibly accounting for the low ventilatory response to CO_2 in the fat-tailed dunnart neonates. This blunted response may be a result of differences in chemoreception, blood buffering capacity or the fact that much of their neonatal development occurs in the pouch (Frappell and Baudinette, 1995; Frappell et al., 2002). The possibility of increased hypercapnia exposure in the

closed pouch environment may be particularly important, with diving and burrowing mammals showing relative insensitivity to CO_2, due to adaptations caused by chronic or intermittent hypercapnia (Boggs et al., 1984; Frappell et al., 2002). While it is possible for the maternal pouch to become hypoxic and hypercapnic, the gaseous composition barely differs from ambient in the pouch of the tammar wallaby during the first 20 postnatal days (Baudinette et al., 1988a), and so is unlikely to account for the attenuated response in adult or neonatal fat-tailed dunnarts. It is also possible that we see an attenuated response to 5 % CO_2 due to the fact that we could not analyse ventilation earlier than 5 minutes post exposure. A study on neonatal rats shows that the maximal response to 8 % CO_2 occurs at 2-3 minutes (Cummings and Frappell, 2009) post exposure, with a slight decline by 5 minutes. Given the comparatively developed state of the neonatal rat, it may be that the decline in ventilatory response occurs at an early time post-exposure in the neonatal dunnart. There is also some evidence to suggest that a size dependency of the $\dot{V}_E$ response to CO_2 exists, with larger newborns possessing a greater ventilatory response than smaller ones (Mortola and Lanthier, 1996).

5.4.3 The effects of hypoxia on breathing and metabolism

Much like hypercapnia, hypoxia had little effect on ventilation at any age with no hyperpnoea exhibited. In fact, hypoxia had a suppressive effect on $\dot{V}_E$, with a sustained decrease in minute ventilation, a response also reported in very small preterm infants (<1500 g) (Alvaro et al., 1992). Regardless, hypoxia still led to a hyperventilatory response (increase in $\dot{V}_E/\dot{V}_{O_2}$) in all but the P12 neonates, owing to its suppressive effects on $\dot{V}_{O_2}$. As with hypercapnia, there is a tendency for the magnitude of the hyperpnoea to be

inversely related to mass specific metabolic rate; that is the hyperpnoea is more pronounced in larger species than in smaller ones (Mortola et al., 1989; Frappell et al., 1992; Gautier, 1996), while the hypometabolism is negatively correlated with size (Mortola et al., 1994). The magnitude of the hyperpnoea in newborns also reflects the maturity of the peripheral chemoreceptors, and hence the degree of neonatal precocity, so it is not entirely surprising that the ventilatory response is absent in the altricial neonatal dunnart. Interestingly, a ventilatory response to hypoxia was not reported in the adult fat-tailed dunnart either, with $\dot{V}_E$ dropping below normoxic levels (Frappell et al., 1992), raising questions about this species' ability to achieve a hypoxic ventilatory response and indicating that perhaps the carotid body of the dunnart is generally less functional.

The overall lack of hyperpnoea during hypoxia in newborns implies that either the chemoafferent input is minimal, or that their inputs are suppressed centrally. Why $\dot{V}_E$ in P5 and P12 dunnarts is suppressed during hypoxia while P0 and P23 animals maintain $\dot{V}_E$ is not known. It has been suggested that central neural inhibition is responsible for the secondary suppression of $\dot{V}_E$ in other animals during hypoxia (Blanco et al., 1984; Coles and Dick, 1996). This could be owing to cessation of phrenic activity due to changes in the release of neurotransmitters onto brainstem respiratory neurons (St-John et al., 1999; Koos et al., 2005). Changes in compliance with hypoxia, leading to an inhibition of the V_T and thus $\dot{V}_E$ responses, have been mostly discounted, despite early studies showing that neonatal exposure to acute hypoxia led to an increase in mechanical impedance (LaFramboise et al., 1983). Contributions from fatigue of the respiratory

muscles, depression of the respiratory neurons, and failure of the peripheral chemoreceptors have also been discounted (Lawson and Long, 1983; Blanco et al., 1984). It should however be noted that all animals used in these previous studies were anesthetised, which changes the activity of respiratory neurons, and the responsiveness of the chemoreceptors.

Despite the lack of ventilatory response, the hypometabolic response observed in the fat-tailed dunnarts is similar to that observed in other species, and is sufficient to increase $\dot{V}_E/\dot{V}_{O_2}$ for the preservation of tissue oxygenation and acid-base balance. Whether the decrease in $\dot{V}_{O_2}$ during hypoxia exposure negates the need for an increase in $\dot{V}_E$ or the whether the absence of a ventilatory response drives the hypometabolism remains unknown. Hypometabolism during hypoxia is an effective strategy as it conserves O_2, but it also lowers tissue CO_2 production, which depresses respiratory drive. It also decreases body temperature and other O_2 dependent functions such as maintenance of muscle tone, cell excitability, tissue development and organ growth (Mortola, 2004). By conserving O_2 delivery to central organs, neonates are more able to protect themselves against the hypoxic challenge, however, an increase in ventilation would promote the delivery of O_2 to the mitochondria for the generation of ATP (Frappell et al., 1992). In some cases, such as in the neonatal dunnart, the hypoxic hypometabolism is so pronounced that $\dot{V}_E$ can fall below the normoxic level (Mortola et al., 1989; Mortola, 1993).

The P12 dunnart produces an unusual response to hypoxia with no increase in convective requirement observed. This response has also been noted in P13 rats where an increase

in $\dot{V}_E/\dot{V}_{O_2}$ was absent, similarly due to a decrease in tidal volume; a response that was different from the rest of the first 3 postnatal weeks (Liu et al., 2002; Wong-Riley et al., 2005). In addition, a comparatively weak metabolic response to hypoxia was also noted in the P13 rat (Liu et al., 2002; Wong-Riley et al., 2005) and P12 dunnart. The inadequate response to hypoxia at P12 (dunnart) and P13 (rat) is indicative of a critical period in the development of the respiratory system. In fact, during this time a reduction in excitatory and increase in inhibitory neurotransmitters has been reported in the rat (Wong-Riley and Liu, 2005). The considerable decrease in V_T/T_I in P12 dunnarts implies that there is a reduction in central respiratory output, which may be related to an increase in inhibitory neurotransmitters, as is the case with the rat neonate (Wong-Riley and Liu, 2005). Neurotransmitters often elicit a different response in neonates than they do in adults (Bonham, 1995). For example, in the newborn opossum glutamate injected into the brainstem induces respiratory pauses, however when injected into an older animal is clearly stimulatory (Farber, 1990). Similarly inhibitory neurotransmitters such as γ-aminobutyric acid (GABA) also have age-dependent effects in the opossum and many other species with GABA having an excitatory effect in the neurons of the newborn, switching to an inhibitory effect in the mature neuron (Michelson and Wong, 1991). At this time in development (P12-13), a switch in GABA receptor subunit expression, a spike in body temperature and increases in metabolic rate (Liu et al., 2002) and ventilation (Wong-Riley et al., 2005) all occur, along with significant decline in tryptophan hydroxylase and serotonin transporter immunoreactivity (Liu and Wong-Riley, 2010b, 2010a), suggesting that normal development can contribute to a narrow window of vulnerability in animals at this postnatal age. These transient changes consequently

result in a system that is less capable of responding to respiratory challenges like hypoxia during a narrow postnatal window which has particular implications for sudden infant death syndrome (SIDS).

In summary, the newborn fat-tailed dunnart exhibits a very low $\dot{V}_E/\dot{V}_{O_2}$ which increases with age. In addition, their ventilatory response to hypoxic and hypercapnic challenge is severely blunted throughout early postnatal life, suggesting that the chemoreflexes are still less capable than anticipated at P23. The lack of chemoresponse may be due to a lack of chemoreceptor development, a failure to properly reset after birth in the relatively hyperoxic environment, or possibly due to mechanical constraint impeding the hyperpnoea. Decreased ability to hyperventilate via a hyperpnoea is overcome by the hypometabolic response to hypoxia at all ages, and to hypercapnia at P0, thereby maintaining tissue oxygenation and pH. The low $\dot{V}_E/\dot{V}_{O_2}$ and subsequent need for the dunnart to rely heavily on skin gas exchange during early life may be partially attributed to the general lack of chemosensitivity.

6 CONCLUDING REMARKS

In most mammals, the respiratory system is required to be sufficiently developed at birth, allowing respiration to meet metabolic demands in a highly compliant chest wall, even with the inherent instabilities of neonatal breathing and in the face of challenges to the respiratory system. However, the newborn fat-tailed dunnart relies almost solely on the skin for gas exchange, with less than 35 % of newborn dunnarts observed to make any respiratory effort; with these small and inconsistent efforts more likely to be equivalent to fetal breathing movements. The inefficient pulmonary ventilation does not meet the neonates' oxygen requirements until between P23 and P35; however this may be of little consequence at a time when the skin can play an important role in providing O_2 and removing CO_2. Skin gas exchange is limited to neonates weighing less than 1 gram, with the small body size and large surface area to volume ratio, along with the low metabolic demands, highly vascularised skin and postnatal presence of cardiovascular shunts all playing a role in successful cutaneous gas exchange.

Any one, or more, of the steps in the oxygen cascade can limit the delivery of O_2 to the mitochondria and consequently contribute to the need for cutaneous gas exchange as an alternative mechanism to deliver O_2. For example, the lack of structural maturity of the respiratory system may render cutaneous gas exchange a necessity in the very small newborn marsupial. At birth, the lungs of the fat-tailed dunnart are nothing more than a few tubular structures, with thick septal walls and a double capillary network, indicative of a lung at the canalicular stage of lung development. The decrease in diffusing capacity due to capillary placement, as well as the decreased surface area available for gas exchange, may present limiting steps in the pathway. In addition, the mechanical

properties of the respiratory pump may also limit the ability of the lungs to efficiently uptake oxygen and therefore limit O_2 delivery.

In the fat-tailed dunnart a sufficiently developed double capillary network was in place with the capillaries in close proximity to the overlying epithelial cells by P45, and thus a functional air-blood barrier established at this time. Interestingly, this age also corresponds to the time when the skin no longer plays a role in gas exchange (~1.2 g) and the first secondary septal crests, and consequently alveoli, were observed. As a consequence of delayed alveolarisation, the surface area available for gas exchange was lower than predicted from allometric equations; suggesting that increased diffusing capacity and decreased surface area to exchange gas both play a role in limiting O_2 availability. Indeed, alveolarisation generally occurs over an extended period of time in marsupials, with well developed alveoli present at the time of pouch vacation; the timing of which also corresponds to the attainment of endothermy and the associated increase in demand for oxygen.

The lung volumes of the newborn marsupials studied here-in were also lower than expected until a body mass of 1 g was reached; the same time that the lung becomes 100 % responsible for gas exchange. The finding of a low lung volume in the marsupial neonate further supports the maxim that cutaneous gas exchange occurs in the marsupial neonate because the respiratory apparatus is not yet capable of meeting the gas exchange requirements of the newborn. There are numerous consequences to low lung volumes in newborns, including the fact that the air sacs have a much greater tendency to collapse. Newborns often minimise this potential problem by maintaining a

dynamic elevation of functional residual capacity above resting lung volume; a strategy that is particularly pronounced in the newborn marsupial (once a regular breathing pattern is established), with the characteristic post-inspiratory pause. Increasing the time frame for gas exchange would also be particularly important for the neonatal dunnart with structurally immature lungs, thereby increasing diffusion time and consequently the capacity to exchange gas.

Despite the primitive appearance of the general lung structure, some secreted surfactant coils were detected in the airways of the fat-tailed dunnart on the first day of life, and the proportion of Alveolar Epithelial Cells (AECs) was remarkably mature with less than 7 % of the AECs undifferentiated at birth (although the presence of glycogen indicates a very recent differentiation).These factors indicate that the epithelial cells are sufficiently differentiated to allow respiration and are not a barrier to pulmonary gas exchange, although the thickened cytoplasmic extensions of Type-I AECs does contribute to the increased diffusion capacity.

In conclusion, a lower than expected convective requirement (minute ventilation / rate of oxygen consumption), low lung volumes and surface areas, delayed fluid clearance from the airways, immature lung structure and vasculature, mechanical distortion and the absence of a reliably expressed breathing pattern at birth point towards constraints on the respiratory system. In addition, the neonates' ventilatory response to hypoxia and hypercapnia was severely blunted, suggesting that the chemoreflexes are not sufficiently developed in the neonate. The lack of chemoresponse generally implies that either chemoafferent input is minimal, or that their inputs are suppressed centrally, possibly

due to either a lack of chemoreceptor development, or a failure to properly reset after birth. However, it is important to remember that mechanical constraint may limit the neonates' ability to mount a ventilatory response when confronted with a challenge and therefore be confused with a lack of chemosensitivity. Despite the lack of ventilatory response, the hypometabolic response observed in the fat-tailed dunnart is sufficient to increase convective requirement during hypoxia (and hypercapnia for the P0 neonate), for the preservation of tissue oxygenation and acid-base balance. Whether the hypometabolism negates any need for a ventilatory response, or the whether the absence of a ventilatory response drives the hypometabolism could be explored in future studies by pharmacologically elevating the metabolic rate during hypoxia using the uncoupling agent 2,4-dinitrophenol.

While the findings presented within indicate that a central rhythm generator exists to some degree, and that the phrenic nerve has made contact with the diaphragm, it is not yet known whether the 13 day gestation is sufficient for the development of the neuromuscular machinery required to drive ventilation, or if the breaths are not being manifested due to some sort of central inhibition in the smallest marsupial newborns.

7 REFERENCES

Allan DW, Greer JJ. 1997a. Development of phrenic motoneuron morphology in the fetal rat. J Comp Neurol 382:469-479.

Allan DW, Greer JJ. 1997b. Embryogenesis of the phrenic nerve and diaphragm in the fetal rat. Journal of Comparative Neurology 382:459-468.

Allan DW, Greer JJ. 1998. Polysialylated NCAM expression during motor axon outgrowth and myogenesis in the fetal rat. J Comp Neurol 391:275-292.

Alvaro R, Alvarez J, Kwiatkowski K, Cates D, Rigatto H. 1992. Small preterm infants (less than or equal to 1500 g) have only a sustained decrease in ventilation in response to hypoxia. Pediatr Res 32:403-406.

Andrewartha SJ, Mitchell NJ, Frappell PB. 2008. Phenotypic differences in terrestrial frog embryos: effect of water potential and phase. J Exp Biol 211:3800-3807.

Avery ME, Cook CD. 1961. Volume-pressure relationships of lungs and thorax in fetal, newborn, and adult goats. J Appl Physiol 16:1034-1038.

Bartlett D, Areson J. 1977. Quantitative lung morphology in newborn mammals. Respiration Physiology 29:193-200.

Bartlett JD. 1971. Origin and regulation of spontaneous deep breaths. Respiration Physiology 12:230-238.

Baudinette RV, Gannon BJ, Ryall RG, Frappell PB. 1988a. Changes in metabolic rates and blood respiratory characteristics during pouch development of a marsupial, Macropus eugenii. Respiration Physiology 72:219-228.

Baudinette RV, Runciman SIC, Frappell PB, Gannon BJ. 1988b. Development of the marsupial cardiorespiratory system. In: Tyndale-Biscoe CH, Janssens PA, editors. The Developing Marsupial. Models for Biomedical Research. Berlin: Springer-Verlag. p Chapter 10: 132-147.

Bennett JH, Breed WG, Hayman DL, Hope RM. 1990. Reproductive and Genetical Studies with a Laboratory Colony of the Dasyurid Marsupial Sminthopsis-Crassicaudata. Australian Journal of Zoology 37:207-222.

Blanco CE, Hanson MA, Johnson P, Rigatto H. 1984. Breathing pattern of kittens during hypoxia. J Appl Physiol 56:12-17.

Boggs DF, Kilgore DL, Birchard GF. 1984. Respiratory physiology of burrowing mammals and birds. Comparative Biochemistry & Physiology 77A:1-7.

Bonham AC. 1995. Neurotransmitters in the CNS control of breathing. Respir Physiol 101:219-230.

Bonora M, Boule M, Gautier H. 1994. Ventilatory strategy in hypoxic or hypercapnic newborns. Biol Neonate 65:198-204.

Bostrom H, Willetts K, Pekny M, Leveen P, Lindahl P, Hedstrand H, Pekna M, Hellstrom M, Gebre-Medhin S, Schalling M, Nilsson M, Kurland S, Tornell J, Heath JK, Betsholtz C. 1996. PDGF-A signaling is a critical event in lung alveolar myofibroblast development and alveogenesis. Cell 85:863-873.

Boyden EA. 1977. Development and growth of the airways. In: Hodson WA, editor. Development of the lung. New York: Dekker. p 3-35.

Brady JP, Dunn PM. 1970. Chemoreceptor reflexes in the newborn infant: effect of CO2 on the ventilatory response to hypoxia. Pediatrics 45:206-214.

Bucher U, Reid L. 1961a. Development of the intrasegmental bronchial tree: the pattern of branching and development of cartilage at various stages of intra-uterine life. Thorax 16:207-218.

Bucher U, Reid L. 1961b. Development of the mucus-secreting elements in human lung. Thorax 16:219-225.

Burri PH. 1984. Fetal and postnatal development of the lung. Annual Review of Physiology 46:617-628.

Burri PH. 1997. Structural aspects of prenatal and postnatal development and growth of the lung. In: McDonald JA, editor. Lung growth and development. New York: Marcel Dekker Inc.

Burri PH. 2006. Structural aspects of postnatal lung development - alveolar formation and growth. Biol Neonate 89:313-322.

Burri PH, Dbaly J, Weibel ER. 1974. The postnatal growth of the rat lung. I. Morphometry. Anatomical record 178:711-730.

Calvert S, Holland R, Hinds L. 1993. Blood O2 transport and Hb types in the embryonic tammar wallaby (Marsupialia, Macropus eugenii). Respiration Physiology 91:99-109.

Calvert SJ, Holland RAB, Gemmell RT. 1994. Respiratory properties of the neonatal blood of the common brushtail possum (Trichosurus vulpecula). Physiological Zoology 67:407-417.

Carroll JL, Bamford OS, Fitzgerald RS. 1993. Postnatal maturation of carotid chemoreceptor responses to O2 and CO2 in the cat. J Appl Physiol 75:2383-2391.

Carroll JL, Fitzgerald RS. 1993. Carotid chemoreceptor responses to hypoxia and hypercapnia in developing kittens. Adv Exp Med Biol 337:387-391.

Castleman WL, Lay JC. 1990. Morphometric and ultrastructural study of postnatal lung growth and development in calves. American Journal of Veterinary Research 51:789-795.

Clements JA, Hustead RF, Johnson RP, Gribetz I. 1961. Pulmonary surface tension and alveolar stability. Tech Rep CRDLR US Army Chem Res Dev Lab 3052:1-24.

Coles SK, Dick TE. 1996. Neurones in the ventrolateral pons are required for post-hypoxic frequency decline in rats. J Physiol 497 (Pt 1):79-94.

Comroe JHJ. 1939. The location and function of the chemoreceptors of the aorta. Am J Physiol 127:176.

Cummings KJ, Frappell PB. 2009. Breath-to-breath hypercapnic response in neonatal rats: temperature dependency of the chemoreflexes and potential implications for breathing stability. Am J Physiol Regul Integr Comp Physiol 297:R124-134.

Davies P, Reid L, Lister G, Pitt B. 1988. Postnatal growth of the sheep lung: A morphometric study. The anatomical record 220:281-286.

Davis SE, Solhied G, Castillo M, Dwinell M, Brozoski D, Forster HV. 2006. Postnatal developmental changes in CO2 sensitivity in rats. J Appl Physiol 101:1097-1103.

De Leo AA, Lefevre C, Topcic D, Pharo E, Cheng JF, Frappell P, Westerman M, Graves JA, Nicholas KR. 2006. Characterization of two whey protein genes in the Australian dasyurid marsupial, the stripe-faced dunnart (Sminthopsis macroura). Cytogenet Genome Res 115:62-69.

Dejours P. 1975. Principles of comparative physiology. Amsterdam: North-Holland Publishing Co. .

Deutsch GH, Pinar H. 2002. Perinatal Lung Development. In: Voelkel NF, MacNee W, editors. Chronic Obstructive Lung Diseases. Hamilton, Ontario: BC Decker. p 7-20.

Eichenwald EC, Ungarelli RA, Stark AR. 1993. Hypercapnia increases expiratory braking in preterm infants. J Appl Physiol 75:2665-2670.

Eugenin J, Nicholls JG. 2000. Control of respiration in the isolated central nervous system of the neonatal opossum, Monodelphis domestica. Brain Research Bulletin 53:605-613.

Farber JP. 1972. Development of pulmonary reflexes and pattern of breathing in the Virginia opossum. Respiration Physiology 14:278-286.

Farber JP. 1978. Laryngeal effects and respiration in the suckling opossum. Respiration Physiology 35:189-201.

Farber JP. 1988. Medullary inspiratory activity during opossum development. Am J Physiol Regul Integr Comp Physiol 254:R578-584.

Farber JP. 1990. Effects on breathing of rostral pons glutamate injection during opossum development. Journal of applied physiology 69:189-195.

Farber JP. 1993. Maximum discharge rates of respiratory neurons during opossum development. J Appl Physiol 75:2040-2044.

Farber JP, Hultgren HN, Tenney SM. 1972. Development of the chemical control of breathing in the Virginia opossum. Respiration Physiology 14:267-277.

Feder ME, Burggren WW. 1985. Skin Breathing in Vertebrates. Scientific American 253:126.

Feldman JL, Janczewski WA. 2006. Point:Counterpoint: The parafacial respiratory group (pFRG)/pre-Botzinger complex (preBotC) is the primary site of respiratory rhythm generation in the mammal. Counterpoint: the preBotC is the primary site of respiratory rhythm generation in the mammal. J Appl Physiol 100:2096-2097; discussion 2097-2098, 2103-2098.

Feldman JL, Mitchell GS, Nattie EE. 2003. Breathing: rhythmicity, plasticity, chemosensitivity. Annu Rev Neurosci 26:239-266.

Ferner K, Zeller U, Renfree MB. 2009. Lung development of monotremes: evidence for the mammalian morphotype. Anat Rec (Hoboken) 292:190-201.

Fisher J, Mortola J. 1980. Statics of the respiratory system in newborn mammals. Respiration Physiology 41:155-172.

Flecknoe S, Harding R, Maritz G, Hooper SB. 2000. Increased lung expansion alters the proportions of type I and type II alveolar epithelial cells in fetal sheep. American Journal of Physiology - Lung Cellular & Molecular Physiology 278:L1180-L1185.

Flecknoe SJ, Wallace MJ, Cock ML, Harding R, Hooper SB. 2003. Changes in alveolar epithelial cell proportions during fetal and postnatal development in sheep. Am J Physiol Lung Cell Mol Physiol 285:L664-670.

Frappell P, Lanthier C, Baudinette RV, Mortola JP. 1992. Metabolism and ventilation in acute hypoxia: a comparative analysis in small mammalian species. American Journal of Physiology 262:R1040-R1046.

Frappell PB. 2008. Ontogeny and allometry of metabolic rate and ventilation in the marsupial: matching supply and demand from ectothermy to endothermy. Comp Biochem Physiol A Mol Integr Physiol 150:181-188.

Frappell PB, Baudinette RV. 1995. Scaling of respiratory variables and the breathing pattern in adult marsupials. Respiration Physiology 100:83-90.

Frappell PB, Baudinette RV, MacFarlane PM, Wiggins PR, Shimmin G. 2002. Ventilation and metabolism in a large semifossorial marsupial: The effect of graded hypoxia and hypercapnia. Physiological & Biochemical Zoology 75:77-82.

Frappell PB, Blevin HA, Baudinette RV. 1989. Understanding respirometry chambers: what goes in must come out. J theor Biol 138:479-494.

Frappell PB, Hinds DS, Boggs DF. 2001. Scaling of respiratory variables and the breathing pattern in birds: An allometric and phylogenetic approach. Physiological & Biochemical Zoology 74:75-89.

Frappell PB, MacFarlane PM. 2006. Development of the respiratory system in marsupials. Respir Physiol Neurobiol 154:252-267.

Frappell PB, Mortola JP. 1989. Respiratory mechanics in small newborn mammals. Respiration Phsyiology 76:25-36.

Frappell PB, Mortola JP. 2000. Respiratory function in a newborn marsupial with skin gas exchange. Respiration Physiology 120:35-45.

Gautier H. 1996. Interactions among metabolic rate, hypoxia, and control of breathing. Journal of Applied Physiology 81:521-527.

Gemmell RT. 1986. Lung development in the marsupial bandicoot, *Isoodon macrourus*. Journal of Anatomy 148:193-204.

Gemmell RT, Nelson J. 1988. The ultrastructure of the lung of two newborn marsupial species, the northern native cat, *Dasyurus hallucatus*, and the brushtail possum, *Trichosurus vulpecula*. Cell and Tissue Research 252:683-685.

Green JA, Frappell PB, Clark TD, Butler PJ. 2008. Predicting rate of oxygen consumption from heart rate while little penguins work, rest and play. Comp Biochem Physiol A Mol Integr Physiol 150:222-230.

Greenlee KJ, Henry JR, Kirkton SD, Westneat MW, Fezzaa K, Lee WK, Harrison JF. 2009. Synchrotron imaging of the grasshopper tracheal system: morphological and physiological components of tracheal hypermetry. Am J Physiol Regul Integr Comp Physiol 297:R1343-1350.

Greer JJ, Allan DW, Martin-Caraballo M, Lemke RP. 1999. An overview of phrenic nerve and diaphragm muscle development in the perinatal rat. J Appl Physiol 86:779-786.

Greer JJ, Funk GD, Ballanyi K. 2006. Preparing for the first breath: prenatal maturation of respiratory neural control. J Physiol 570:437-444.

Greer JJ, Smith JC, Feldman JL. 1992. Respiratory and locomotor patterns generated in the fetal rat brain stem-spinal cord in vitro. J Neurophysiol 67:996-999.

Guthrie RD, LaFramboise WA, Standaert TA, Van Belle G, Woodrum DE. 1985. Ventilatory interaction between oxygen and carbon dioxide in the preterm primate. Pediatr Res 19:528-533.

Hanson MA, Kumar P, Williams BA. 1989. The effect of chronic hypoxia upon the development of respiratory chemoreflexes in the newborn kitten. Journal of Physiology (London) 411:563-574.

Harding R, Hooper SB. 1996. Regulation of lung expansion and lung growth before birth. Journal of Applied Physiology 81:209-224.

Hilaire G, Duron B. 1999. Maturation of the mammalian respiratory system. Physiological Reviews 79:325-360.

Hill JP, Hill WCO. 1955. The growth stages of the pouch young of the native cat (*Dasyurus viverrinus*) together with observations on the anatomy of the newborn young. Transactions of the zoological society of London 28:349-352.

Hinds LA, Tyndale-Biscoe CH, Shaw G, Fletcher TP, Renfree MB. 1990. Effects of prostaglandin and prolactin on luteolysis and parturient behaviour in the non-pregnant tammar, Macropus eugenii. J Reprod Fertil 88:323-333.

Holland RA, Gooley AA, Hope RM. 1998. Embryonic globins of the marsupial the tammar wallaby: bird like and mammal like. Clin Exp Pharmocol Physiol 25:740-744.

Holland RAB, Calvert SJ, Hope RM, Chesson CM. 1994. Blood O2 transport in newborn and adult of a very small marsupial (*Sminthopsis crassicaudata*). Respiration Physiology 98:69-81.

Holland RAB, Rimes AF, Comis A, Tyndale-Biscoe CH. 1988. Oxygen carriage and carbonic anhydrase activity in the blood of a marsupial, the Tammar Wallaby (*Macropus eugenii*), during early development. Respiration Physiology 73:69-86.

Hooper SB, Kitchen MJ, Siew ML, Lewis RA, Fouras A, te Pas AB, Siu KK, Yagi N, Uesugi K, Wallace MJ. 2009. Imaging lung aeration and lung liquid clearance at birth using phase contrast X-ray imaging. Clin Exp Pharmacol Physiol 36:117-125.

Hooper SB, Kitchen MJ, Wallace MJ, Yagi N, Uesugi K, Morgan MJ, Hall C, Siu KK, Williams IM, Siew M, Irvine SC, Pavlov K, Lewis RA. 2007. Imaging lung aeration and lung liquid clearance at birth. FASEB J 21:3329-3337.

Hooper SB, Wallace MJ. 2006. Role of the physicochemical environment in lung development. Clin Exp Pharmacol Physiol 33:273-279.

Hughes RL, Hall LS. 1988. Structural adaptations of the newborn marsupial. In: Tyndale-Biscoe CH, Jannsens PA, editors. The developing marsupial: Models for biomedical research. Berlin: Springer-Verlag.

Hughes RL, Hall LS, Tyndale-Biscoe CH, Hinds LA. 1989. Evolutionary implications of macropod organogenesis. In: Grigg G, Jarman P, Hume I, editors. Kangaroos, wallabies and rat-kangaroos. NSW: Surrey Beaty & Sons.

Janczewski WA, Onimaru H, Homma I, Feldman JL. 2002. Opioid-resistant respiratory pathway from the preinspiratory neurones to abdominal muscles: in vivo and in vitro study in the newborn rat. J Physiol 545:1017-1026.

Jansen A, Chernick V. 1983. Development of respiratory control. Physiological Reviews 63:437-483.

Jansen AH, Chernick V. 1991. Fetal breathing and development of control of breathing. Journal of Applied Physiology 70:1431-1446.

Kaiser A, Klok CJ, Socha JJ, Lee WK, Quinlan MC, Harrison JF. 2007. Increase in tracheal investment with beetle size supports hypothesis of oxygen limitation on insect gigantism. Proc Natl Acad Sci U S A 104:13198-13203.

Kennedy EP, Lehninger AL. 1948. Intracellular structures and the fatty acid oxidase system of rat liver. J Biol Chem 172:847.

Kitchen MJ, Lewis RA, Yagi N, Uesugi K, Paganin D, Hooper SB, Adams G, Jureczek S, Singh J, Christensen CR, Hufton AP, Hall CJ, Cheung KC, Pavlov KM. 2005. Phase contrast X-ray imaging of mice and rabbit lungs: a comparative study. Br J Radiol 78:1018-1027.

Kitchen MJ, Paganin D, Lewis RA, Yagi N, Uesugi K, Mudie ST. 2004. On the origin of speckle in x-ray phase contrast images of lung tissue. Physics in Medicine and Biology 49:4335-4348.

Koos BJ, Kawasaki Y, Kim YH, Bohorquez F. 2005. Adenosine A2A-receptor blockade abolishes the roll-off respiratory response to hypoxia in awake lambs. Am J Physiol Regul Integr Comp Physiol 288:R1185-1194.

Kosch PC, Stark AR. 1984. Dynamic maintenance of end-expiratory lung volume in full-term infants. J Appl Physiol 57:1126-1133.

Krause W, Cutts J, Leeson C. 1976. Type II pulmonary epithelial cells of the newborn opossum lung. Am J Anat 146:181-188.

Krause WJ, Leeson CR. 1975. Postnatal development of the respiratory system of the opossum. 2. Electron microscopy of the epithelium and pleura. Acta Anatomica 92:28-44.

Krauss A, Klain DB, Waldman S, Auld PAM. 1965. Ventilatory response to carbon dioxide in newborn infants. Pediatr Res 9:46-50.

LaFramboise WA, Guthrie RD, Standaert TA, Woodrum DE. 1983. Pulmonary mechanics during the ventilatory response to hypoxemia in the newborn monkey. J Appl Physiol 55:1008-1014.

Laskowski MB, Owens JL. 1994. Embryonic expression of motoneuron topography in the rat diaphragm muscle. Dev Biol 166:502-508.

Lawson EE, Long WA. 1983. Central origin of biphasic breathing pattern during hypoxia in newborns. J Appl Physiol 55:483-488.

Lechner AJ, Banchero N. 1982. Advanced pulmonary development in newborn guinea pigs (Cavia porcellus). Am J Anat 163:235-246.

Lewis RA, Hall CJ, Hufton AP, Evans S, Menk RH, Arfelli F, Rigon L, Tromba G, Dance DR, Ellis IO, Evans A, Jacobs E, Pinder SE, Rogers KD. 2003. X-ray refraction effects: application to the imaging of biological tissues. The Brittish Journal of Radiology 76:301-308.

Lewis RA, Yagi N, Kitchen MJ, Morgan MJ, Paganin D, Siu KKW, Pavlov K, Williams I, Uesugi K, Wallace MJ, Hall CJ, Whitley J, Hooper SB. 2005. Dynamic imaging of the lungs using x-ray phase contrast. Physics in Medicine and Biology 50:5031-5040.

Lindahl P, Karlsson L, Hellstrom M, Gebre-Medhin S, Willetts K, Heath JK, Betsholtz C. 1997. Alveogenesis failure in PDGF-A-deficient mice is coupled to lack of distal spreading of alveolar smooth muscle cell progenitors during lung development. Development 124:3943-3953.

Liu Q, Wong-Riley MT. 2002. Postnatal expression of neurotransmitters, receptors, and cytochrome oxidase in the rat pre-Botzinger complex. J Appl Physiol 92:923-934.

Liu Q, Wong-Riley MT. 2010a. Postnatal changes in the expressions of serotonin 1A, 1B, and 2A receptors in ten brain stem nuclei of the rat: implication for a sensitive period. Neuroscience 165:61-78.

Liu Q, Wong-Riley MT. 2010b. Postnatal changes in tryptophan hydroxylase and serotonin transporter immunoreactivity in multiple brainstem nuclei of the rat: implications for a sensitive period. J Comp Neurol 518:1082-1097.

Liu YY, Wong-Riley MT, Liu JP, Jia Y, Liu HL, Jiao XY, Ju G. 2002. GABAergic and glycinergic synapses onto neurokinin-1 receptor-immunoreactive neurons in the pre-

Botzinger complex of rats: light and electron microscopic studies. Eur J Neurosci 16:1058-1066.

MacFarlane PM, Frappell PB. 2001. Convection requirement is established by total metabolic rate in the newborn tammar wallaby. Respiration Physiology 126:221-231.

MacFarlane PM, Frappell PB, Mortola JP. 2002. Mechanics of the respiratory system in the newborn tammar wallaby. Journal of Experimental Biology 205:533-538.

Makanya AN, Haenni B, Burri PH. 2003. Morphometry and allometry of the postnatal lung development in the quokka wallaby (Setonix brachyurus): a light microscopic study. Respiratory Physiology & Neurobiology 134:43-55.

Makanya AN, Mortola JP. 2007. The structural design of the bat wing web and its possible role in gas exchange. J Anat 211:687-697.

Makanya AN, Sparrow MP, Warui CN, Mwangi DK, Burri PH. 2001. Morphological analysis of the postnatally developing marsupial lung: The quokka wallaby. anatomical record 262:253-265.

Makanya AN, Tschanz SA, Haenni B, Burri PH. 2007. Functional respiratory morphology in the newborn quokka wallaby (Setonix brachyurus). Journal of Anatomy 211:26-36.

Martin RJ, Carlo WA, Robertson SS, Day WR, Bruce EN. 1985. Biphasic response of respiratory frequency to hypercapnea in preterm infants. Pediatr Res 19:791-796.

McGowan SE. 1992. Extracellular matrix and the regulation of lung development and repair. FASEB J 6:2895-2904.

Mercer RR, Crapo JD. 1990. Spatial distribution of collagen and elastin fibers in the lungs. J Appl Physiol 69:756-765.

Merchant JC. 1979. The effect of pregnancy on the interval between one oestrus and the next in the tammar wallaby, Macropus eugenii. J Reprod Fertil 56:459-463.

Mercurio AR, Rhodin JA. 1976. An electron microscopic study on the type I pneumocyte in the cat: differentiation. Am J Anat 146:255-271.

Michelson HB, Wong RK. 1991. Excitatory synaptic responses mediated by GABAA receptors in the hippocampus. Science 253:1420-1423.

Milic-Emili J, Grunstein MM. 1976. Drive and timing components of ventilation. Chest 70:131-133.

Miller NJ, Orgeig S, Daniels CB, Baudinette RV. 2001. Postnatal development and control of the pulmonary surfactant system in the tammar wallaby Macropus eugenii. Journal of Experimental Biology 204:4031-4042.

Milsom WK. 1990. Mechanoreceptor modulation of endogenous respiratory rhythms in vertebrates. American Journal of Physiology 259:R898-R910.

Mortola J. 1987. Dynamics of breathing in newborn mammals. Physiological Reviews 67:187-243.

Mortola J, Lauzon A, Mott B. 1987. Expiratory flow pattern and respiratory mechanics. Can J Physiol Pharmacol 65:1142-1145.

Mortola J, Magnante D, Saetta M. 1985a. Expiratory pattern of newborn mammals. Journal of Applied Physiology 58:528-533.

Mortola J, Saetta M, Fox. G, Smith B, Weeks S. 1985b. Mechanical aspects of chest wall distortion. J Appl Physiol 59:295-304.

Mortola J, Tenney S. 1986. Effects of hyperoxia on ventilatory and metabolic rates of newborn mice. Respiration Physiology 63:267-274.

Mortola JP. 1984. Breathing pattern in newborns. Journal of Applied Physiology 56:1533-1540.

Mortola JP. 1985. Establishment of the end-expiratory level (FRC) in newborn mammals. In: Walters DV, Strang LB, Geubelle F, editors. International Symposium on Physiology and Pathophysiology of the Fetal and Neonatal Lung. Brussels: MTP Press Limited, Lancaster. p 129-136.

Mortola JP. 1993. Hypoxic hypometabolism in mammals. NIPS 8:79-82.

Mortola JP. 2001. Respiratory Physiology of Newborn Mammals. A Comparative Perspective. Baltimore: John Hopkins University Press.

Mortola JP. 2004. Implications of hypoxic hypometabolism during mammalian ontogenesis. Respiratory Physiology & Neurobiology 141:345-356.

Mortola JP, Fisher JT, Smith B, Fox G, Weeks S. 1982. Dynamics of breathing in infants. Journal of Applied Physiology 52:1209-1215.

Mortola JP, Frappell PB, Woolley PA. 1999. Breathing through skin in a newborn mammal. Nature 397:660.

Mortola JP, Lanthier C. 1996. The ventilatory and metabolic response to hypercapnia in newborn mammalian species. Respiration Physiology 103:263-270.

Mortola JP, Matsuoka T, Saiki C, Naso L. 1994. Metabolism and ventilation in hypoxic rats: effect of body mass. Respiration Physiology 97:225-234.

Mortola JP, Rezzonico R, Lanthier C. 1989. Ventilation and oxygen consumption during actue hypoxia in newborn mammals: a comparative analysis. Respiration Physiology 78:31-43.

Morton S. 1978. Torpor and nest-shaping in free-living Sminthopsis crassicaudata (Marsupialia) and Mus musculus (Rodentia). J Mamm 59:569-575.

Mund SI, Stampanoni M, Schittny JC. 2008. Developmental alveolarization of the mouse lung. Dev Dyn 237:2108-2116.

Murphy CR, Smith JR. 1970. Age determination of pouch young and juvenile Kangaroo Island wallabies. Transactions of the Royal Society of South Australia 94:15-20.

Nattie E. 1999. CO2, brainstem chemoreceptors and breathing [Review]. Progress in Neurobiology 59:299-331.

Nattie E. 2006. Why do we have both peripheral and central chemoreceptors? J Appl Physiol 100:9-10.

Neubauer JA, Melton JE, Edelman NH. 1990. Modulation of respiration during brain hypoxia. J Appl Physiol 68:441-451.

Olver RE, Walters DV, S MW. 2004. Developmental regulation of lung liquid transport. Annu Rev Physiol 66:77-101.

Onimaru H, Homma I. 2006. Point:Counterpoint: The parafacial respiratory group (pFRG)/pre-Botzinger complex (preBotC) is the primary site of respiratory rhythm generation in the mammal. Point: the PFRG is the primary site of respiratory rhythm generation in the mammal. J Appl Physiol 100:2094-2095.

Pask A, Renfree MB, Marshall Graves JA. 2000. The human sex-reversing ATRX gene has a homologue on the marsupial Y chromosome, ATRY: implications for the evolution of mammalian sex determination. Proc Natl Acad Sci U S A 97:13198-13202.

Pask AJ, Paplinska JZ, Shaw G, Graves JA, Renfree MB. 2007. Marsupial WT1 has a novel isoform and is expressed in both somatic and germ cells in the developing ovary and testis. Sex Dev 1:169-180.

Piiper J, Scheid P. 1992. Gas exchange in vertebrates through lungs, gills and skin. Physiology 7:199-203.

Porra L, Monfraix S, Berruyer G, Le Duc G, Nemoz C, Thomlinson W, Suortti P, Sovijarvi ARA, Bayat S. 2004. Effect of tidal volume on distribution of ventilation assessed by synchrotron radiation CT in rabbit. J Appl Physiol 96:1899-1908.

Randall D, Gannon B, Runciman S, Baudinette RV. 1984. Chapter 29. Gas transfer by the neonate in the pouch of the tammar wallaby, Macropus eugenii. In: Seymour RS, editor. Respiration and metabolism of embryonic vertebrates. Dordrecht, Netherlands: Dr W. Junk Publishers. p 423-436.

Randall GCB. 1992. Perinatal adaptation in animals. Animal Reproduction Science 28:309-318.

Reeves R. 1977. The interaction of body temperature and acid-base balance in ectothermic vertebrates. Annual Review of Physiology 39:559-586.

Renfree MB. 1973. Proteins in the uterine secretions of the marsupial Macropus eugenii. Dev Biol 32:41-49.

Renfree MB. 1995. Monotreme and marsupial reproduction. Reprod Fertil Dev 7:1003-1020.

Renfree MB, Fox DJ. 1975. Pre- and postnatal development of lactate and malate dehydrogenases in the marsupial Didelphis marsupialis virginiana. Comp Biochem Physiol B 52:347-350.

Renfree MB, Lewis AM. 1996. Cleavage in vivo and in vitro in the Marsupial Macropus eugenii. Reprod Fertil Dev 8:725-742.

Ribbons KA, Baudinette RV, McMurchie EJ. 1989. The development of pulmonary surfactant lipids in a neonatal marsupial and the rat. Respiration Physiology 75:1-10.

Rigatto H, Desai U, Leahy F, Kalapesi Z, Cates D. 1981. The effect of 2% CO2, 100% O2, theophylline and 15% O2 on "inspiratory drive" and "effective" timing in preterm infants. Early Hum Dev 5:63-70.

Rigatto H, Kwiatkowski KA, Hasan SU, Cates DB. 1991. The ventilatory response to endogenous CO2 in preterm infants. Am Rev Respir Dis 143:101-104.

Runciman SIC, Baudinette RV, Gannon BJ. 1996. Postnatal development of the lung parenchyma in a Marsupial: The Tammar Wallaby. Anatomical Record 244:193-206.

Runciman SIC, Baudinette RV, Gannon BJ, Lipsett J. 1998a. Morphometric analysis of postnatal lung development in the tammar wallaby: light microscopy. Respiration Physiology 112:325-337.

Runciman SIC, Baudinette RV, Gannon BJ, Lipsett J. 1998b. Morphometric estimate of gas-exchange tissue in the new-born tammar wallaby, Macropus eugenii. Respiration Physiology 111:177-187.

Runciman SIC, Baudinette RV, Gannon BJ, Lipsett J. 1999. Morphometric analysis of postnatal lung development in a marsupial: Transmission electron microscopy. Respiration Physiology 118:61-75.

Runciman SIC, Gannon BJ, Baudinette RV. 1995. Central cardiovascular shunts in the perinatal marsupial. The Anatomical Record 243:71-83.

Saetta M, Mortola JP. 1987. Interaction of hypoxic and hypercapnic stimuli on breathing pattern in the newborn rat. J Appl Physiol 62:506-512.

Saiki C, Mortola JP. 1996. Effect of CO2 on the metabolic and ventilatory responses to ambient temperature in conscious adult and newborn rats. Journal of Physiology 491:261-269.

Saunders NR, Hinds LA. 1997. Marsupial Biology: Recent Research, New Perspectives. Sydney: University of New South Wales Press Ltd.

Schittny JC, Mund SI, Stampanoni M. 2008. Evidence and structural mechanism for late lung alveolarization. Am J Physiol Lung Cell Mol Physiol 294:L246-254.

Sera T, Uesugi K, Yagi N. 2005. Morphometric deformations of small airways and alveoli under quasi-static inflation process. J Physiol Anthropol Appl Human Sci 24:465-468.

Sevcik P, Vojtova H, Stejskal J, Hillova L. 1955. [Role of Escherichia coli B5 O55 in the etiology of infantile and neonatal diarrhea.]. Cesk Pediatr 10:694-697.

Smith CA, Rodman JR, Chenuel BJ, Henderson KS, Dempsey JA. 2006. Response time and sensitivity of the ventilatory response to CO2 in unanesthetized intact dogs: central vs. peripheral chemoreceptors. J Appl Physiol 100:13-19.

Smith JC, Ellenberger HH, Ballanyi K, Richter DW, Feldman JL. 1991. Pre-Botzinger complex: a brainstem region that may generate respiratory rhythm in mammals. Science 254:726-729.

Socha JJ, Lee WK, Harrison JF, Waters JS, Fezzaa K, Westneat MW. 2008. Correlated patterns of tracheal compression and convective gas exchange in a carabid beetle. J Exp Biol 211:3409-3420.

St-John WM, St Jacques R, Li A, Darnall RA. 1999. Modulation of hypoxic depressions of ventilatory activity in the newborn piglet by mesencephalic mechanisms. Brain Res 819:147-149.

Stahl WR. 1967. Scaling of respiratory variables in mammals. Journal of Applied Physiology 22:453-460.

Starcher BC. 2000. Lung elastin and matrix. Chest 117:229S-234S.

Strang LB. 1991. Fetal lung liquid: secretion and reabsorption. Physiological Reviews 71:991-1016.

Szdzuy K, Zeller U, Renfree M, Tzschentke B, Janke O. 2008. Postnatal lung and metabolic development in two marsupial and four eutherian species. J Anat 212:164-179.

Taylor C, Weibel E. 1981. Design of the mammalian respiratory system. I. Problem and strategy. Respiration Physiology 44:1-10.

te Pas AB, Davis PG, Hooper SB, Morley CJ. 2008. From liquid to air: breathing after birth. J Pediatr 152:607-611.

Tenney SM, Remmers JE. 1963. Comparative quantitative morphology of the mammalian lung: diffusing area. Nature 197:54-56.

Thurlbeck WM. 1975. Postnatal growth and development of the lung. Am Rev Respir Dis 111:803-844.

Tibben E, Holland R, Tyndale-Biscoe C. 1991. Blood oxygen carriage in the marsupial, tammar wallaby (Macropus eugenii), at prenatal and neonatal stages. Respiration Physiology 84:93-104.

Tyndale-Biscoe CH, Janssens PA. 1988. The Developing Marsupial: Models for Biomedical Research. Berlin: Springer-Verlag.

Tyndale-Biscoe CH, Renfree MB. 1987. Reproductive Physiology of Marsupials: Cambridge University Press.

Viemari JC, Burnet H, Bevengut M, Hilaire G. 2003. Perinatal maturation of the mouse respiratory rhythm-generator: in vivo and in vitro studies. Eur J Neurosci 17:1233-1244.

Vyas H, Milner AD, Hopkins IE. 1981. Intrathoracic pressure and volume changes during the spontaneous onset of respiration in babies born by cesarean section and by vaginal delivery. J Pediatr 99:787-791.

Wakefield MJ, Graves JA. 2003. The kangaroo genome: Leaps and bounds in comparative genomics. EMBO reports 4:143-147.

Walker MT, Gemmell RT. 1983. Organogenesis of the pituitary, adrenal, and lung at birth in the wallaby, *Macropus rufogriseus*. The American Journal of Anatomy 168:331-344.

Wang T, Hicks JW. 1996. The interaction of pulmonary ventilation and the right-left shunt on arterial oxygen levels. J Exp Biol 199:2121-2129.

West JB. 1995. Respiratory physiology- the essentials. Baltimore: Williams & Wilkins.

Westneat MW, Betz O, Blob RW, Fezzaa K, Cooper WJ, Lee WK. 2003. Tracheal respiration in insects visualized with synchrotron x-ray imaging. Science 299:558-560.

Wong-Riley MT, Liang HL, Eells JT, Chance B, Henry MM, Buchmann E, Kane M, Whelan HT. 2005. Photobiomodulation directly benefits primary neurons functionally inactivated by toxins: role of cytochrome c oxidase. J Biol Chem 280:4761-4771.

Wong-Riley MT, Liu Q. 2005. Neurochemical development of brain stem nuclei involved in the control of respiration. Respir Physiol Neurobiol 149:83-98.

Yagi N, Suzuki Y, Umetani K, Kohmura Y, Yamasaki K. 1999. Refraction-enhanced x-ray imaging of mouse lung using synchrotron radiation source. Med Phys 26:2190-2193.

Zeltner TB, Burri PH. 1987. The postnatal development and growth of the human lung. Respiration Physiology 67:269-282.

Zeltner TB, Caduff JH, Gehr P, Pfenninger J, Burri PH. 1987. The postnatal development and growth of the human lung. I. Morphometry. Respiration Physiology 67:247-267.

Zoetis T, Hurtt ME. 2003. Species comparison of lung development. Birth Defects Research 68:121-124.